GEORGIA INSTITUTE OF TECHNOLOGY
OFFICE OF CONTRACT ADMINISTRATION

RESEARCH PROJECT INITIATION

Date: October 6, 1975

Project Title: Single Wheel Gas Turbine Topping Unit for Coal Burning Power Plants

Project No: E-25-658

Principal Investigator: Dr. T. W. Jackson/Dr. G. T. Colwell

Sponsor: Energy Research & Development Admin., Oak Ridge Operations, Oak Ridge, Tenn. 37830

Agreement Period: From July 1, 1975 Until June 30, 1976

Type Agreement: Contract No. E-(40-1)-4959

Amount: $25,000 ERDA
1,320 GIT Contribution
$26,320 Total Estimated Cost

Reports Required:
Publication Preprints; Publication Reprints; Annual Progress Report; Final Report.

Sponsor Contact Person (s):

Mr. Earl Mason
Research Contracts, Procedures & Reports Branch
Contract Division, US Energy Research & Development Administration
Oak Ridge Operations
P.O. Box E
Oak Ridge, Tennessee 37830
Phone: (615) 483-8611

Assigned to: Mechanical Engineering

COPIES TO:

Principal Investigator (2)	Library
School Director	Rich Electronic Computer Center
Dean of the College	Photographic Laboratory
Director, Research Administration	Project File
Director, Financial Affairs (2)	
Security-Reports-Property Office ✓	
Patent Coordinator	Other

RA-3 (9-75)

GEORGIA INSTITUTE OF TECHNOLOGY
OFFICE OF CONTRACT ADMINISTRATION

SPONSORED PROJECT TERMINATION

Date: May 2, 1977

Project Title: Single Wheel Gas Turbine Topping Unit for Coal Burning Power Plants

Project No: E-25-658

Project Director: Dr. T. W. Jackson/Dr. G. T. Colwell

Sponsor: Energy Research and Development Administration
Oak Ridge Operations

Effective Termination Date: 6/30/76

Clearance of Accounting Charges: 6/30/76

Grant/Contract Closeout Actions Remaining:

_ Final Invoice and Closing Documents
_ Final Fiscal Report
X Final Report of Inventions
X Govt. Property Inventory & Related Certificate
_ Classified Material Certificate
_ Other _____

Assigned to: Mechanical Engineering (School/Laboratory)

COPIES TO:

Project Director
Division Chief (EES)
School/Laboratory Director
Dean/Director—EES
Accounting Office
Procurement Office
Security Coordinator (OCA)
Reports Coordinator (OCA)
Library, Technical Reports Section
Office of Computing Services
Director, Physical Plant
EES Information Office
Project File (OCA)
Project Code (GTRI)
Other _____

CA—4 (3/76)

E-25-658

ORO-4959-1

PROGRESS REPORT

ERDA Contract No. E-(40-1)-4959
(Georgia Tech Project No. E-25-658)

SINGLE WHEEL GAS TURBINE TOPPING UNIT FOR COAL BURNING POWER PLANTS

15 March 1976

by

Thomas W. Jackson
Professor of Energy Engineering

and

Gene T. Colwell
Assoc. Professor of Mechanical Engineering

Georgia Institute of Technology
Atlanta, Georgia 30332

PROGRESS REPORT

SINGLE WHEEL GAS TURBINE TOPPING UNIT FOR COAL BURNING POWER PLANTS

INTRODUCTION

The work statement for ERDA Contract E-(40-1)-4959 is as follows:

> "The Contractor shall conduct a study of the calculation of theoretical estimates of turbine and compressor parameters. The work shall consist of the following tasks:
>
> 1. The drag turbine and compressor will be mathematically modeled, based on existing one-dimensional and three-dimensional computer programs. The model will allow the analysis of the effects of varied turbine and compressor parameters.
>
> 2. Using the model described in Task 1, detailed comprehensive calculations will be made of efficiencies for a turbine-compressor combination used as a topping unit for a conventional steam power plant.
>
> 3. Results of the calculations performed in Task 2 will be assembled in a final report. The report will include the rationale and basis for the efficiency calculations. The report will be sufficiencly detailed so as to allow outside experts in the field to assess the potential of a subsequent prototype test turbine and will provide recommendations for further research and development on the single wheel gas turbine in terms of its promise of offering a novel, more efficient system for fossil-energy fueled advanced power systems."

During the past 9 months the principal investigators, Drs. Colwell and Jackson, have each spent at least 15 percent of their time on the subject project. They will continue at this rate or more until the end of the subject contract period, 1 July 1976. In addition, a graduate student, Mr. Andrew Coons, has worked on the project as a portion of his requirements for a Masters degree in Mechanical Engineering. Undergraduate students have also contributed by attacking specific portions of the overall problem associated with combining high temperature turbines with central station power plants.

PROJECT PROGRESS

During the year the following has or will be accomplished:

1. Dr. Colwell has prepared a paper utilizing the three dimensional program and data of a former student, Mr. A. Yalcin, entitled "Flow Fields in Moving Curved Channels." (No further three dimensional effort will be undertaken during the contract period.) The paper has been submitted for possible publication to COMPUTERS AND FLUIDS.

2. Drs. Colwell and Jackson have supervised Mr. Andrew Coons in the restructuring and modeling of the one-dimensional program to obtain compressor and turbine pressure and flow rate maps, as well as, efficiencies for a large range of passage shapes and flow rates. Combined engine calculations, with and without turbine flow area variation, have been obtained.

3. Drs. Colwell and Jackson have evaluated the potentials of the system, turbine-compressor combination, as a topping unit for a conventional steam power plant. They have also extended their considerations to the possibility of utilizing the turbine alone with conventional axial flow compressors.

4. Drs. Colwell and Jackson have combined their efforts and incorporated their conclusions in a renewal proposal which is being forwarded to ERDA under separate cover.

The following papers and reports have or will be prepared before the completion of the current contract.

1. "Flow Fields in Moving Curved Channels" by Gene T. Colwell and Ali Ihsan Yalcin. Submitted for possible publication to COMPUTERS AND FLUIDS. (A copy of the paper is attached.)

2. Masters thesis entitled "Performance of Viscous Topping Turbine for Application in Fossil Fuel Power Plant" by Andrew M. Coons (to be submitted during Spring Quarter 1976)

3. Final report to be submitted by Drs. Colwell and Jackson at end of contract period.

In reference to the final report, it will encompass the following:

1. The mathematical formulation of the one dimensional computer program for the compressor and turbine and its rationale.

2. A summation of the results obtained including efficiencies of the turbine and compressor for various flow rates. The parameters will also be examined for passage variations and the stationary wall effect.

3. A summation of the data obtained in 2. when combined into a turbine-compressor combination and used as a topping turbine for a conventional steam power plant.

4. Recommendations for further work as follows:

   a. It is proposed to match the compressor (axial flow with various assumed efficiencies) to the single wheel turbine in 1, 2, 3 or more units in both parallel and series flow modes.

   b. It is proposed to optimize the groove sizes for particular pressure ratios, flow rates, and inlet temperatures.

   c. It is proposed to determine turbine fin temperatures as a function of flow rates, turbine inlet temperatures, wheel speeds, and pressure ratios.

   d. It is proposed to determine the overall Power Plant efficiencies using a complete system comprising axial flow compressors and the viscous single wheel turbine in 1, 2, 3 or more units in both parallel and series flow modes.

   e. It is proposed to speculate on the research accomplished for

      (1) possible economic benefits for coal burning plants,

      (2) possibilities of advancing the work to prototype stages for various applications, and

      (3) possibilities of using modifications of the system in other energy situations; such as, a total turbine for geothermal power extraction, etc.

FINANCIAL CONSIDERATIONS

It is anticipated that all funds alloted to the project will be expended by 1 July 1976.

FLOW FIELDS IN MOVING CURVED CHANNELS

Gene T. Colwell
Associate Professor

and

Ali Ihsan Yalcin
Graduate Student

School of Mechanical Engineering
Georgia Institute of Technology
Atlanta, Georgia

November, 1975

ABSTRACT

The laminar steady flow of air through moving narrow deep circumferential grooves on a rotor is studied. Fluid enters the moving grooves from a stationary inlet nozzle with uniform velocity and exits into a stationary diffuser after approximately 150 degrees of rotation. Three dimensional developing velocity profiles and pressure distributions are presented for a variety of operating conditions. Computed overall head-flow characteristics are found to be in relatively close agreement with the simple Couette model where both walls are taken to be moving at the same rate and in the same direction.

C O N T E N T S

INTRODUCTION

For several years the flow of air and combustion products around the periphery of rotors with narrow deep circumferential slots has been under study at the Georgia Institute of Technology. These studies were motivated by a need to understand the flow fields which develop in a new type of gas turbine engine which was invented at the Institute (1). This novel engine which is shown schematically in Figure 1 combines compression and expansion processes on a single rotor. The work described in the present paper was aimed at developing an understanding of how the laminar three dimensional flow field behaves on the compressor side of the turbine at very low rotational speeds. The next stage of the work will be to examine turbulent conditions which will exist in the flow passages of the machine at almost all operating conditions of interest.

To the author's knowledge, no previously published literature exists which treats exactly the problem under study. There are, however, many references which are of interest and use in selecting computational schemes and in evaluating results. Professor Rice and his colleages (2,3) have published a number of papers over a period of several years which describe results of studies of "Tesla" Turbomachines. In the Tesla arrangement fluid enters around the periphery of the rotor, spirals inwardly between closely spaced disks, and exits along the rotor axis. The governing equations are of course the same for the peripheral flow arrangement reported on in the present paper and the Tesla machine but the boundary conditions are quite different.

Boyd and Rice (2) numerically solved Navier-Stokes type equations for the Tesla turbine to yield detailed information on development of

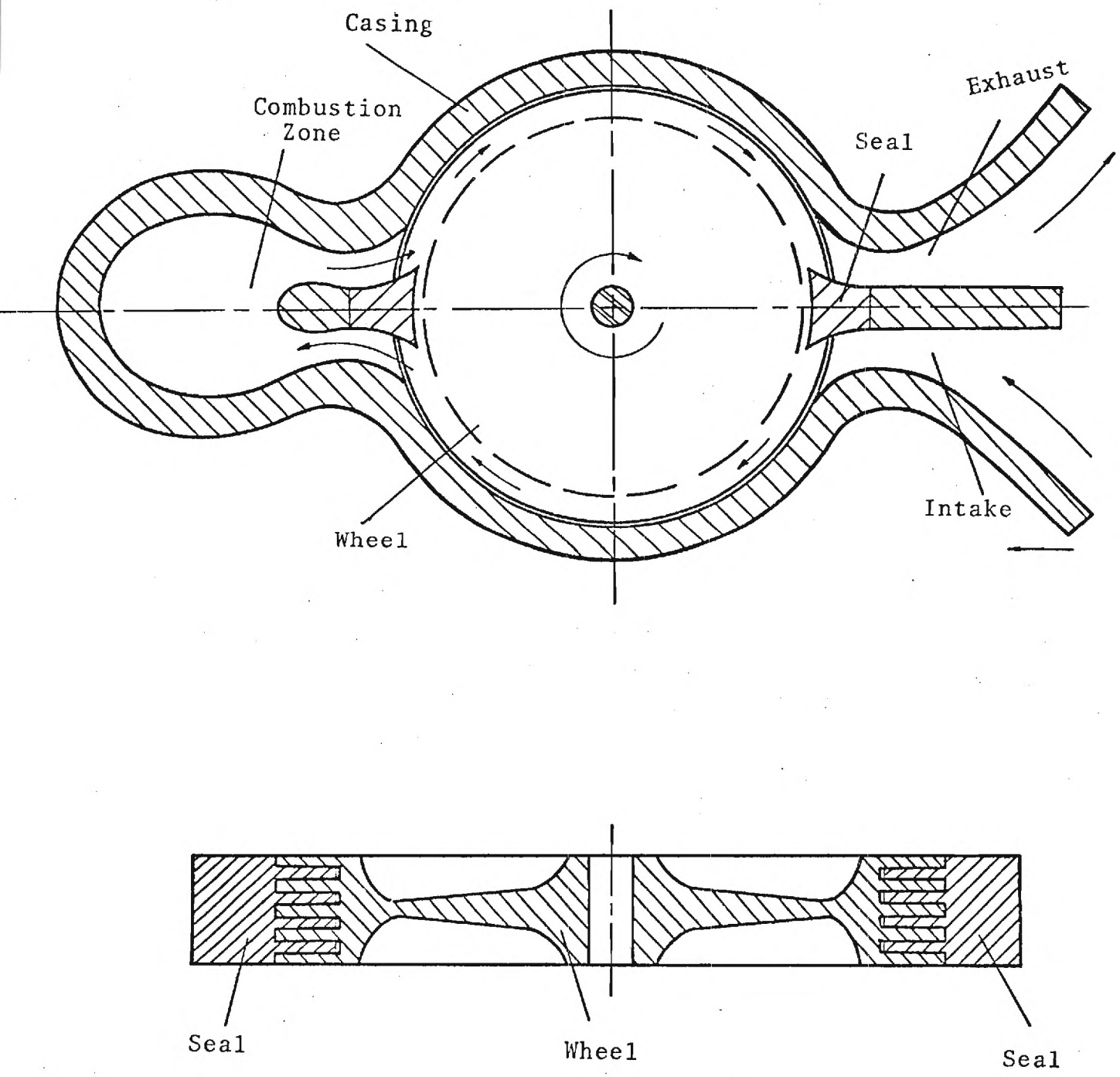

Figure 1. Viscous Drag Turbine

the velocity and pressure fields in the machine under laminar steady conditions. They considered both uniform inlet velocity and parabolic inlet velocity. The discussion concerning solution schemes in Reference 2 was of considerable value to the present project. Lawn and Rice (3) computed overall design parameters for laminar inward flow disk turbines. These parameters were obtained by integrating profiles of the type presented in Reference 2. The design charts include information on volume flow rates, Reynolds numbers, pressure changes through the turbine, and efficiencies. The efficiency which is defined in terms of torque transfer and stagnation pressure change is reported to reach values of near 0.8 under certain conditions.

Rastogi and Whitelaw (4) made a study of the effects of longitudinal curvature on boundary layers. Although they were primarily interested in turbulent boundary layers, they did report results of computations on one laminar case. A wall jet was placed on both concave and convex surfaces and variations with curvature at various longitudinal stations were determined for average boundary layer velocity and wall shear stress. These data are of interest to the present study only in a roughly qualitative manner. However, they do indicate that large concave or convex curvatures have rather small effects on overall performance parameters for non-separated boundary layers. Reference 4 indicates maximum variations in mean longitudinal velocities and wall shear stresses of about ten to fifteen per cent for convex and concave surfaces with radius of curvature of 10 cm and slot Reynolds number of 2000.

Coney and El-Shaarawi (5) theoretically examined the problem of laminar axial viscous flow in an annulus with a rotating inner cylinder. Their results show how three dimensional velocity profiles develop in

the axial direction from the inlet to fully developed conditions. They made direct numerical calculations of velocities and pressures from linearised finite difference equations developed from governing differential equations. Although the throughflow directions and channel geometries are quite different in the work being reported on herein and those reported in Reference 5, there is considerable similarity in the shapes of the parametric curves. Conover (6) studied experimentally the laminar velocity field between rotating and stationary disks with and without radial inflow. The manner in which radial velocities change with axial location is of particular interest since they exhibit some of the same backflow characteristics that circumferential velocities exhibit in the present case. Reference 6 also gives some interesting information relative to limits of stability for the model studied.

Hasinger and Kehrt (7) reported on an analytical and experimental study of mixed flow shear pumps. Their arrangement included axial inlet flow, spiral flow between rotating conical surfaces, and mixed exhaust flow. This paper is very useful because of the excellent physical descriptions of energy transfer between rotor and fluid, velocity profile developments, various losses, and overall parametric performance. They present a "design" chart with radius, average fluid tangential velocity, rotor velocity, flow rate, disk spacing, kinematic viscosity, and efficiency as parameters. This chart, of course, can not be applied to the machine presently under study at the Georgia Institute of Technology. However, the overall effects of changing for example disk spacing are qualitatively similar. It is also interesting to note that a parabolic profile was assumed in Reference 7 for the tangential velocity between the disks. It has been found in the present studies

that, for the peripheral flow compressor, tangential velocity profiles do become fully developed and approximately parabolic a short distance from the inlet at high flow rates. When flow rates are low, near shut-off, a region of backflow exists near the mid-point between the disks and of course the velocity profile is quite different from a parabola.

NOMENCLATURE

A_t	nozzle throat or total slot inlet area, (L^2)
g	gravitational constant, $\left(\frac{M - L}{F - T^2}\right)$
h	height of a slot, (L)
i,j,k	peripheral, radial and axial directions, respectively
k	ratio of specific heats
L,M,N	number of increments on flow field in peripheral, radial and axial direction, respectively
$\dot{m}$	mass flow rate into slots $\left(\frac{M}{T}\right)$
M_{No}	nozzle throat or slot inlet Mach number
N_{Re}	$\bar{\rho}_i \Omega w^2/\bar{\mu}_i$ = mechanical Reynolds number
$\bar{p}$	pressure, (F/L^2)
p	$\bar{p}/(\bar{\rho}\Omega^2 R^2)$ = dimensionless pressure
$\bar{p}_o$	nozzle inlet stagnation pressure, $\left(\frac{F}{L^2}\right)$
$\bar{p}_i$	slot inlet pressure $\left(\frac{F}{L^2}\right)$
Q	volume flow rate into slots, $\left(\frac{L^3}{T}\right)$
r	$\bar{r}/R$ = dimensionless radial length coordinate
R	radius of wheel from center to the base of a slot (L)
R_c	universal gas constant, $\left(\frac{L - F}{t - m}\right)$
$\bar{r},\bar{z}$	radial and axial space coordinates, respectively, (L)
v_θ	$\bar{v}_\theta/\Omega R$ = dimensionless peripheral velocity component
v_r	$\bar{v}_r/\Omega h$ = dimensionless radial velocity component
v_z	$\bar{v}_z/\Omega w$ = dimensionless axial velocity component
$\bar{v}_r,\bar{v}_\theta,\bar{v}_z$	radial, peripheral and axial velocity components, respectively, (L/T)
T_o	nozzle inlet stagnation temperature, (t)
w	width of a slot, (L)

z	$\bar{z}/w$ = dimensionless axial length coordinate
Δr	h/M = dimensionless radial space increment
$\Delta\theta$	θ/L = dimensionless peripheral space increment
Δz	z/N = dimensionless axial space increments
$\Delta v_\theta, \Delta v_r, \Delta v_z$	dimensionless incremental changes of peripheral, radial and axial velocity components between adjacent peripheral planes
Δp	dimensionless incremental change of pressure across adjacent peripheral planes
$\bar{\mu}$	viscosity of fluid, $\left(\frac{M - T}{L^2}\right)$
$\bar{\mu}_i$	slot inlet viscosity, $\left(\frac{M - T}{L^2}\right)$
μ	$\bar{\mu}/\bar{\mu}_i$ = dimensionless viscosity
Ω	angular velocity of wheel, $\left(\frac{1}{T}\right)$
ρ	$\bar{\rho}/\bar{\rho}_i$ = dimensionless density
$\bar{\rho}$	density of fluid, $\left(\frac{M}{L^3}\right)$
$\bar{\rho}_o$	nozzle inlet stagnation density, $\left(\frac{M}{L^3}\right)$
$\bar{\rho}_i$	slot inlet density, $\left(\frac{M}{L^3}\right)$
$\bar{\theta}$	peripheral space coordinate (radians)
θ	$\bar{\theta}/\Theta$ = dimensionless peripheral coordinate
Θ	angle between nozzle exit and diffuser inlet with respect to center of wheel, (radians)

THEORY

A mathematical model is developed which, after simplification, allows direct numerical calculations. Rather general governing equations along with boundary conditions are reduced, by order of magnitude analysis, to a much more compact form. These are then written in numerical form and the resulting linear algebriac equations are solved using a Gaussian elimination scheme. The developments summarized herein are presented in detail by Yalcin (8).

Governing Equations

Assuming that the flow is laminar, incompressible, steady, and essentially isothermal the three differential scalar momentum equations may be written for cylindrical coordinates:

r-momentum equation,

$$\bar{\rho}\left(\bar{v}_r \frac{\partial \bar{v}_r}{\partial \bar{r}} + \frac{\bar{v}_\theta}{\bar{r}} \frac{\partial \bar{v}_r}{\partial \bar{\theta}} - \frac{\bar{v}_\theta^2}{\bar{r}} + \bar{v}_z \frac{\partial \bar{v}_r}{\partial \bar{z}}\right) = -\frac{\partial \bar{p}}{\partial \bar{r}} + \bar{\mu}\left[\frac{\partial}{\partial \bar{r}}\left(\frac{1}{\bar{r}} \frac{\partial}{\partial \bar{r}} (\bar{r}\bar{v}_r)\right)\right.$$

$$\left. + \frac{1}{\bar{r}^2} \frac{\partial^2 \bar{v}_r}{\partial \bar{\theta}^2} - \frac{2}{\bar{r}^2} \frac{\partial \bar{v}_\theta}{\partial \bar{\theta}} + \frac{\partial^2 \bar{v}_r}{\partial \bar{z}^2}\right] \quad ;$$

θ-momentum equation,

$$\bar{\rho}\left(\bar{v}_r \frac{\partial \bar{v}_\theta}{\partial \bar{r}} + \frac{\bar{v}_\theta}{\bar{r}} \frac{\partial \bar{v}_\theta}{\partial \bar{\theta}} + \frac{\bar{v}_r \bar{v}_\theta}{\bar{r}} + \bar{v}_z \frac{\partial \bar{v}_\theta}{\partial \bar{z}}\right) = -\frac{1}{\bar{r}} \frac{\partial \bar{p}}{\partial \bar{\theta}} + \bar{\mu}\left[\frac{\partial}{\partial \bar{r}}\left(\frac{1}{\bar{r}} \frac{\partial}{\partial \bar{r}} (\bar{r}\bar{v}_\theta)\right)\right.$$

$$\left. + \frac{1}{\bar{r}^2} \frac{\partial^2 \bar{v}_\theta}{\partial \bar{\theta}^2} + \frac{2}{\bar{r}^2} \frac{\partial \bar{v}_r}{\partial \bar{\theta}} + \frac{\partial^2 \bar{v}_\theta}{\partial \bar{z}^2}\right] \quad ;$$

z-momentum equation,

$$\bar{\rho}\left(\bar{v}_r \frac{\partial \bar{v}_z}{\partial \bar{r}} + \frac{\bar{v}_\theta}{\bar{r}} \frac{\partial \bar{v}_z}{\partial \bar{\theta}} + \bar{v}_z \frac{\partial \bar{v}_z}{\partial \bar{z}}\right) = - \frac{\partial \bar{p}}{\partial \bar{z}} + \bar{\mu}\left[\frac{1}{\bar{r}} \frac{\partial}{\partial \bar{r}}\left(\bar{r} \frac{\partial \bar{v}_z}{\partial \bar{r}}\right) + \frac{1}{\bar{r}^2} \frac{\partial^2 \bar{v}_z}{\partial \bar{\theta}^2} + \frac{\partial^2 \bar{v}_z}{\partial \bar{z}^2}\right] .$$

The steady incompressible continuity equation is

$$\frac{1}{\bar{r}}\left[\frac{\partial}{\partial \bar{r}}\left(\bar{r}\bar{v}_r\right)\right] + \frac{1}{\bar{r}}\left(\frac{\partial \bar{v}_\theta}{\partial \bar{\theta}}\right) + \frac{\partial \bar{v}_z}{\partial \bar{z}} = 0 .$$

The coordinate system is illustrated in Figure 2 which shows the flow through one slot of the compressor. A cross-section of a slot is shown in Figure 3. Surface A is stationary and represents the casing while surfaces B and C are located on the rotor and are moving. Appropriate boundary conditions for the flow field under study are:

$\bar{v}_\theta = \Omega\bar{r}$ on planes B and C

$\bar{v}_\theta = 0$ on plane A

$\bar{v}_z = 0$ on planes A, B, C and centerline

$\bar{v}_r = 0$ on planes A, B, C

$\left.\frac{\partial \bar{v}_\theta}{\partial \bar{z}}\right|_k = 0$ due to symmetry

$\left.\frac{\partial \bar{v}_r}{\partial \bar{z}}\right|_k = 0$ due to symmetry

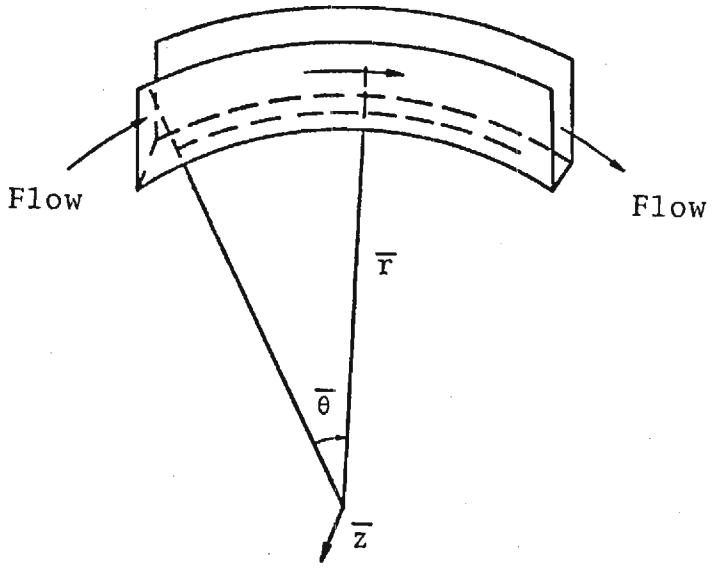

Figure 2. Coordinate System

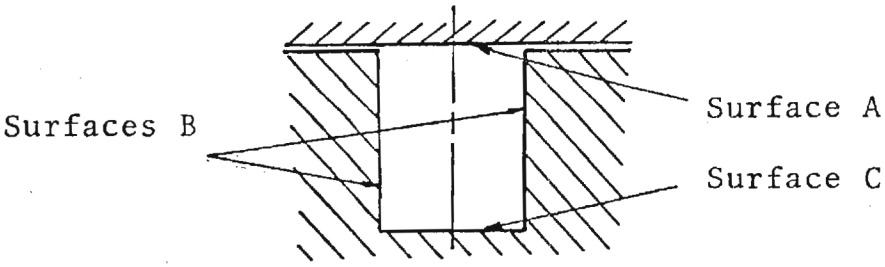

Figure 3. Slot Nomenclature

$$\frac{\partial \bar{v}_z}{\partial \bar{z}} = 0 \qquad \text{on planes B}$$

$$\bar{v}_\theta = v_{in},\ \bar{v}_z = 0,\ \bar{v}_r = 0 \quad \text{at inlet}$$

Equations in Dimensionless Form

The variables involved are non-dimensionalized by characteristic quantities such that the resulting quotients are of order one. To facilitate the order of magnitude analysis, the depth of slot to wheel radius ratio, h/R, and width of slot to wheel radius, w/R, are assumed to be much less than one.

$$r = \frac{\bar{r}}{R}\ ;\ \theta = \frac{\bar{\theta}}{\Theta}\ ;\ z = \frac{\bar{z}}{w}\ ;\ v_r = \frac{\bar{v}_r}{\Omega h}\ ;\ v_\theta = \frac{\bar{v}_\theta}{\Omega R}\ ;\ v_z = \frac{\bar{v}_z}{\Omega w}\ ;$$

$$\rho = \frac{\bar{\rho}}{\bar{\rho}_i}\ ;\ \mu = \frac{\bar{\mu}}{\bar{\mu}_i}\ ;\ p = \frac{\bar{p}}{\bar{\rho}_i \Omega^2 R^2}\ ;\ N_{Re} = \frac{\bar{\rho}_i \Omega w^2}{\bar{\mu}}$$

Using the above dimensionless variables in place of the dimensional ones yield the following set of equations:

Continuity equation,

$$\frac{\Omega h R}{R}\frac{\partial}{\partial r}(r\, v_r) + \frac{\Omega R}{\Theta}\frac{\partial v_\theta}{\partial \theta} + \frac{R\Omega w}{w}\, r\, \frac{\partial v_z}{\partial z} = 0$$

r-momentum equation,

$$\bar{\rho}_i \rho \left(\frac{\Omega^2 h^2}{R} v_r \frac{\partial v_r}{\partial r} + \frac{\Omega^2 h R}{R\Theta}\frac{v_\theta}{r}\frac{\partial v_r}{\partial \theta} - \frac{\Omega^2 R^2}{R}\frac{v_\theta^2}{r} + \frac{\Omega^2 w h}{w}\bar{v}_z \frac{\partial \bar{v}_r}{\partial z} \right) =$$

$$- \frac{\bar{\rho}_i \Omega^2 R^2}{R}\frac{\partial p}{\partial r} + \bar{\mu}_i \mu \left[\frac{R\Omega h}{R^3}\frac{\partial}{\partial r}\left(\frac{1}{r}\frac{\partial}{\partial r}(r\, v_r) \right) + \frac{\Omega h}{\Theta^2 R^2}\frac{1}{r^2}\frac{\partial^2 v_r}{\partial \theta^2} \right.$$

$$\left. - \frac{\Omega R}{\Theta R^2}\frac{2}{r^2}\frac{\partial v_\theta}{\partial \theta} + \frac{\Omega h}{w^2}\frac{\partial^2 v_r}{\partial z^2} \right]$$

θ-momentum equation,

$$\bar{\rho}_i\rho\left(\frac{\Omega^2 hR}{R}\,v_r\,\frac{\partial v_\theta}{\partial r}+\frac{\Omega^2R^2}{\Theta R}\,\frac{v_\theta}{r}\,\frac{\partial v_\theta}{\partial\theta}+\frac{\Omega^2hR}{R}\,\frac{v_r v_\theta}{r}+\frac{\Omega^2wR}{w}\,v_z\,\frac{\partial v_\theta}{\partial z}\right)=$$

$$-\frac{\bar{\rho}_i\Omega^2R^2}{\Theta R}\,\frac{1}{r}\,\frac{\partial p}{\partial\theta}+\bar{\mu}_i\mu\left[\frac{\Omega R^2}{R^3}\,\frac{\partial}{\partial r}\left(\frac{1}{r}\,\frac{\partial}{\partial r}\,(rv_\theta)\right)+\frac{\Omega R}{\Theta^2R^2}\,\frac{1}{r^2}\,\frac{\partial^2 v_\theta}{\partial\theta^2}+\right.$$

$$\left.\frac{\Omega h}{\Theta R^2}\,\frac{2}{r^2}\,\frac{\partial v_r}{\partial\theta}+\frac{\Omega R}{w^2}\,\frac{\partial^2 v_\theta}{\partial z^2}\right]$$

z-momentum equation,

$$\bar{\rho}_i\rho\left(\frac{\Omega^2 hw}{R}\,v_r\,\frac{\partial v_z}{\partial r}+\frac{\Omega^2Rw}{R\Theta}\,\frac{v_\theta}{r}\,\frac{\partial v_z}{\partial\theta}+\frac{\Omega^2w^2}{w}\,v_z\,\frac{\partial v_z}{\partial z}\right)=$$

$$-\frac{\bar{\rho}_i\Omega^2R^2}{w}\,\frac{\partial p}{\partial z}+\bar{\mu}_i\mu\left[\frac{\Omega Rw}{R^3}\,\frac{1}{r}\,\frac{\partial}{\partial r}\left(r\,\frac{\partial v_z}{\partial r}\right)+\frac{\Omega w}{\Theta^2R^2}\,\frac{1}{r^2}\,\frac{\partial^2 v_z}{\partial\theta^2}+\frac{\Omega w}{w^2}\,\frac{\partial^2 v_z}{\partial z^2}\right]$$

An order of magnitude analysis was next made in order to eliminate terms which are negligible in the equations. The resulting equations are:

Continuity,

$$\frac{1}{\Theta}\,\frac{\partial v_\theta}{\partial\theta}+r\,\frac{\partial v_z}{\partial z}=0\quad;$$

r-momentum equation,

$$-\frac{v_\theta^2}{r}=-\frac{\partial p}{\partial r}+\left(\frac{h}{R}\right)\left(\frac{1}{N_{Re}}\right)\frac{\partial^2 v_r}{\partial z^2}\quad;$$

θ-momentum equation,

$$\frac{1}{\Theta}\,\frac{v_\theta}{r}\,\frac{\partial v_\theta}{\partial\theta}+v_z\,\frac{\partial v_\theta}{\partial z}=-\frac{1}{\Theta}\,\frac{\partial p}{r\partial\theta}+\left(\frac{1}{N_{Re}}\right)\left(\frac{\partial^2 v_\theta}{\partial z^2}\right)\quad;\ \text{and}$$

z-momentum equation,

$$\frac{\partial p}{\partial z}=0\,.$$

Boundary conditions are:

$v_\theta = 0$ on plane A,

$v_\theta = r$ on plane B,

$v_\theta = 1$ on plane C,

$v_z = 0$ on planes A, B, C and centerline,

$v_r = 0$ on planes A, B and C,

$\frac{\partial v_\theta}{\partial z} = 0$ on centerline

$\frac{\partial v_z}{\partial z} = 0$ on plane B, and

$\frac{\partial v_r}{\partial z} = 0$ on centerline.

Inlet conditions are specified as zero approach velocity at nozzle entrance and slug-type flow into the grooves. The nozzle throat area is set equal to the total cross-sectional slot area. When Mach number at the nozzle throat (inlet to the grooves), area and nozzle inlet stagnation conditions are specified, the mass flow rate, slot inlet static pressure, and density can be computed using the following equations which were written for one dimensional isentropic flow.

$$\dot{m} = A_t \sqrt{\frac{kg}{R_c}} \left(\frac{\bar{p}_o}{\sqrt{T_o}} \right) \frac{M_{No}}{\left(1 + \frac{(k-1)}{2} M_{No}^2 \right)^{\left(\frac{k+1}{2(k-1)} \right)}}$$

$$\bar{p}_i = \bar{p}_o \Big/ \left(1 + \frac{k-1}{2} M_{No}^2 \right)^{\frac{k}{k-1}}$$

$$\bar{\rho}_i = \bar{\rho}_o \Big/ \left(1 + \frac{k-1}{2} M_{No}^2\right)^{\frac{1}{k-1}}$$

$$Q = \dot{m}/\bar{\rho}_i$$

These same equations were used to describe flow in the diffuser at compressor exit. Figure 4 shows assumed and computed velocity profiles at various locations in the compressor. Only two slots are shown in the diagram whereas many slots would be used in a typical machine.

Equations in Numerical Form

There are various methods of solving the set of governing equations with related boundary conditions which have been described. Boyd and Rice (2) studied a somewhat similar problem and used a linearizing technique which they found to work well. Basically the same approach has been taken in the present solution.

The slot in which the fluid flows was divided into L-segments in the peripheral direction from nozzle to diffuser, M-radial stations from the base of the slot to the shroud, and N-sections from the center of a slot to the moving wall on either side of it. An illustration of the lattice is shown in Figure 5. Initially, defining equations are approximated by a finite difference scheme such that all variables assume their values at the next peripheral station. Tangential derivatives utilize backward difference schemes whereas all others are approximated by centered difference methods. In light of these measures the equations become

Equation of continuity,

$$\frac{v_\theta(i+1,j,k) - v_\theta(i,j,k)}{\Theta\Delta\theta} + r_j \frac{v_z(i+1,j,k+1) - v_z(i+1,j,k-1)}{2\Delta z} = 0 ;$$

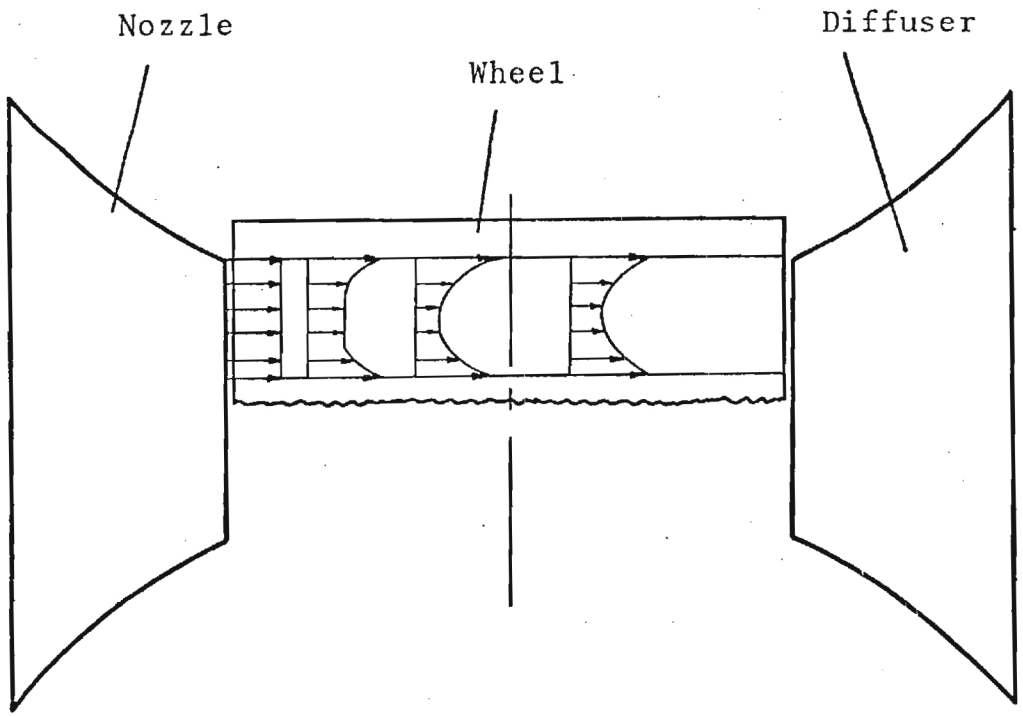

Figure 4. Meridional Velocity Development

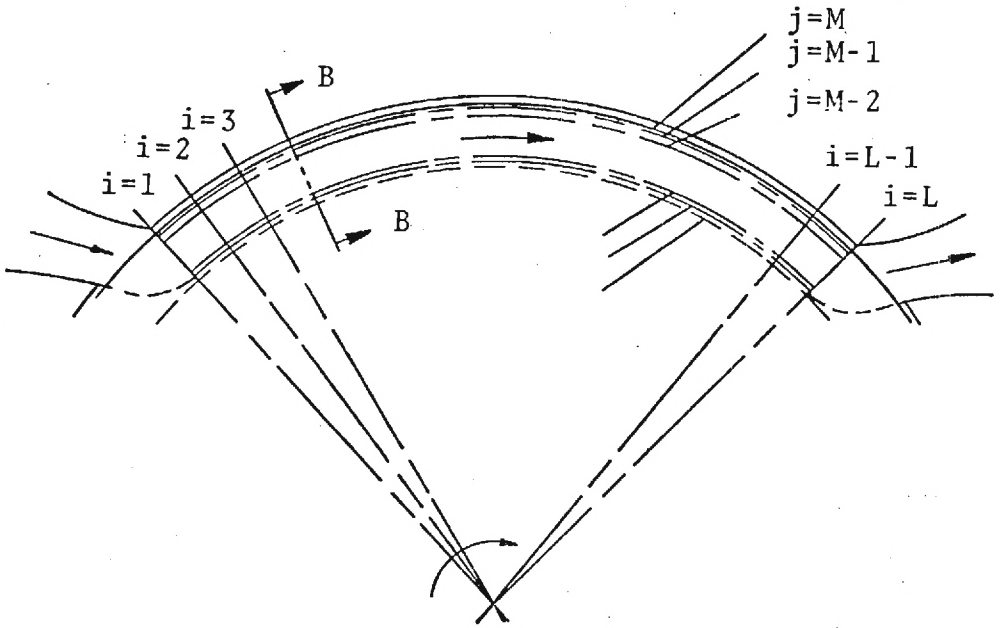

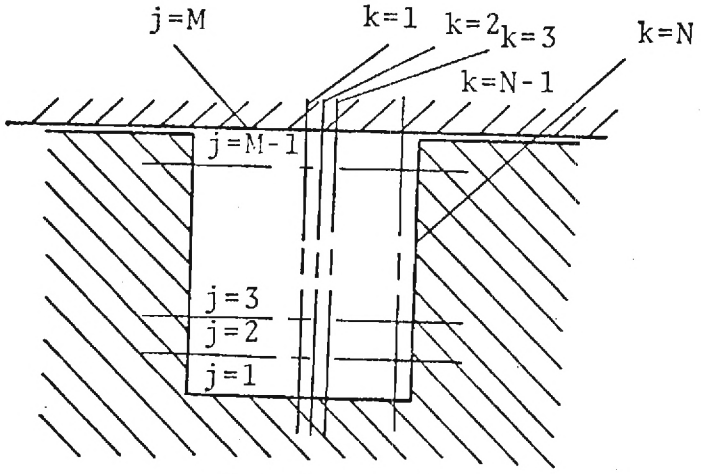

Section B-B

Figure 5. Grid Spacing

r-momentum equation,

$$-\frac{1}{r_j}\left[v_\theta(i+1,j,k)\right]^2 = -\frac{p(i+1,j+1) - p(i+1,j-1)}{2\Delta r} +$$

$$\left(\frac{h}{R}\right)\left(\frac{1}{N_{Re}}\right)\left(\frac{v_r(i+1,j,k+1) - 2v_r(i+1,j,k) + v_r(i+1,j,k-1)}{(\Delta z)^2}\right) \quad ; \text{ and}$$

θ-momentum equation,

$$\frac{v_\theta(i+1,j,k)}{r_j}\,\frac{v_\theta(i+1,j,k) - v_\theta(i,j,k)}{\Theta\Delta\theta} +$$

$$v_z(i+1,j,k)\,\frac{v_\theta(i+1,j,k+1) - v_\theta(i+1,j,k-1)}{2\Delta z} =$$

$$-\frac{p(i+1,j)-p(i,j)}{r_j\Theta\Delta\theta} + \frac{1}{N_{Re}}\left[\frac{v_\theta(i+1,j,k+1)-2v_\theta(i+1,j,k)+ v_\theta(i+1,j,k-1)}{(\Delta z)^2}\right]$$

Boundary conditions are:

$v_\theta(i+1,M,k) = 0$

$v_\theta(i+1,j,N) = r_j$

$v_z(i+1,j,1) = v_z(i+1,j,N) = v_z(i+1,1,k) = v_z(i+1,M,k) = 0$

$v_r(i+1,j,N) = v_r(i+1,1,k) = v_r(i+1,M,k) = 0$

$3v_\theta(i+1,j,1)-4v_\theta(i+1,j,2)+ v_\theta(i+1,j,3) = 0$

$3v_z(i+1,j,N)-4v_z(i+1,j,N-1)+ v_z(i+1,j,N-2) = 0$

$7v_r(i+1,j,1)-8v_r(i+1,j,2)+ v_r(i+1,j,3) = 0$

The z-momentum equation is incorporated into the above equations by setting pressure variables independent of axial gradients. The fact that the above equations are still non-linear means that they are very difficult to solve directly. To overcome this problem a new set of variables are introduced:

$$\Delta v(j,k) = v(i+1,j,k) - v(i,j,k)$$

$$\Delta v_z(j,k) = v_z(i+1,j,k) - v_z(i,j,k)$$

$$\Delta v_r(j,k) = v_r(i+1,j,k) - v_r(i,j,k)$$

$$\Delta p(j) = p(i+1,j) - p\ (i,j).$$

Substituting the variables into the equations and neglecting any term that contains products of the variables which are small, the following set of equations and boundary conditions are obtained:

Equation of continuity,

$$2\left(\frac{\Delta z}{\Theta r_j \Delta\theta}\right) \Delta v_\theta(j,k) - \Delta v_z(j,k-1) + \Delta v_z(j,k+1) = v_z(i,j,k-1) - v_z(i,j,k+1);$$

r-momentum equation,

$$-\left(\frac{2}{r_j}\right)\left(\frac{R\Delta z}{h}\right)\left[v_\theta(i,j,k)\right] \Delta v_\theta(j,k) - \left(\frac{1}{N_{Re}\Delta z}\right) \Delta v_r(j,k-1) + \left(\frac{2}{N_{Re}\Delta z}\right)$$

$$\Delta v_r(j,k) - \left(\frac{1}{N_{Re}\Delta z}\right) \Delta v_r(j,k+1) + g\left(\frac{1}{2\Delta r}\right)\left(\frac{R\Delta z}{h}\right) \Delta p(j+1) - g$$

$$\left(\frac{1}{2\Delta r}\right)\left(\frac{R\Delta z}{h}\right) \Delta p(j-1) = \left(\frac{1}{r_j}\right)\left(\frac{R\Delta z}{h}\right)\left[v_\theta(i,j,k)\right]^2 - g\left(\frac{1}{2\Delta r}\right)\left(\frac{R\Delta z}{h}\right)$$

$$\left[p(i,j+1) - p(i,j-1)\right] + \left(\frac{1}{N_{Re}\Delta z}\right)\left[v_r(i,j,k+1) - 2v_r(i,j,k) + v_r(i,j,k-1)\right];$$

and

θ-momentum equation,

$$\left[-\left(\frac{1}{N_{Re}\Delta z}\right) - 0.5\ v_z(i,j,k)\right] \Delta v_\theta(j,k-1) + \left[\left(\frac{\Delta z}{\Theta\Delta\theta r_j}\right) v_\theta(i,j,k) + 2\left(\frac{1}{N_{Re}\Delta z}\right)\right] \Delta v_\theta(j,k) + \left[0.5\ v_z(i,j,k) - \frac{1}{N_{Re}\Delta z}\right] \Delta v_\theta(j,k+1) +$$

$$\left(0.5\ [v_\theta(i,j,k+1) - v_\theta(i,j,k-1)]\right) \Delta v_z(j,k) + g\left[\frac{\Delta z}{\Theta r_j \Delta\theta}\right] \Delta p(j) =$$

$$\left(\frac{1}{N_{Re}\Delta z}\right)\left[v_\theta(i,j,k+1) - 2v_\theta(i,j,k) + v_\theta(i,j,k-1)\right] -$$

$$0.5\, v_z(i,j,k)\left[v_\theta(i,j,k+1) - v_\theta(i,j,k-1)\right] .$$

Boundary conditions are

$$\Delta v_\theta(j,N) = r_j - v_\theta(i,j,N)$$

$$\Delta v_\theta(M,k) = 0$$

$$\Delta v_z(j,1) = \Delta v_z(j,N) = \Delta v_z(M,k) = \Delta v_z(1,k) = 0$$

$$\Delta v_r(j,N) = \Delta v_r(M,k) = \Delta v_r\ (1,k) = 0$$

$$3\Delta v_\theta(j,1) - 4\Delta v_\theta(j,2) + \Delta v_\theta(j,3) = -3v_\theta(i,j,1) + 4v_\theta(i,j,2) - v_\theta(i,j,3)$$

$$\Delta v_z(j,N-2) - 4\Delta v_z(j,N-1) = - v_z(i,j,N-2) + 4v_z(i,j,N-1)$$

$$7\Delta v_r(j,1) - 8\Delta v_r(j,2) + \Delta v_r(j,3) = - 7v_r(i,j,1) + 8v_r(i,j,2) - v_r(i,j,3).$$

Equations of continuity and momentum are applied to the internal nodes on a peripheral plane and boundary conditions are defined at lattice points on the boundaries. Since shroud and base of the groove pressures are unknown, the radial gradient is expanded in a forward difference method in the radial direction depending upon whether the node is on an axial plane next to the base of the groove or on the last one before the shroud, respectively.

After this special treatment the number of unknowns on any particular peripheral plane is 3(M-2)(N-1). Owing to symmetry and known values of certain variables on the solid boundaries and centerline, the number of unknowns has been substantially decreased.

Solution Technique

Upon careful investigation of the equations and boundary conditions it is evident they constitute a set of linear algebraic equations that can

be fitted into the format below:

$$\{A\}[X] = [C]$$

where matrix A contains the coefficients of the variables involved, X is a vector composed of 3(M-2)(N-1) unknown Δ-variables and C is a constant vector that includes all elements that are on the right of the equality sign of the equations.

The reason that the elements in vectors A and C are known is that they are composed of quantities that are either geometric parameters, system characteristics, and/or variables calculated or known from previous computations or by boundary conditions.

Among the various methods of solution of a linear system of equations, Gaussian elimination is particularly suitable in the present case because matrix A is sparse; that is, the rows and the columns have considerable numbers of zero elements. The principle of solution is to reduce matrix A to a triangular system by a series of divisions and subtractions. The set of equations are originally in the form:

$$a_{11}x_1 + a_{12}x_2 + \ldots + a_{1,n-1}x_{n-1} + a_{1,n}x_n = c_1$$

$$a_{21}x_1 + a_{22}x_2 + \ldots + a_{2,n-1}x_{n-1} + a_{2,n}x_n = c_2$$

$$\vdots \qquad \vdots \qquad \vdots \qquad \vdots \qquad \vdots$$

$$a_{n}x_1 + a_{n,2}x_2 + \ldots + a_{n,n-1}x_{n-1} + a_{n,n}x_n = c_n$$

The first equation is initially divided by a_{11} (assuming that $a_{11} \neq 0$) and the result is used to eliminate x_1 from all succeeding equations. Next, the modified second equation is divided by the coef-

ficient of x_2 in that equation and the result is used to eliminate x_2 from the succeeding equations, and so forth. After this elimination process has been carried out n-times, the resultant set, which is equivalent to the original one except for the effect of any round-offs committed, is of the form

$$x_1 + a'_{1,2}x_2 + \ldots + a'_{1,n}x_n = c'_1$$

$$x_2 + \ldots + a'_{2,n}x_n = c'_2$$

$$x_{n-1} + a'_{n-1,n}x_n = c'_{n-1}$$

$$x_n = c'_n$$

where $a'_{i,j}$, c'_i designate specific numerical values. The solution is completed by working backwards from the last equation, to obtain successively x_n, x_{n-1}, $\ldots$, x_1.

Solving the linear system of equations with the method cited above yields the unknown Δ-variables. Δ-variables, by definition, are differences in magnitude of velocity components or pressure between consecutive peripheral planes such that the value on the first plane is always known by inlet conditions or previous similar calculations. Thus, Δ-variables yield, indirectly, velocity components and pressures on each node of a peripheral plane.

For the next set of calculations a similar matrix is set up and the coefficients and constant matrix elements are calculated with inclusion of new velocity components and pressures. This logic is followed until the exit stage is reached. The computer logic behind the method of solution is presented in Figure 6.

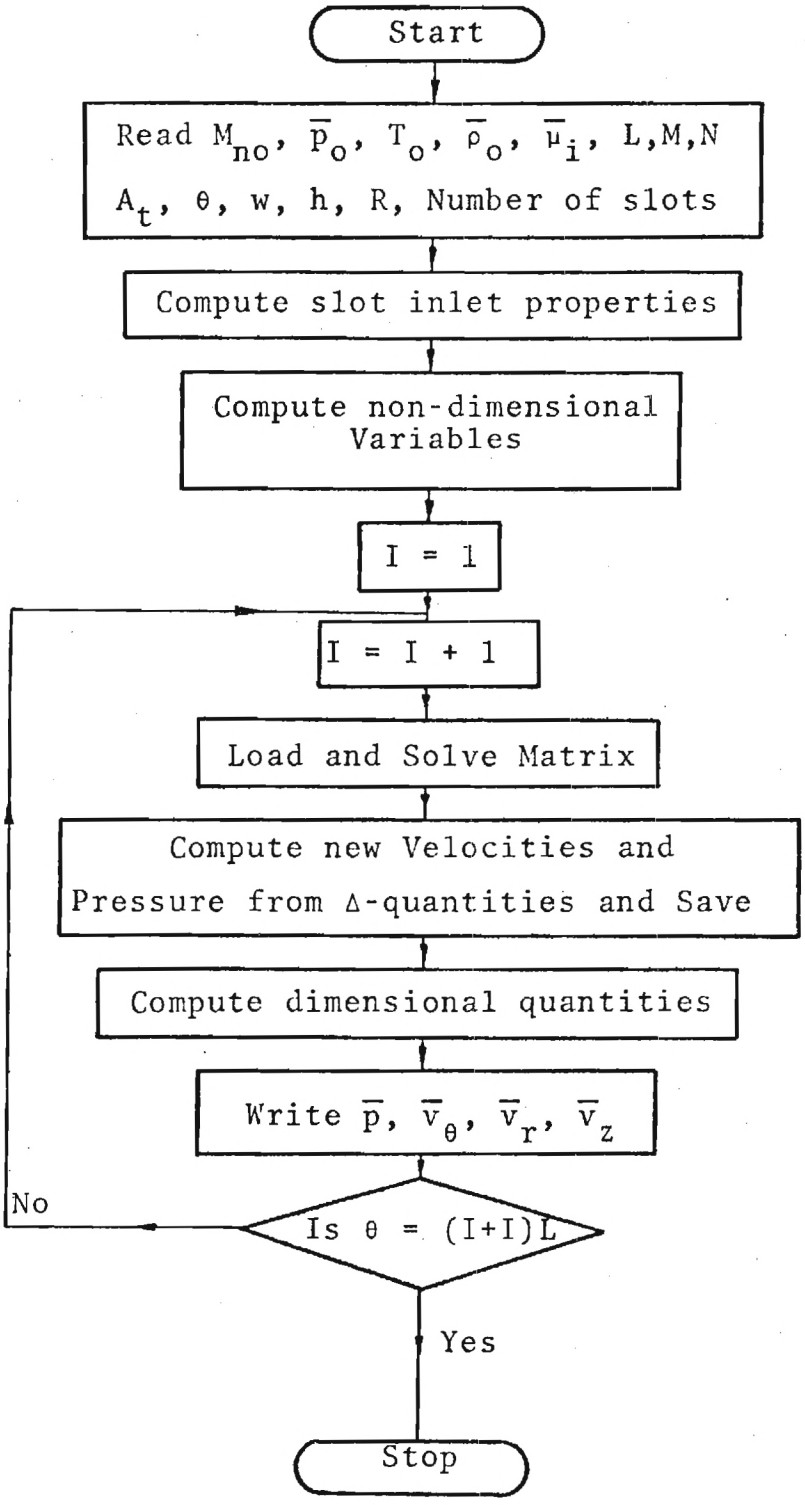

Figure 6. Computation Scheme

The axial and radial variations of the peripheral velocity are averaged by using Simpson's one-third rule for double integration to get the mean exit velocity. Subsequent checks of the accuracy of the computations are made by calculating the mass flow rate which should, ideally, be conserved. If the increments in the radial direction are chosen to be equal, the average exit pressure can be computed by a simple arithmetic mean.

RESULTS

The computational techniques discussed above were used to study a number of flow fields which might develop in a low speed circumferential flow viscous machine. In all cases the flow was restricted to the laminar regime by limiting Reynolds number based on average through-flow velocity and hydraulic radius to values less than 2000.

Table I shows parameters chosen for eight different cases which were typical of those studied in the project. It should be noted that the Reynolds numbers shown are machine Reynolds numbers based on rotational speed and slot width.

Figure 7 through 10 show how circumferential velocity profiles develop from inlet to exit for cases I through IV described in Table I. The profiles are symmetrical in the z direction and thus are shown only from the wall to the center of the passage ($z = w/2$). Also it should be noted that each plot is for a single value of r. A study of the four figures shows that velocity profiles become fully developed rather quickly as the fluid moves from the inlet towards the exit. It is also significant to note that velocities near the center of the passage are negative for fully developed flow when the inlet velocity is low (see Case III).

Figure 11 shows how v_θ changes with r for $z = 0.5$ at various θ locations. In this particular case, inlet velocities are low and thus when the flow becomes fully developed (where $\theta = 0.132$), v_θ values are negative at the midpoint of the passage. All velocities approach zero on the outer wall and approach the wheel surface velocity at the inner wall.

TABLE I. PARAMETERS

$\theta = 150°$, $\bar{\rho}_{in} = 1.201 \frac{kg}{m^3}$, $\bar{p}_{in} = 1$ atm

$w = 0.0197$ cm, $h = 0.197$ cm

Case	R(cm)	Ω $\frac{Rev}{Min}$	N_{Re}	V_{in} $\frac{M}{Sec}$
I	1.38	1,500	17.04	7.57
II	1.97	1,000	11.36	7.57
III	1.97	1,000	11.36	3.10
IV	1.38	1,500	17.04	4.47
V	1.97	2,000	22.72	17.86
VI	1.97	2,000	22.72	19.96

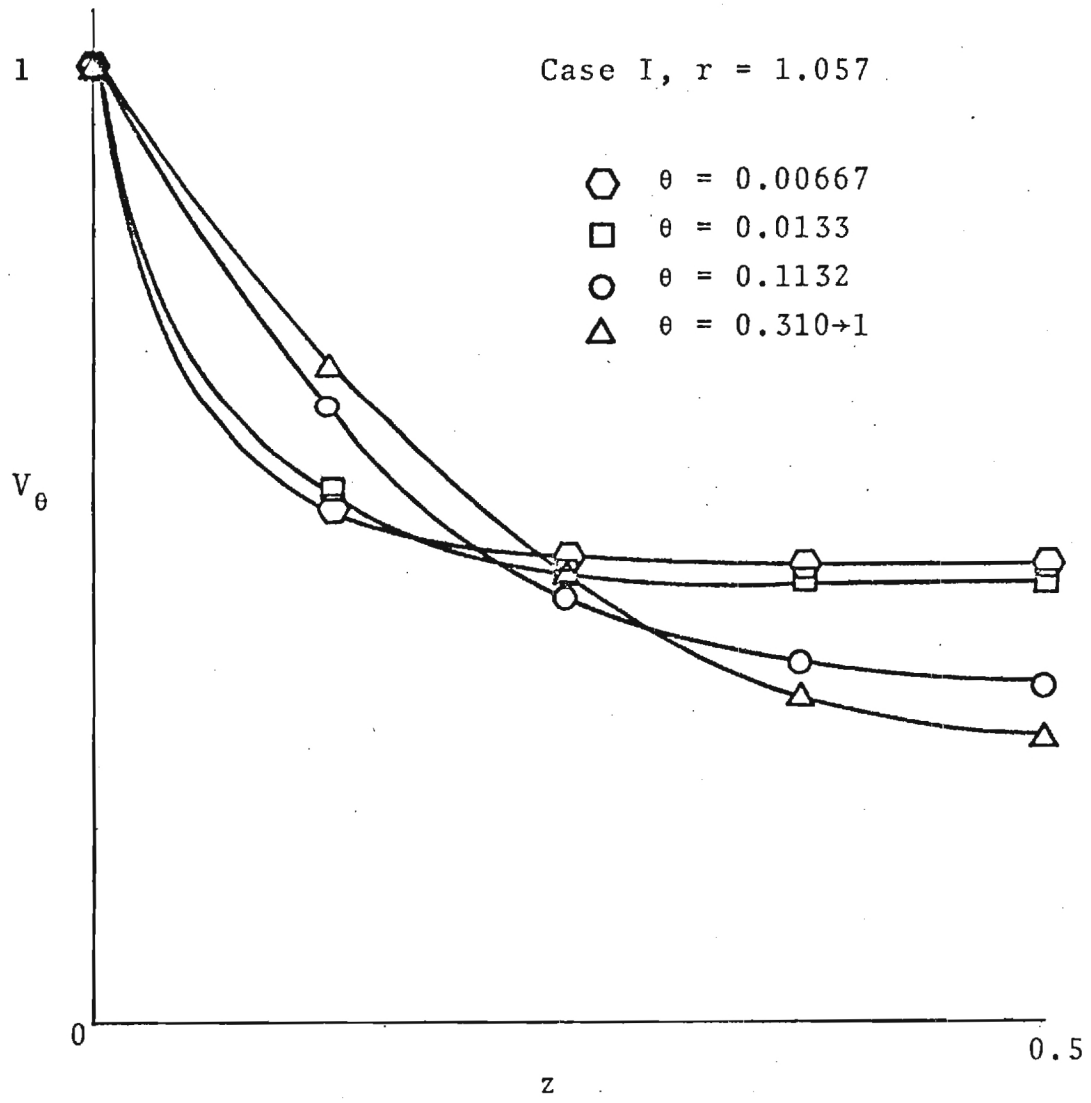

Figure 7. Tangential Velocity Development

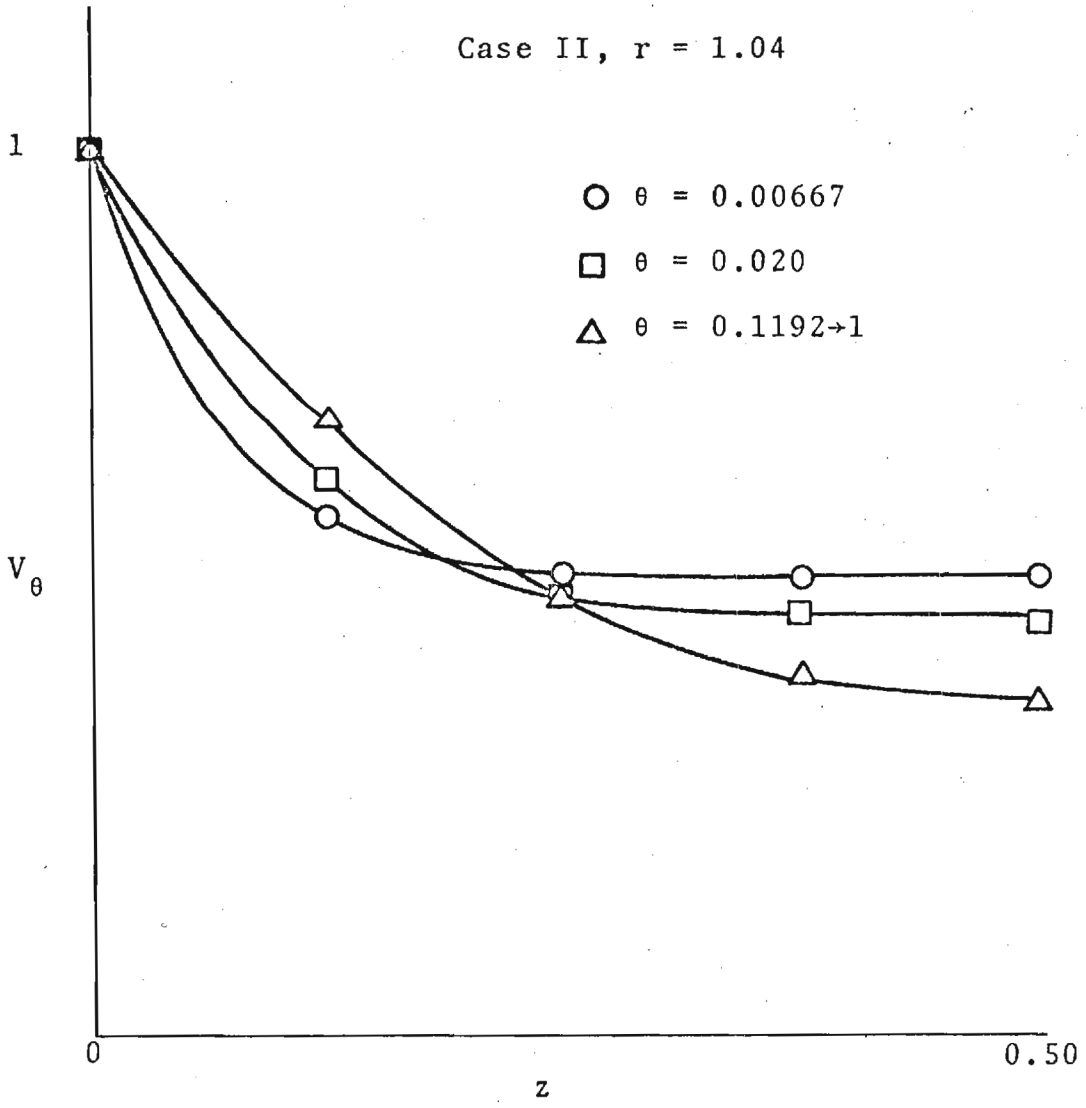

Figure 8. Tangential Velocity Development

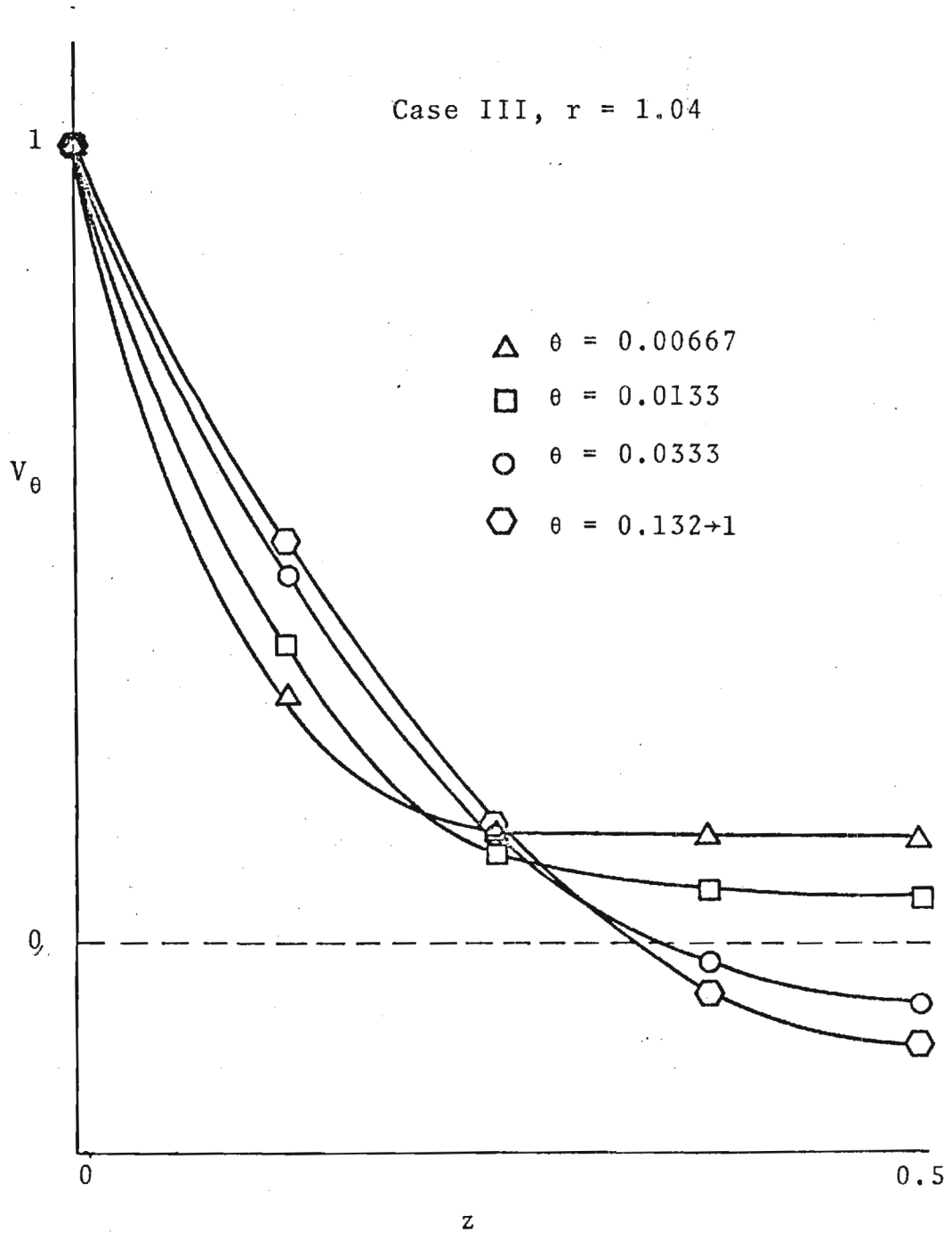

Figure 9. Tangential Velocity Development

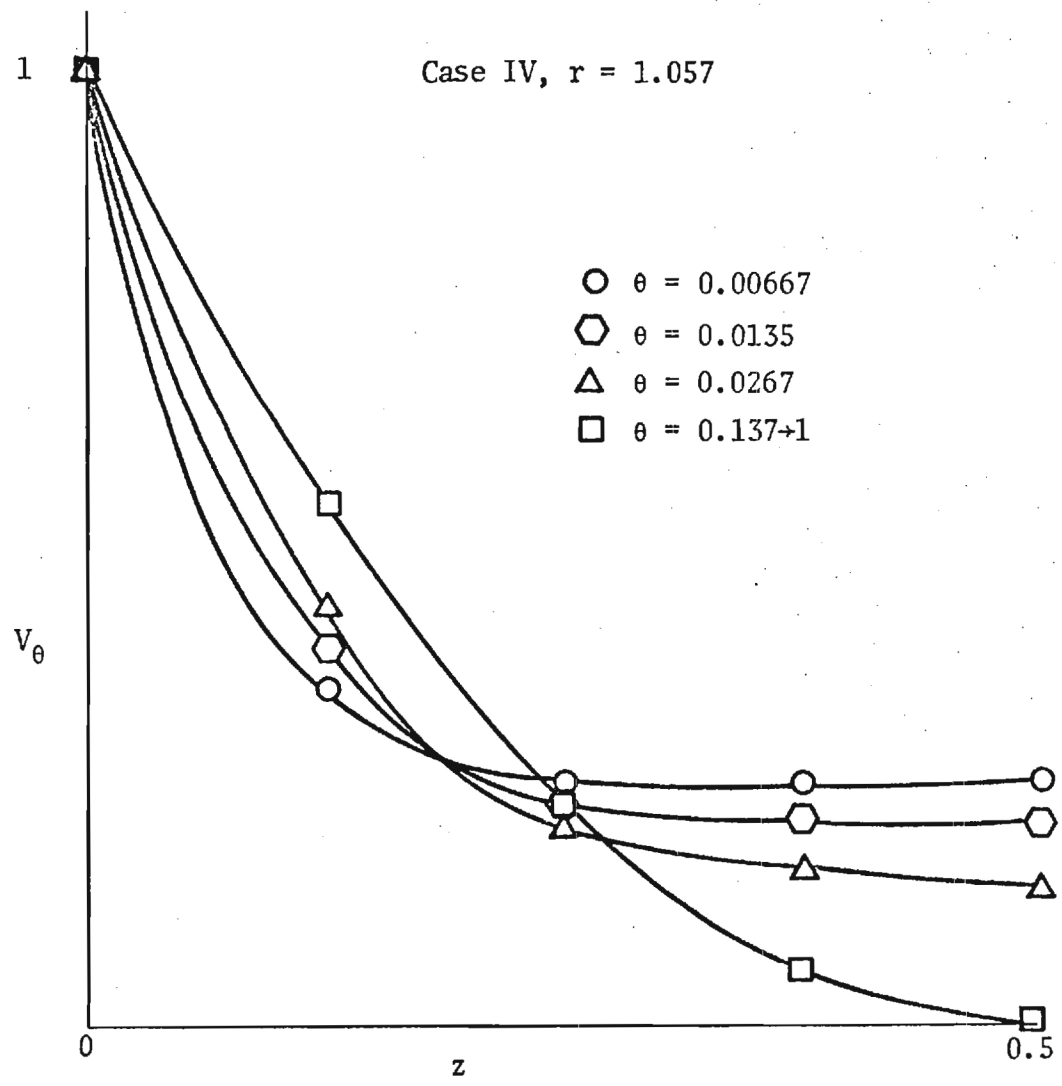

Figure 10. Tangential Velocity Development

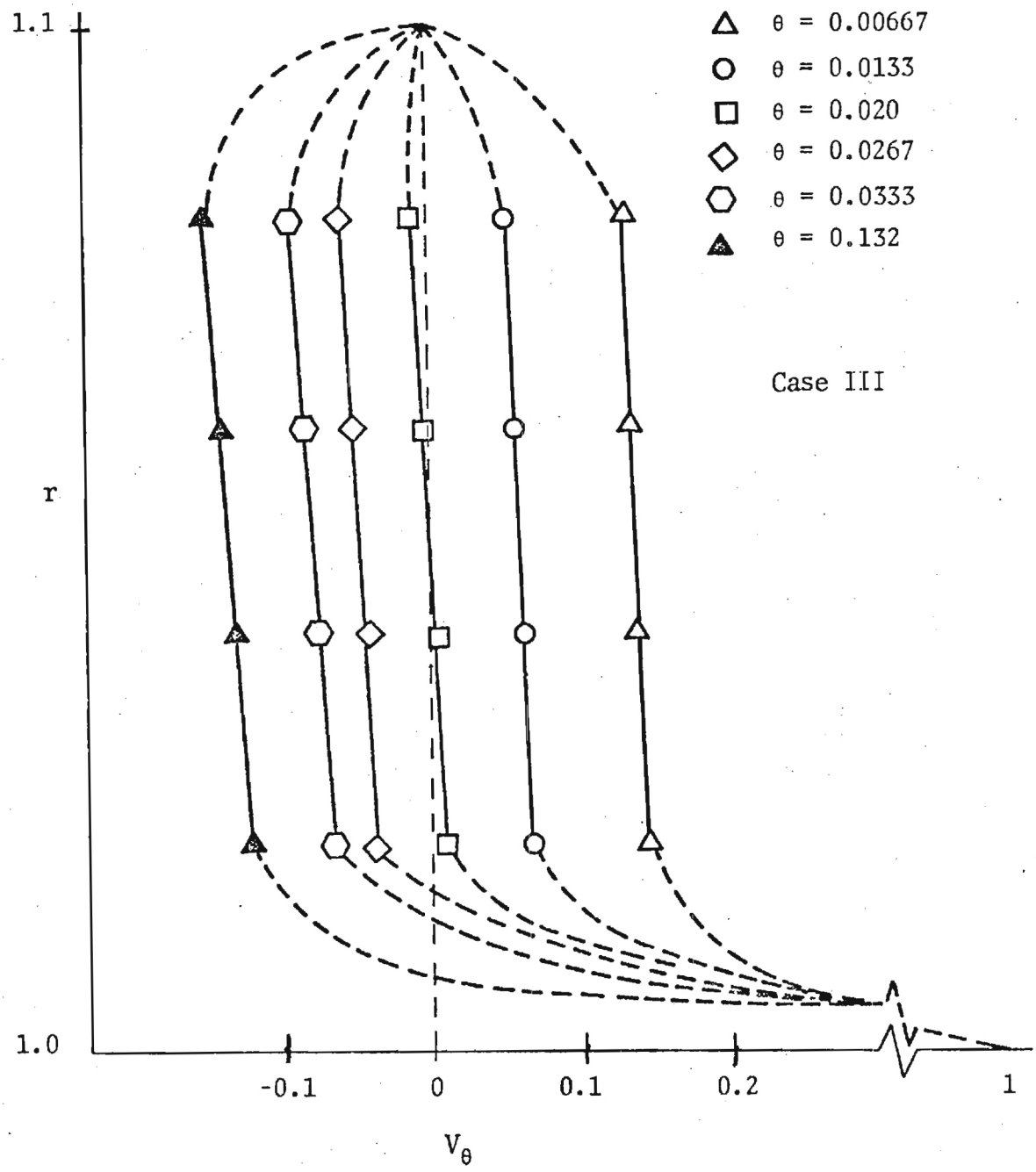

Figure 11. Centerline Tangential Velocities

Figure 12 shows variation of v_z with z at various angular locations for a fixed value of r. The profiles are symmetrical with respect to z so that profiles are shown only between the wall and the midpoint of a passage. The magnitude of axial velocity components are largest at passage inlet and approach zero as the flow becomes fully developed. Figure 13 shows how the radial velocity component varies with z at different θ locations for a fixed value of r. These velocities are relatively large near passage inlet and become much smaller downstream. The profiles are symmetrical about the midpoint of the passage in the axial direction.

Figure 14 shows typical pressure rise along the periphery of the wheel for Cases V and VI in Table I. The geometries and rotational speeds in Cases V and VI are the same - only the inlet velocity is changed. Case V has a smaller inlet velocity than VI and hence the pressure increases more rapidly around the periphery of the wheel. It is clear that after the flow becomes fully developed the pressure rise is linear with increasing angle as measured from the inlet.

Figure 15 shows radial pressure gradients in the r direction at the passage exit plane for Cases V and VI. These gradients are linear with increasing r and in all cases studied they are relatively small. Figure 16 shows head rise versus flow rate as computed using the method presented in this paper and using fully developed couette and poiseuille models. The couette flow model considers a fully developed flow field between two infinite parallel planes which are moving at a velocity equal to the surface speed of the rotor. The poiseuille model considers fully developed flow in a straight tube with boundaries moving at rotor surface speed. A hydraulic radius for the retangular slot is used in

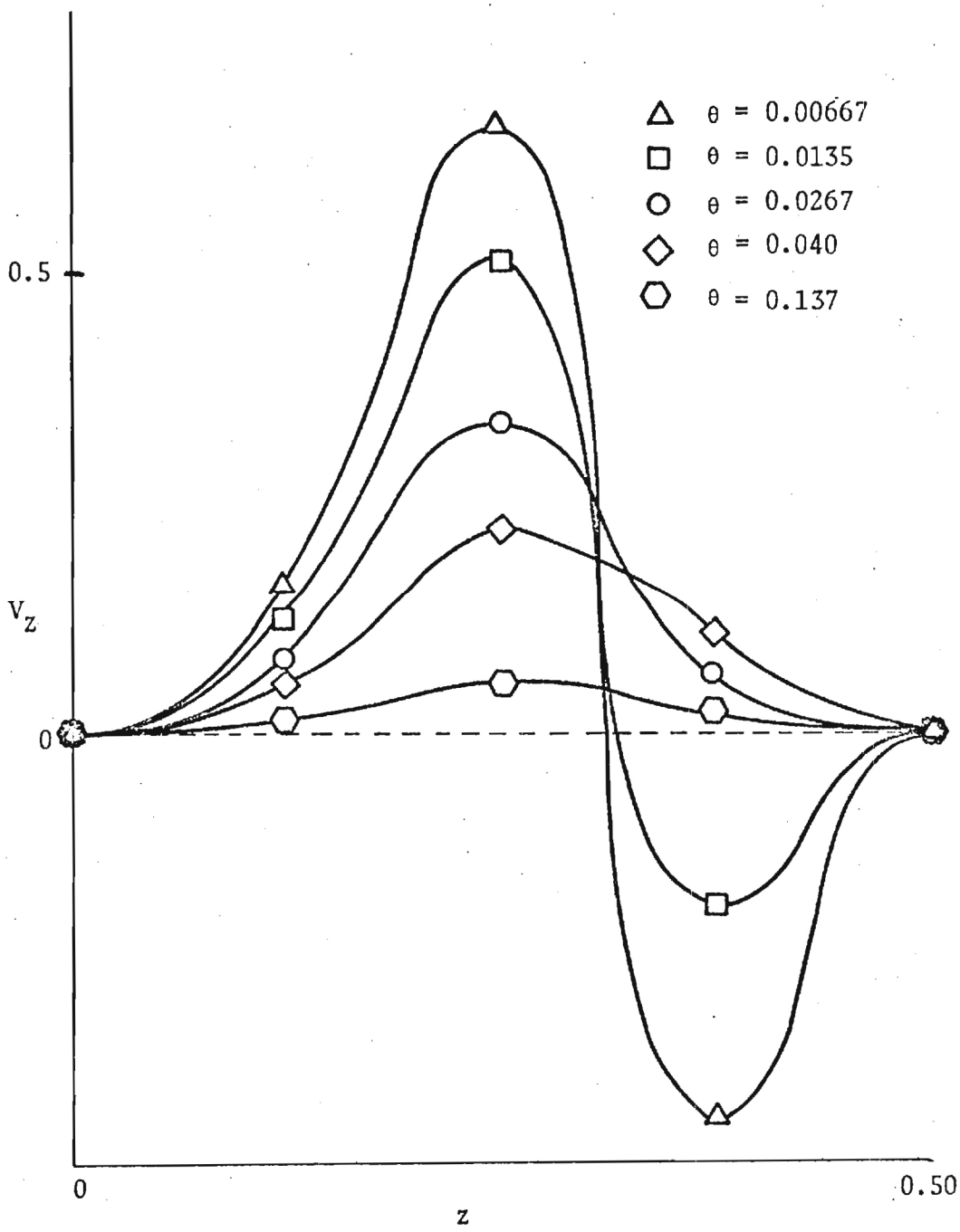

Figure 12. Axial Velocity Development

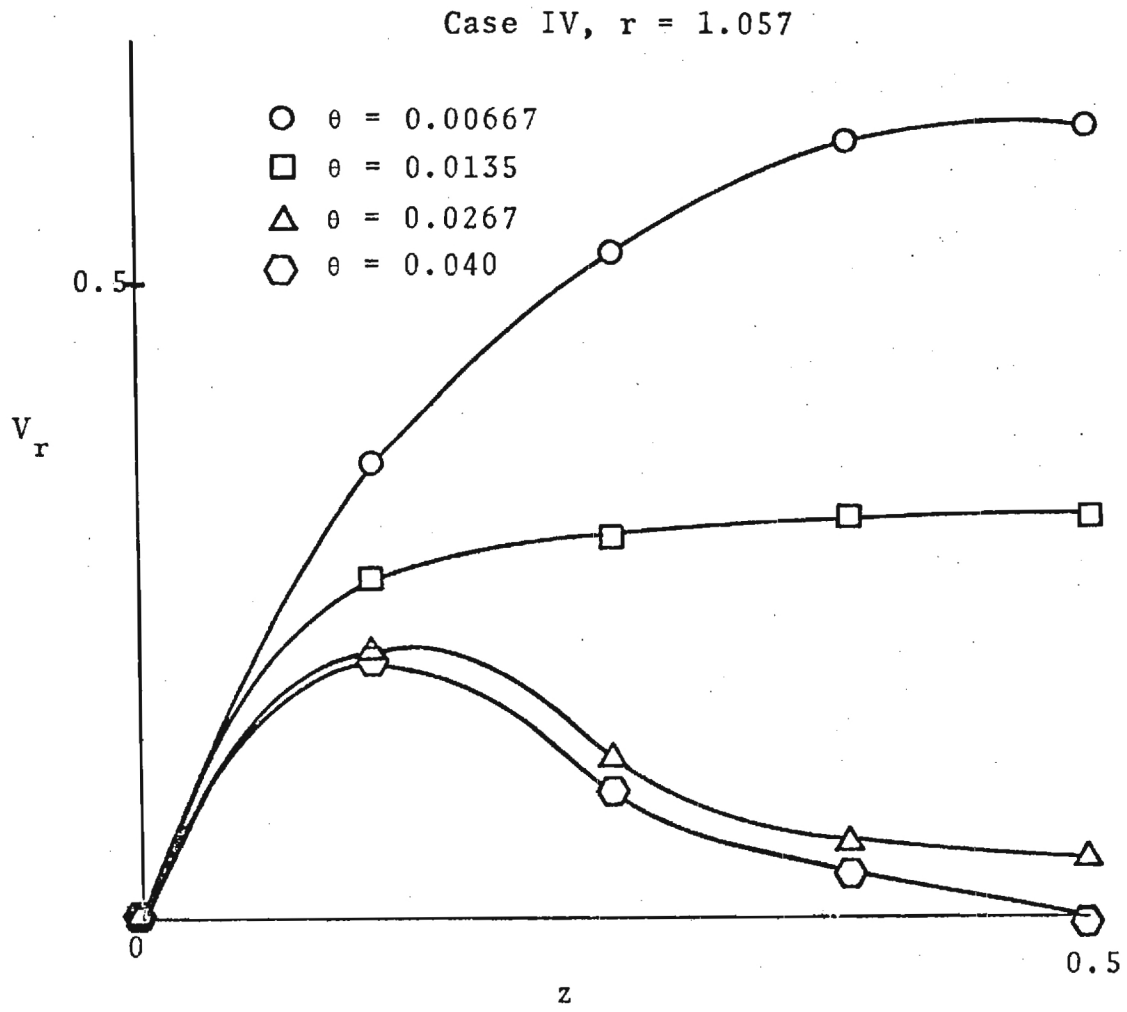

Figure 13. Radial Velocity Development

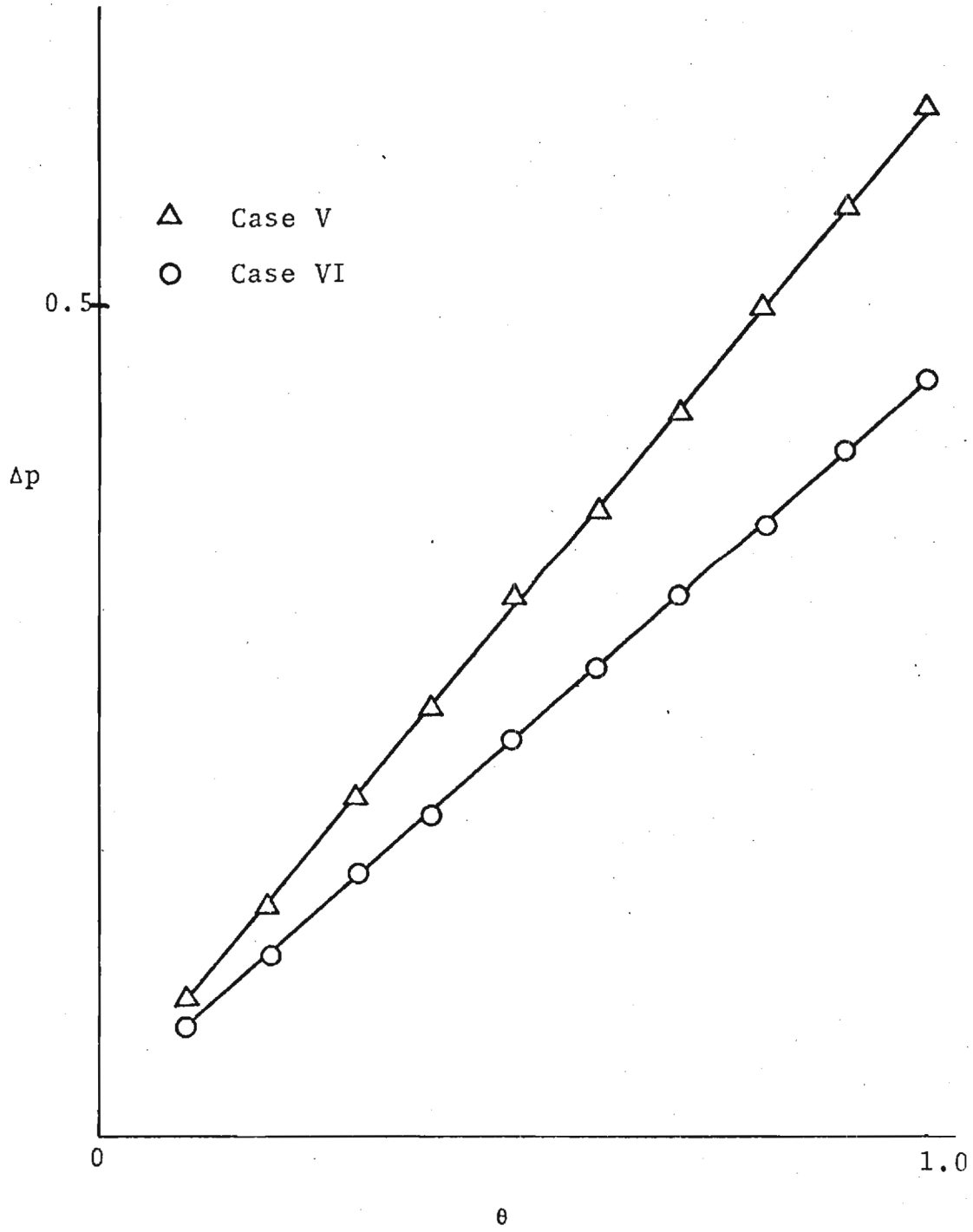

Figure 14. Head Rise Along The Periphery

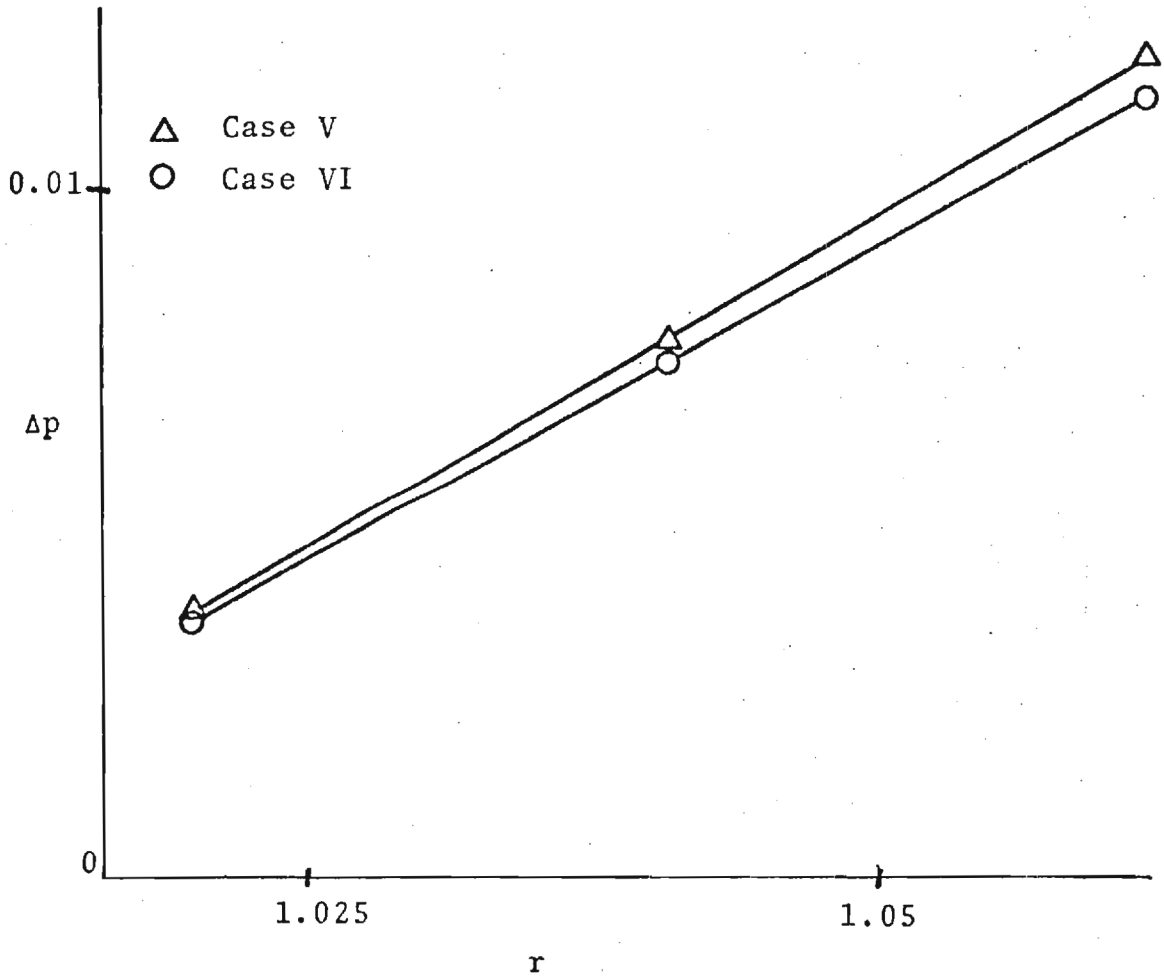

Figure 15. Radial Pressures At Exit Plane

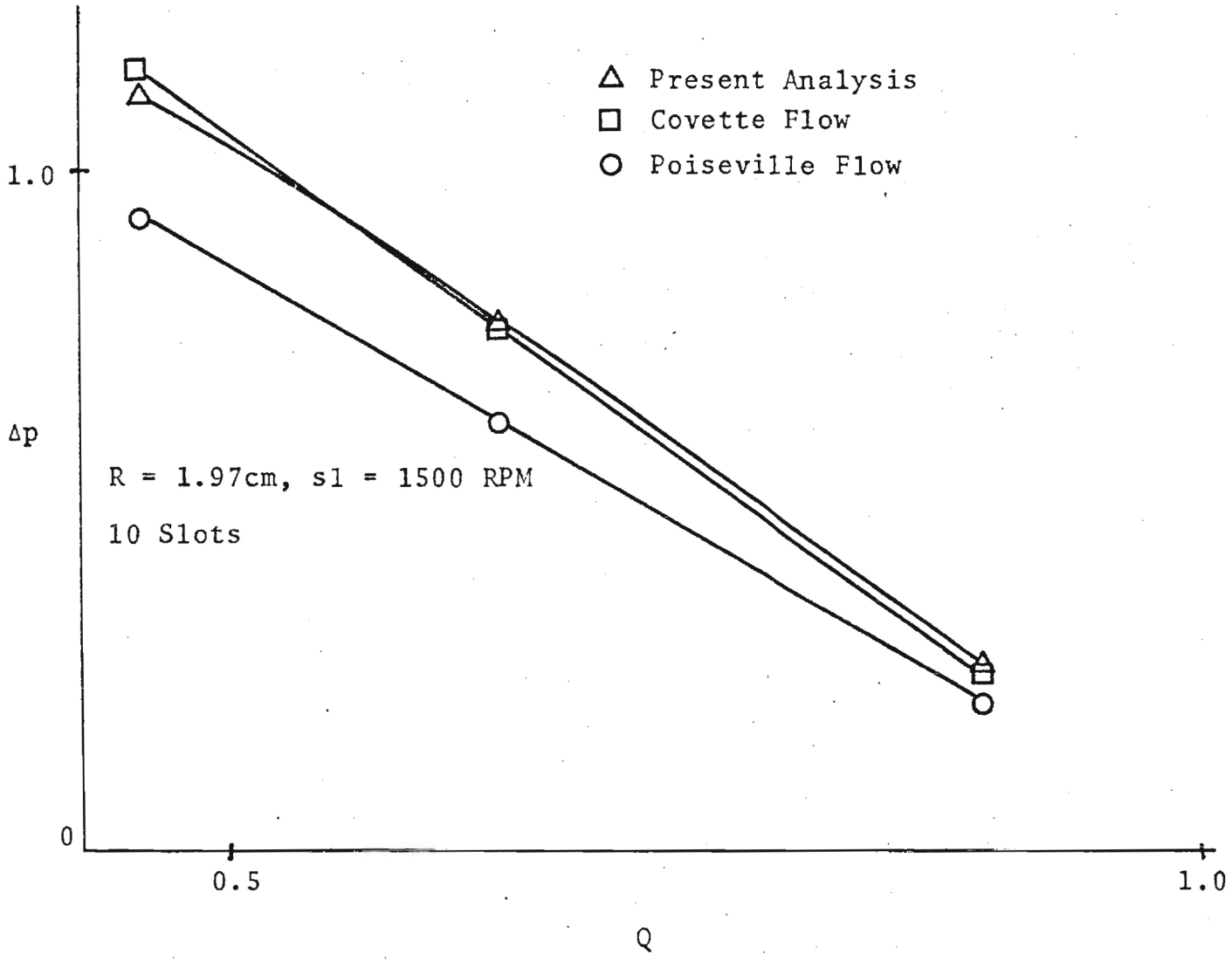

Figure 16. Head Flow Comparisons

the poiseuille equations. As expected the couette model closely approximates overall head versus flow characteristics. It is however of no value in studying the three dimensional flow patterns near the passage inlet. The poiseuille model only approximately predicts overall performance.

REFERENCES

1. Colwell, G. T. and T. W. Jackson, "Turbine-Compressor", U.S. Patent 3,751,908, August 14, 1973.

2. Boyd, K. E. and W. Rice, "Laminar Inward Flow of an Incompressible Fluid Between Rotating Disks, With Full Peripheral Admission", Journal of Applied Mechanics, Vol. 35, Vol. 90, No. 2, June 1968.

3. Lawn, M. J. and W. Rice, "Calculated Design Data for the Multiple-Disk Turbine Using Incompressible Fluid", ASME 74-FE-9, 1974.

4. Rastogi, A. K. and J. H. Whitelaw, "Proceedure for Predicting the Influence of Longitudinal Curvature on Boundary-Layer Flows", ASME 71-WA/FE-37, 1971.

5. Coney, J. E. R. and M. A. I. El-Shaarawi, "A Contribution to the Numerical Solution of Developing Laminar Flow in the Entrance Region of Concentric Annuli with Rotating Inner Walls", ASME 74-FE-28, 1974.

6. Conover, R. A., "Laminar Flow Between a Rotating Disk and a Parallel Stationary Wall With and Without Radial Inflow", ASME 68-FE-30, 1968.

7. Hasinger, S. H. and L. G. Kehrt, "Investigation of a Shear-Force Pump", ASME 62-WA-193, 1962.

8. Yalcin, A. I., "Theoretical Study of a Viscous Turbine", M.S. Thesis, Georgia Institute of Technology, Atlanta, Georgia, 1975.

LIST OF FIGURES

ORO-4959-2
E-25-658

FINAL REPORT

ERDA Contract No. E-(40-1)-4959
(Georgia Tech Project No. E-25-658)

SINGLE WHEEL GAS TURBINE TOPPING UNIT FOR COAL BURNING POWER PLANTS

21 June 1976

by

Thomas W. Jackson
Professor of Energy Engineering

and

Gene T. Colwell
Professor of Mechanical Engineering

Georgia Institute of Technology
Atlanta, Georgia 30332

FINAL REPORT

SINGLE WHEEL GAS TURBINE TOPPING UNIT FOR COAL BURNING POWER PLANTS

INTRODUCTION

The work statement for ERDA Contract E-(40-1)-4959 is as follows:

> "The Contractor shall conduct a study of the calculation of theoretical estimates of turbine and compressor parameters. The work shall consist of the following tasks:
>
> 1. The drag turbine and compressor will be mathematically modeled, based on existing one-dimensional and three-dimensional computer programs. The model will allow the analysis of the effects of varied turbine and compressor parameters.
>
> 2. Using the model described in Task 1, detailed comprehensive calculations will be made of efficiencies for a turbine-compressor combination used as a topping unit for a conventional steam power plant.
>
> 3. Results of the calculations performed in Task 2 will be assembled in a final report. The report will include the rationale and basis for the efficiency calculations. The report will be sufficiently detailed so as to allow outside experts in the field to assess the potential of a subsequent prototype test turbine and will provide recommendations for further research and development on the single wheel gas turbine in terms of its promise of offering a novel, more efficient system for fossil-energy fueled advanced power systems."

During the 12 months of the contract the principal investigators Drs. Colwell and Jackson have each spent more than 15 percent of their time on the project. In addition they have supervised a graduate student, Mr. Andrew M. Coons, who has obtained a Masters degree in Mechanical Engineering, and who has, in his thesis entitled "Performance of a Viscous Topping Turbine," mathematically modeled a drag turbine and compressor. Attached hereto as Appendix A is a copy of Mr. Coons' thesis.

DISCUSSION

The thesis in the appendix together with the paper "Flow Fields in Moving Curved Channels," which was submitted with the project progress report dated 15 March 1976, covers all of the requirements of the subject contract. It is anticipated that a journal paper will be prepared, at a later date, covering the results presented in the thesis by Coons.

The results obtained from the research effort have indicated that the high temperature turbine has some applicability. For instance, Coons' thesis gives the following recommendations:

1. A survey should be made of operating power plants to determine the extent to which the topping turbine plus axial flow compressors can be used. Estimates of the effects of the viscous topping turbine on the steam cycle should be evaluated.

2. Heat transfer evaluations should be made to determine the effects of heat transfer on system performance more exactly.

3. A system should be optimized for an existing power plant.

In addition, the principal investigators have in a continuation proposal, dated 15 March 1976, proposed the following;

"It is proposed that the Single-Wheel Viscous Turbine be supplemented by an axial flow compressor and that 1, 2, 3 or more viscous turbine regenerative type units be utilized to complete a topping unit for conventional steam power plants burning powdered coal.

The modification proposed will require extensive calculations to match the axial flow compressor to various combinations of single wheel units. Parallel flow as well as series flow will be considered.

Detailed computer calculations will be made to secure an ideal match considering heat transfer effects in the single wheel units. Fin temperatures in the wheel will be calculated for various combined temperatures, flow areas, and various axial flow compressor efficiencies. The detailed calculations will provide sufficient information so that the compressor and viscous turbine parameters are available

1. to match the compressor (of various efficiencies) with the single wheel turbine in 1, 2, 3 or more units in both parallel and series flow modes.

2. to optimize the groove sizes for particular pressure ratios, flow rates, and inlet temperatures.

3. to permit the determination of turbine fin temperatures as a function of flow rates, turbine inlet temperatures, wheel speeds, and pressure ratios.

4. to determine the overall Power Plant efficiencies using a complete system.

In addition to the calculations the rationale and basis for the analyses will be presented. Also it is proposed to speculate on the research accomplished for

1. possible economic benefits for coal burning plants,

2. possibilities of advancing the work to prototype stages for various applications, and

3. possibilities of using modifications of the system in other energy situations; such as, a total turbine for geothermal power extraction, etc."

CONCLUSIONS

The research has been concluded successfully and has indicated that the high temperature (to 4000°R) viscous turbine could have an important role in increasing the efficiency of fossil fuel power plants.

It is also concluded that the research effort should, in view of the potential benefits (See proposal dated 15 March 1976 for continuation of ERDA Contract E-(40-1)-4959 and entitled "Single Wheel Gas Turbine Topping Unit for Coal Burning Power Plants"), be continued in the theoretical mode for another year. At the end of the year it is anticipated that a firm decision can be made on prototype development.

APPENDIX A

PERFORMANCE OF A VISCOUS

TOPPING TURBINE

Approved:

G. T. Colwell 5-5-76

G. T. Colwell, Chairman

T. W. Jackson

T. W. Jackson, Chairman

C. W. Gorton

C. W. Gorton

Date approved by Chairman: 5-5-76

TABLE OF CONTENTS

LIST OF TABLES

LIST OF ILLUSTRATIONS

GLOSSARY OF ABBREVIATIONS

H	slot height (inch)
W	slot width (inch)
DIA	rotor diameter (inch)
WIDTH	turbine length (ft)
dA	change in slot flow area across control volume element $(in)^2$
dP	change in pressure across control volume element (psi)
dT	change in temperature across control volume element (°R)
$d\rho$	change in density across control volume element (lb_m/in^3)
dV	change in velocity across control volume element (in/sec)
DX	length of control volume element (in)
S	wheel rim speed (in/sec)
q	heat transfer from rotor to air (Btu/lb_m)
τ_c	shear stress between air and static outer wall (psi)
τ_w	shear stress between air and rotor (psi)
V	air velocity absolute (in/sec)
P	air pressure (psia)
P_1	air inlet stagnation pressure (psia)
P_2	air exit stagnation pressure (psia)
T	air temperature (°R)

ρ	air density (lb_m/in^3)
$\dot{M}$	total mass flowrate (lb_m/sec)
MD	mass flowrate per slot (lb_m/sec)
t	time (sec)
AA	total turbine flow area (in^2)
A	flow area per slot (in^2)
g_c	Newton constant, 32.174 ft-lb_m/lb_f-sec^2
M	mass in control volume (lb_m)
F	forces on control volume (lb_f)
Q	heat addition (Btu/sec)
W_s	mechanical work (Btu/sec)
h	enthalpy (Btu/lb_m)
$\bar{n}$	control volume surface normal
h_w	convection factor (Btu/in^2-°R-sec)
C_p	specific heat at constant pressure (Btu/lb_m-°R)
T_w	wheel surface temperature (°R)
R	gas constant, 53.3 ft-lb_f/lb_m-°R
D_h	hydraulic diameter (in)
Re	Reynolds number
μ	air viscosity lb_m/ft-sec
f	friction factor
k	ratio of specific heats C_p/C_v = 1.4
eff_T	turbine efficiency
T_1	inlet stagnation temperature (°R)
T_2	exit stagnation temperature (°R)
eff_u	unit efficiency
hp	horsepower output

SUMMARY

One-dimensional mathematical models have been developed which approximate flow behavior in a viscous turbine and a viscous compressor. The models were validated by comparison with available experimental data for the viscous compressor and by comparison with limiting cases where the solutions are known. Detailed performance characteristics, including efficiency, pressure ratio, and shaft horsepower, of both turbine and compressor were generated.

Potential use of a viscous topping turbine for application in fossil fuel power plants has been studied. Unit operation with single and multiple wheel staged turbines has been evaluated for efficiency and net output in shaft horsepower. The effects of varying flow area, heat transfer, and supersonic flow have been studied.

Results of varied turbine and compressor parameters have been displayed in graphical fashion. The concept has been evaluated and the results indicate a possibility of providing a more efficient system to derive electrical energy from fossil fuel. Recommendations for further study are included.

CHAPTER I

INTRODUCTION

1-1. The Concept of the Viscous Turbine

The idea of using topping turbines in fossil fuel plants in order to increase overall efficiency of electrical power generation has been known for a long time. However, conventional gas turbines are not suitable for use in coal burning power plants due to blade erosion caused by impingement of unburned particles and ash. In addition, turbine inlet temperatures are limited.

Several years ago at the Georgia Institute of Technology, Drs. T. W. Jackson and G. T. Colwell conceived an idea for a grooved disk, as shown in Figure 1-1, operating as a viscous turbine which may have the temperature and durability characteristics needed for installation in the burner locations on existing coal boilers. The turbine, without complex surfaces for blades, would operate on viscous drag as the high temperature combustion gases passed through the grooves at high velocities.

An overall efficiency analysis of a topping turbine unit, including compressor and viscous turbines in an electrical steam plant, is illustrated in Figure 1-2. The benefit of the topping turbine is that it utilizes expansion

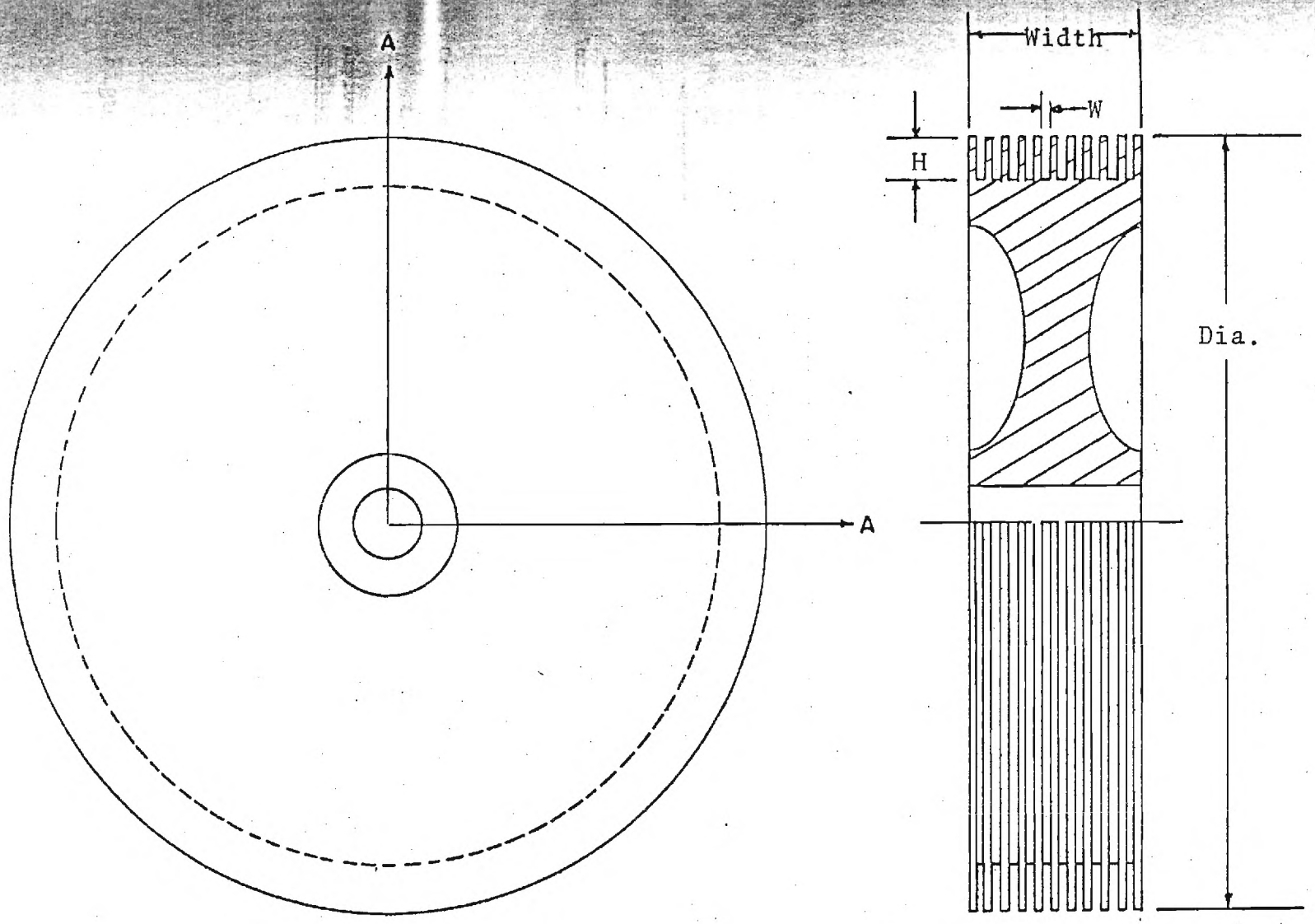

Figure 1-1. Wheel Geometry

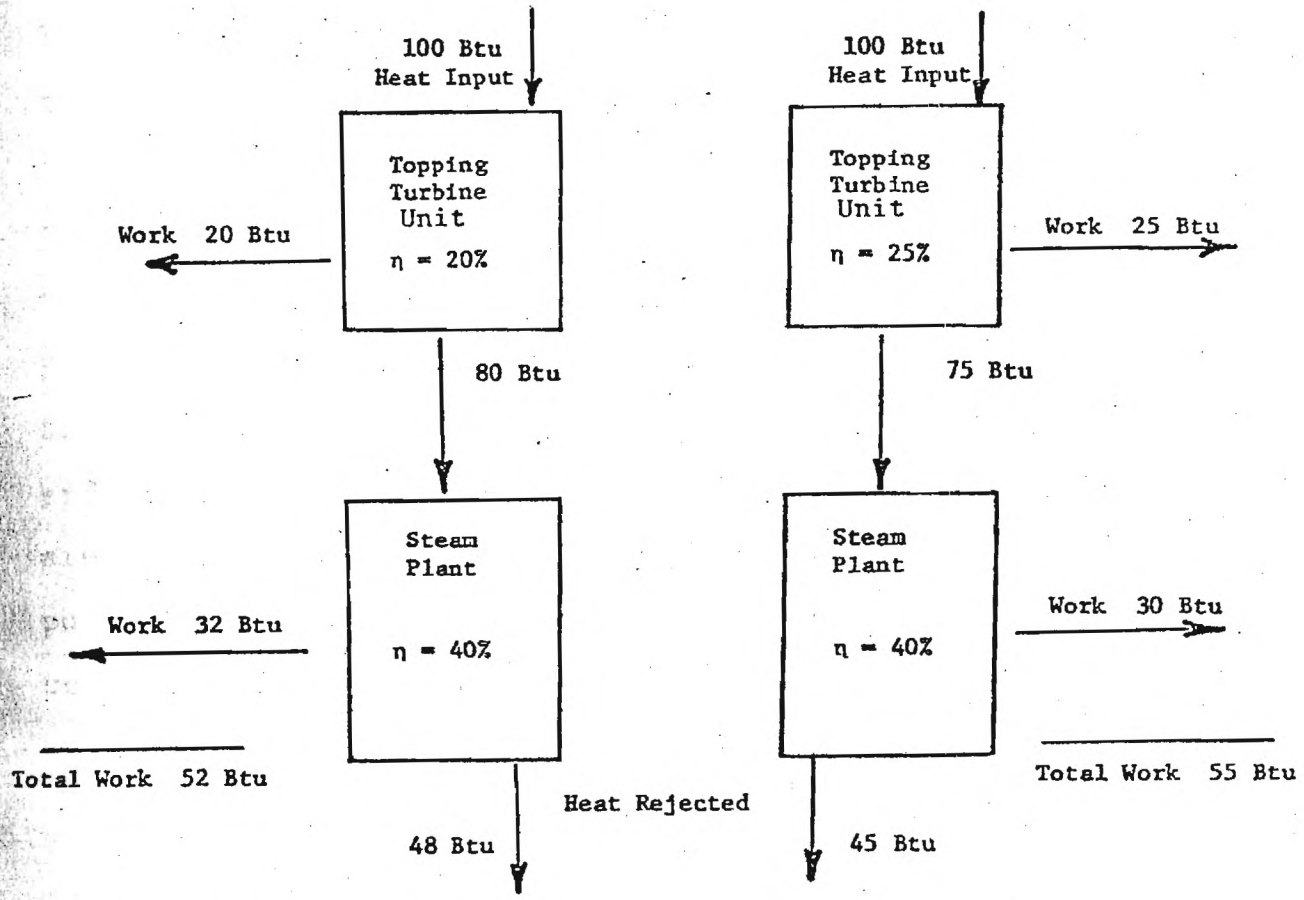

Combined Efficiency

$$\eta_T = \frac{52}{100} = 52\%$$

Improvement over ordinary plant

$$I = \frac{12}{40} = 30\%$$

$$\eta_T = \frac{55}{100} = 55\%$$

$$I = \frac{15}{40} = 37.5\%$$

Figure 1-2. Schematic Diagrams of Generating Systems Using Coal Burning Topping Turbines and Estimates of Output Improvements for Two Topping Turbine Efficiencies of 20% and 25% Over a Standard Steam Plant Operating at 40% Efficiency

of the combustion gases to obtain output above and beyond ordinary plant operation without additional heat input. The heat energy leaving the turbine is available for use in the conventional Rankine-steam cycle. By similar analysis to Figure 1-2, a 10 percent thermal efficiency from the topping turbine unit will yield a 15 percent improvement over ordinary steam plants. An entire unit utilizing the grooved disk as turbine and compressor was considered feasible until this study revealed relatively low compressor efficiency and that only limited turbine pressure ratios are possible due to choking. Higher unit efficiencies are possible by combining a series of turbines with an axial compressor at a higher pressure ratio.

1-2. Literature Survey

The concept of the viscous turbine has been studied and refined at Georgia Tech. Under Dr. Colwell's direction, a viscous compressor was analyzed both experimentally and theoretically by Dusadeenoad in 1970 [1].* Further investigation by Caldwell [2] displayed the importance of effective sealing on efficiency. Based on this work, a patent was issued to Drs. Jackson and Colwell jointly in 1973 [3]. The compressor was further demonstrated in a three-dimensional theoretical study for laminar incompressible flow by Yalcin [4].

---

*Numbers in brackets indicate references.

Though the earliest recognition of a viscous turbine was by Nikolai Tesla [5] in 1913, no reference has been located which gives performance characteristics of a high speed viscous turbine. This thesis has employed fundamental engineering concepts to predict turbine and compressor performance. Texts by John [6], Schlichting [7], White [8] and Reynolds [9] were used to develop the models employed. Material properties were taken from Kreith [10] and Keenan and Kaye [11]. A computer manual by Cooper and Smith also served as a valuable reference [12].

CHAPTER II

THEORETICAL DEVELOPMENT

2-1. Turbine and Compressor Models

Theoretical performance characteristics of the viscous turbine and compressor are generated with one-dimensional mathematical models. The models consist of a series of finite elements which compose the turbine or compressor arc on the circumference of the wheel. Each element is represented by a stationary control volume as shown in Figure 2-1. The effects of variable area are included in the mathematical equations, however, they reduce to the non-variable form when $dA = 0$.

The fundamental equations of continuity, momentum, and energy coupled with the equation of state for air must be satisfied within each control volume element. The shear stresses on the surfaces of the elements are determined using laminar and turbulent friction factors for duct flow. Forces in the directions shown in Figure 2-1 are considered positive. Heat into the fluid and work on the fluid are also positive. The turbine will have negative values for τ_w, q, and work. These are handled in a general way in the derivations.

2-2. Fundamental Equations

Steady mass flow through the arc greatly reduces the

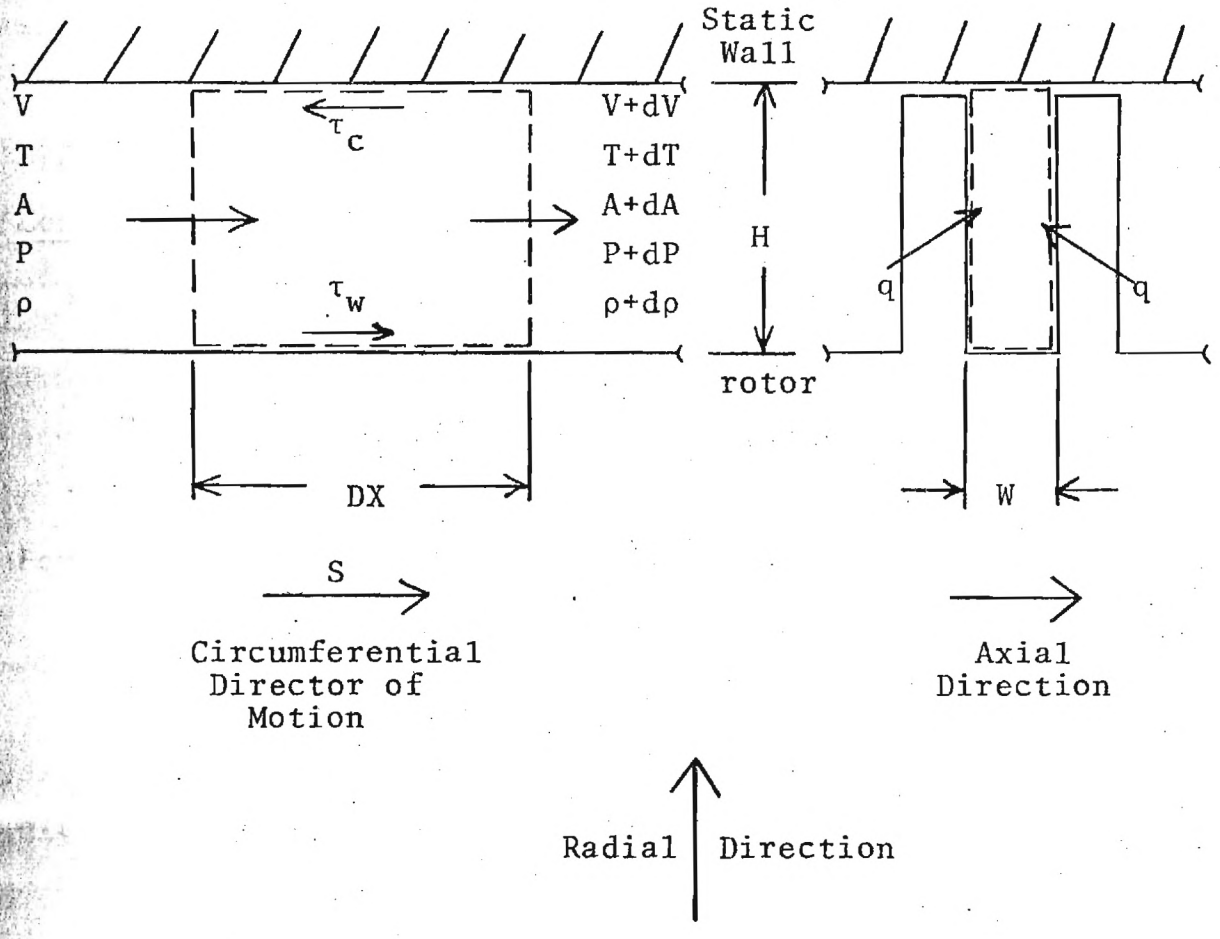

Figure 2-1. Control Volume

complexity of the fundamental equations. The equations are further simplified by choosing the intervals sufficiently small such that material properties specific heat and viscosity are constant within each element. With sufficiently small intervals, second and third order differentials may also be considered negligible. For example, $d\rho dV << d\rho V$. Thus $d\rho dV$ is assumed zero.

Continuity Equation

Conservation of mass in control volume form is:

$$\frac{dM}{dt} = \frac{\alpha}{\alpha t} \iiint_{c.v.} \rho \, dVol + \iint_{s} \rho \, \bar{V} \cdot \bar{n} \, dA$$

For steady flow,

$$0 = (\rho+d\rho)\ (V+dV)\ (A+dA) - \rho VA$$

Neglecting second and third order differentials,

$$\frac{d\rho}{\rho} + \frac{dA}{A} + \frac{dV}{V} = 0$$

$$d\rho = - \frac{\rho dV}{V} - \frac{\rho dA}{A}$$

And the mass flowrate is:

$$\dot{M} = \rho VA = \text{constant}$$

Momentum Equation

Rate of change of momentum in a control volume is:

$$\frac{d(MV)}{dt} = \frac{\alpha}{\alpha t} \iiint_{c.v.} \rho V \, dVol + \iint_{s} V\rho(\bar{V}\cdot\bar{n})dA$$

By Newton's Second Law,

$$\frac{d(MV)}{dt} = q_c \quad \Sigma\bar{F}$$

Summing forces in Figure 2-2 and neglecting second order differentials,

$$\Sigma F = -(p+dp)(A+dA) + (p+p/2)dA$$

$$+ pA + \tau_w(2H+W)DX - \tau_c W(DX)$$

Where,

$\tau_w > 0$ in the compressor

$\tau_w < 0$ in the turbine

Now,

$$\frac{d(MV)}{dt} = \rho AVdV$$

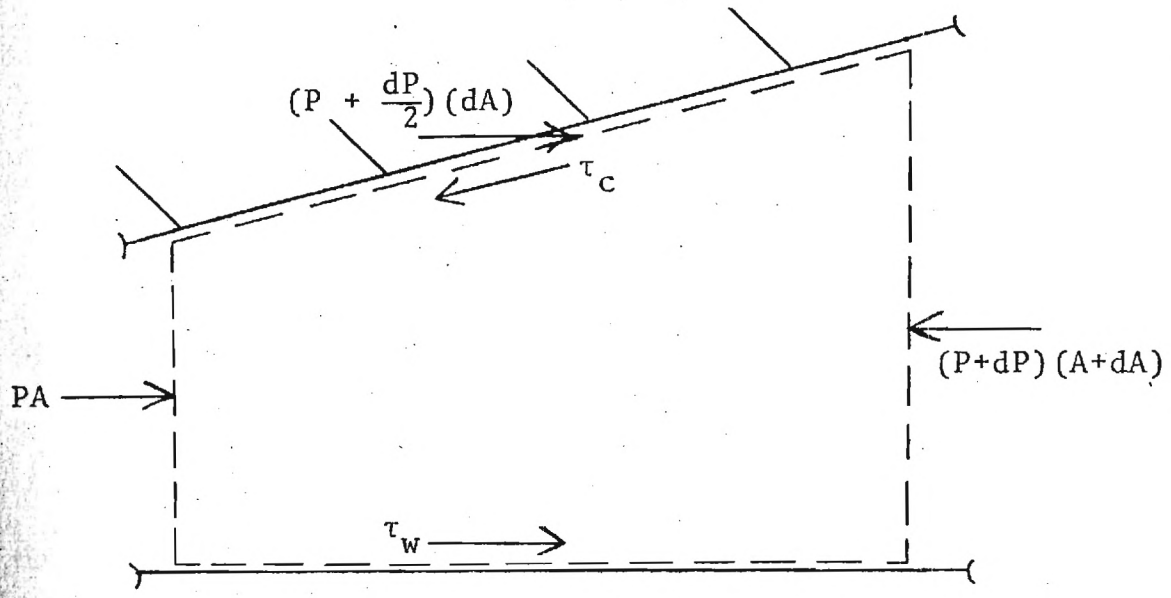

Figure 2-2. Control Volume Force Balance

$$-AdP + \tau_w (2H+W)DX - \tau_c W(DX) = \frac{\rho AVdV}{q_c}$$

Letting $A = HW$, $\rho AV = \dot{M}$

$$dP = \frac{-\dot{M}dV}{HWq_c} + \frac{\tau_w(2H+W)DX}{HW} - \frac{\tau_c DX}{H}$$

Energy Equation

Rate change of energy in a control volume is:

$$\frac{dE}{dt} = \frac{\alpha}{\alpha t} \iiint_{c.v.} e\rho dVol + \iint_{s} e\rho(\bar{V}\cdot\bar{n})dA$$

$$e = u + \frac{V^2}{2q_c}$$

$$\frac{dE}{dt} = \frac{d}{dt}\,(Q+W_s) - \frac{p}{\rho}\,\dot{M}$$

where Q represents heat addition, W_s represents mechanical work, and $-p/\rho\dot{M}$ is flow work.

Since

$$h = u + \frac{P}{\rho}$$

then,

$$\frac{d(W_s+Q)}{dt} = \iint_s (h + \frac{V^2}{2q_c})\rho(\bar{V}\cdot\bar{n})dA$$

Simplifying and neglecting second order differentials,

$$\frac{dW_s}{dt} + \frac{dQ}{dt} = \dot{M}(dh + \frac{VdV}{q_c})$$

$$\frac{dW_s}{dt} = \text{(shear force) x (wheel speed)}$$

$$\frac{dW_s}{dt} = \tau_w(2H+W)DX\ S$$

$$\frac{dQ}{dt} = \left(\begin{matrix}\text{Convection}\\ \text{Factor}\end{matrix}\right) \times (\text{Area}) \times \left(\begin{matrix}\text{Temperature}\\ \text{Difference}\end{matrix}\right)$$

$$\frac{dQ}{dt} = h_w\ (2H+W)DX(T_w-T)$$

Assuming air to be a perfect gas,

$$dh = C_p dT$$

Then,

$$\frac{\tau_w(2H+W)DX(S)}{\dot{M}} + \frac{h_w(2H+W)DX(T_w-T)}{\dot{M}} = C_p dT + \frac{VdV}{g_c}$$

$$dT = \frac{-VdV}{c_p g_c} + \frac{\tau_w(2H+W)DX(S)}{C_p\dot{M}} + \frac{h_w(2H+W)DX(T_w-T)}{C_p\dot{M}}$$

State Equation

The state equation for air as a perfect gas is:

$$Pv = RT$$

$$\rho = P/RT$$

$$d\rho = \frac{dP}{RT} - \frac{P}{RT^2}\,dT$$

Where,

$$R = 53.3 \frac{\text{ft lb}_f}{\text{lb}_m \ ^\circ R}$$

2-3. Wall Stresses and Convection Factors

Reynold's number (Re) for flow in pipes of non-circular cross section is based on hydraulic diameter.

$$D_h = \frac{2HW}{(H+W)}$$

Then for Re and τ_c relative to the stationary housing,

$$Re = \frac{\rho \ V \ D_h}{M}$$

$$\tau_c = f\rho V^2/8 \ q_c$$

And for Re and τ_w relative to the rotating wheel,

$$Re = \frac{\rho |(S-V)| D_h}{M}$$

$$\tau_w = \frac{f\rho |S-V| (S-V)}{8 \ q_c}$$

If S>V, as in the compressor, τ_w will be greater than zero.

However, if S<V the above relation will generate a negative τ_w as required by the turbine.

Empirical correlations for Re and f are

$$f = 64/Re \qquad Re < 2000$$

$$\frac{1}{\sqrt{f}} = 2.0 \log_{10} (Re\sqrt{f}) - .8 \qquad Re > 2000$$

(Reference 7, equations 5.11, 20.30), and by Reynold's analogy,

$$h_w = \frac{f\rho|S-V|C_p}{8.0}$$

2-4. Simultaneous Solution of Fundamental Equations

A summary of the fundamental equations is now given.

Continuity

$$d\rho = \frac{-\rho dV}{V} - \frac{\rho dA}{A}$$

Momentum

$$dP = \frac{-\dot{M}\, dV}{HW\, g_c} + C_1$$

where

$$C_1 = \frac{\tau_w (2H+W)DX}{HW} - \frac{\tau_c DX}{H}$$

Energy

$$dT = \frac{-VdV}{C_p g_c} + C_2$$

where,

$$C_2 = \frac{\tau_w (2H+W)DX(S)}{C_p \dot{M}} + \frac{h_w (2H+W)DX(T_w-T)}{C_p \dot{M}}$$

State

$$d\rho = \frac{dP}{RT} - \frac{P}{RT^2} dT$$

These constitute four coupled equations with four unknowns. Since $d\rho$, dP, and dT are all first order functions of dV, the fundamental equations may be solved in a straightforward manner by substituting the continuity momentum, and energy equations into the state equation. With some simplification, this yields:

$$dV = C_4/C_3$$

where,

$$C_3 = [-\rho/V + \frac{\dot{M}}{HWRTg_c} - \frac{PV}{RT^2 C_p g_c}]$$

and

$$C_4 = [\frac{C_1}{RT} - \frac{C_2 P}{RT^2} + \frac{\rho dA}{A}]$$

Then $d\rho$, dP and dT follow directly as functions of C_4 and C_3 ($dV = C_4/C_3$).

$$d\rho = \frac{-\rho}{V} \frac{C_4}{C_3}$$

$$dP = \frac{-\dot{M}}{HW\ g_c} \frac{C_4}{C_3} + C_1$$

$$dT = \frac{-V}{C_p\ g_c} \frac{C_4}{C_3} + C_2$$

2-5. Efficiency Definitions

Turbine efficiency is defined as the ratio of actual turbine work output to the isentropic work between the same pressures.

$$\text{eff}_T = \frac{(\text{Shear Force}) \times (\text{Wheel Speed})}{(\text{Isentropic Work } P_1 \to P_2)}$$

$$= \frac{|\tau_w| (2H+W)(DX)S}{C_p\ T_1\ \dot{M}\ [1-(\frac{P_2}{P_1})^{\frac{1-k}{K}}]}$$

Compressor efficiency is the reciprocal of the turbine efficiency. It is the ratio of isentropic work to actual work.

$$\text{eff}_c = \frac{(\text{isentropic work } P_1 \rightarrow P_2)}{(\text{shear force}) \times (\text{wheel speed})} = \frac{C_p T_1 \dot{M}[(\frac{P_2}{P_1})^{\frac{1-k}{k}} - 1]}{\tau_w (2H+W)DX(S)}$$

Unit Efficiency

The turbine, when combined with a compressor and heat source, forms a unit operating as an open Brayton cycle shown in Figure 2-3. An open Brayton cycle with reheat is shown in Figure 2-4.

The efficiency of either unit is defined by

$$\text{eff}_u = \frac{(\text{Total Turbine Work}) - (\text{Compressor Work})}{(\text{Total Heat Input})}$$

If an axial compressor with 80 percent efficiency is used, the work of compression is

$$\text{Compressor Work} = \frac{\dot{M} C_p \ 530°R \ [(\frac{P_2}{14.7})^{\frac{1-k}{k}} - 1]}{.8}$$

The total turbine work is shear force by wheel speed.

$$\text{Turbine Work} = \tau_w (2H+W)DX(S)$$

and the heat inputs are

$$\text{Initial Heat Input} = C_p \dot{M} (T_3 - T_2)$$

$$\text{Reheat} = C_p \dot{M} (T_{4a} - T_{3a})$$

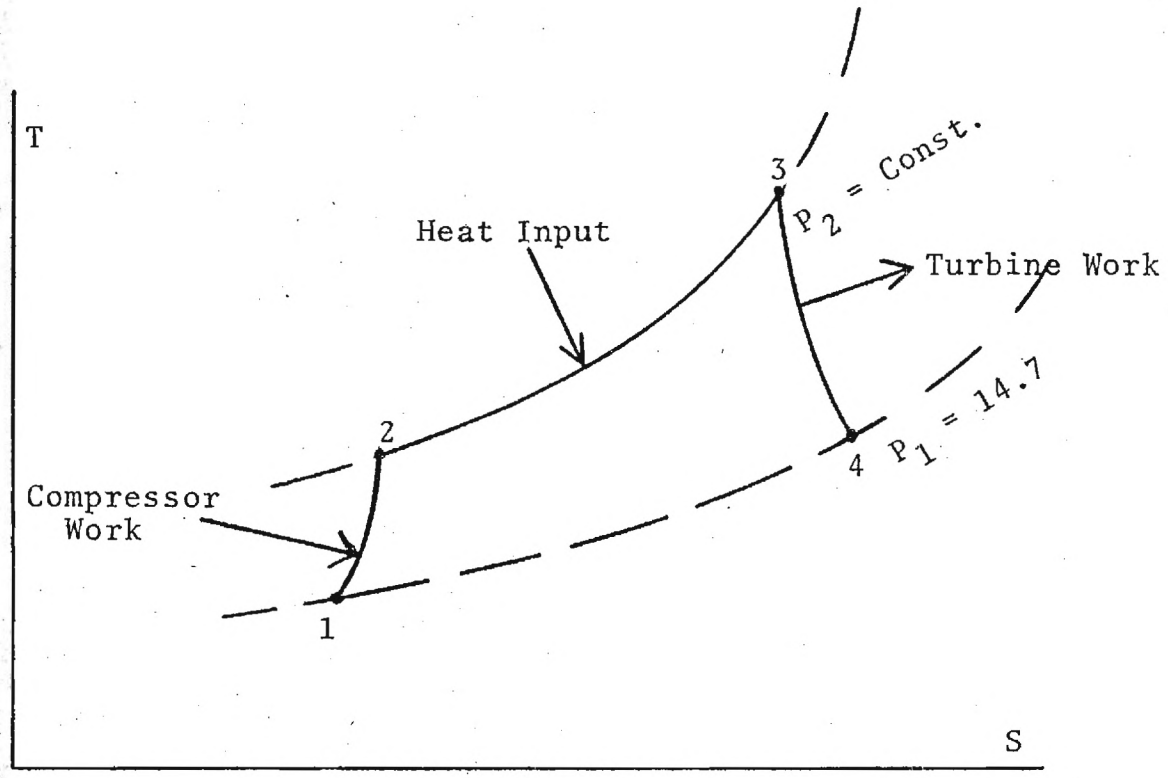

Figure 2-3. Open Brayton Cycle

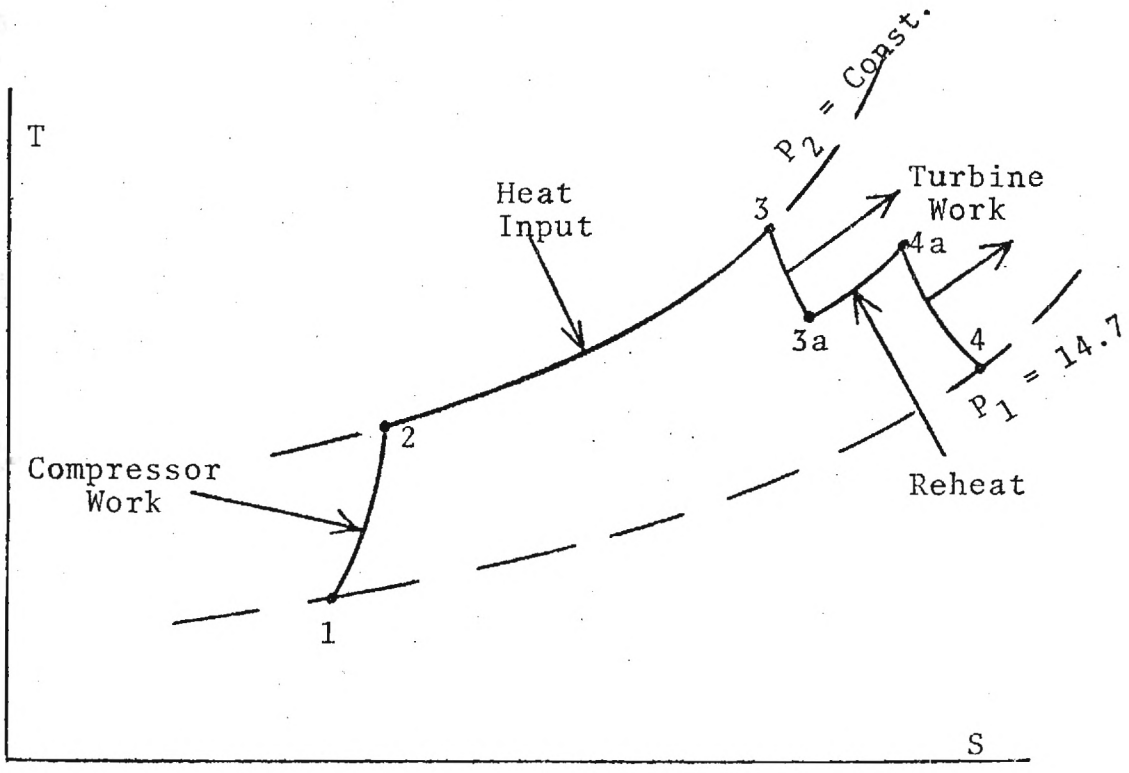

Figure 2-4. Open Brayton Cycle with Reheat

CHAPTER III

SOLUTION TECHNIQUES

3-1. Computer Analysis (Non-Variable Area)

The arc length of the turbine or compressor is divided into one hundred finite increments, each of which constitutes a control volume as shown in Figure 2-1. The length of each element is dependent on the wheel diameter and the degrees of arc desired (Figure 3-1). Iterating the control volume analysis a hundred times has the effect of marching through the turbine or compressor. Various flowrates are used to map and then optimize performance.

The same analysis was performed using a single control volume attached to the disk. This control volume was allowed to sweep through the arc at the wheel speed. Properties within the element were transient as the control volume moved through the arc. The results were identical. However, due to the complexity of the single element transient analysis, the iteration technique has been employed exclusively in this report.

A computer program has been written to perform the analysis required to determine turbine and compressor operational characteristics. All parameters related to the geometry or operation of the disk as well as entrance

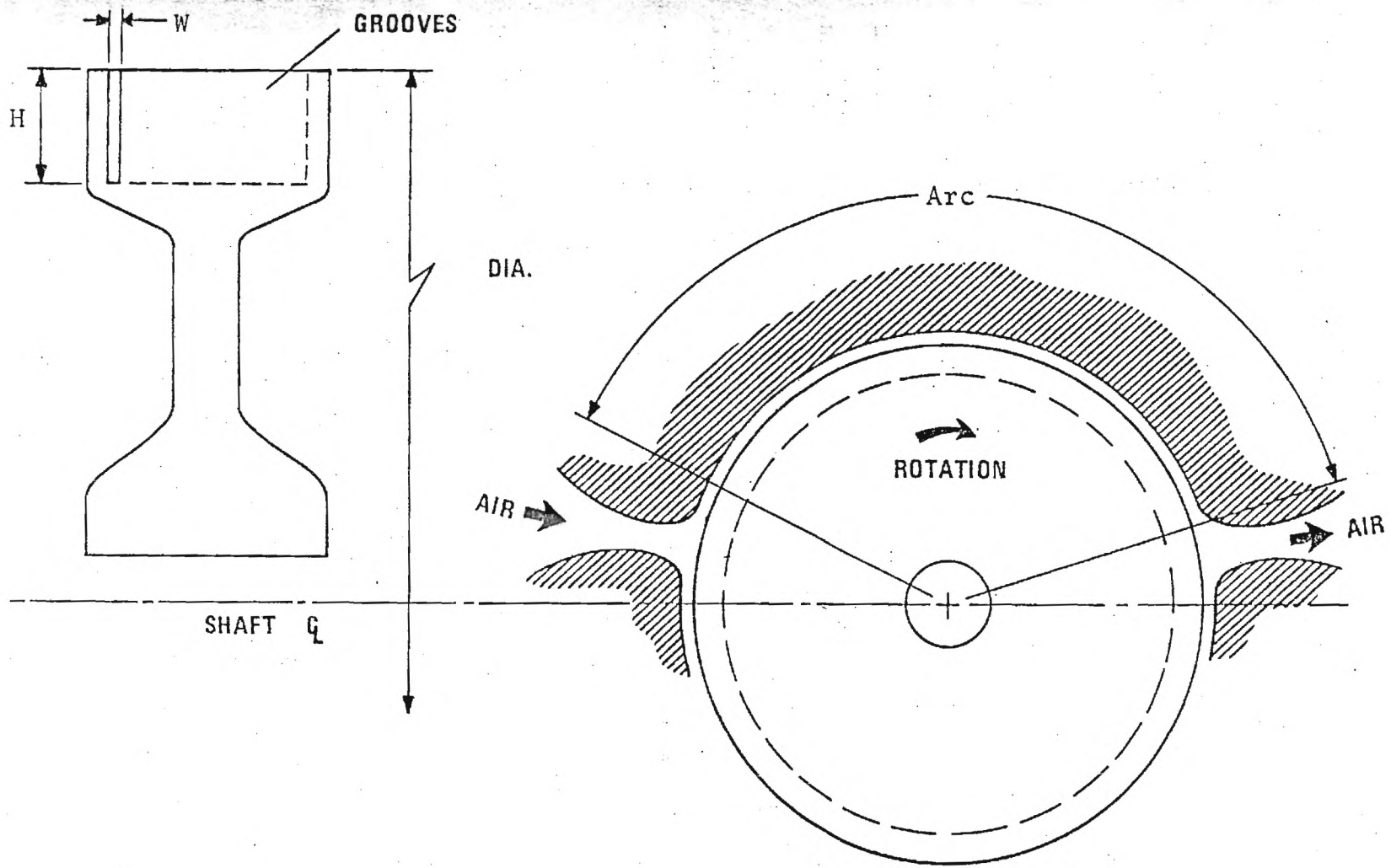

Figure 3-1. Geometry of Larger Rotor

conditions may be varied. The program, given in Appendix A, is in standard Fortran IV-G user language. Subroutines, which employ a plotter to display generated data, are called as necessary.

A simplified flowchart is shown in Figure 3-2. Geometry and speed of the turbine or compressor along with stagnation properties of the entering air are read into the computer. Mass flowrates are then selected starting at just above zero and increasing to choked flow. Static properties and velocity are calculated using standard isentropic relations. The control volume analysis as described in Chapter II is now iterated to determine exit properties at each element from the entrance properties plus the differentials calculated (eq. P(J+1) = P(J) + d(P).

Material properties, specific heat and viscosity, are primarily a function of air temperature which varies along the arc. They are described within each control volume element by the following curve fitting relationships:

Viscosity, lb_m/ ft-sec

$$\mu = 1.285 \left(\frac{T}{560°R}\right)^{1.35} \left(\frac{1000°R}{T+440°R}\right)$$

Specific heat, Btu/lb_m-°R

$$C_p = \left(\frac{T}{1000} - 1\right) .02 + .2486$$

PERFORMANCE OF A VISCOUS TOPPING TURBINE

A THESIS

Presented to

The Faculty of the Division

of Graduate Studies

By

Andrew M. Coons

In Partial Fulfillment

of the Requirements for the Degree

Master of Science in Mechanical Engineering

Georgia Institute of Technology

June, 1976

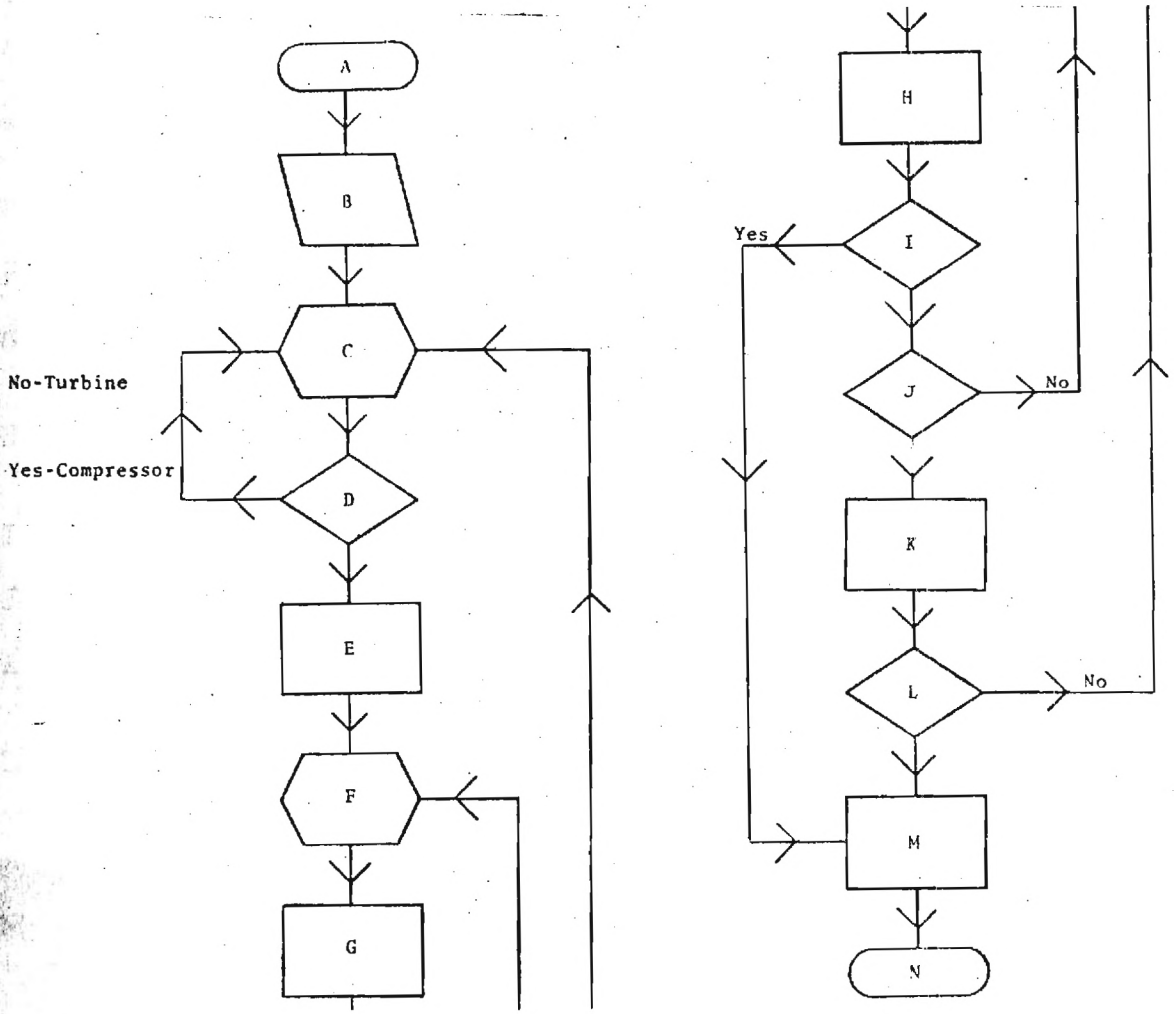

Figure 3-2. Program Flowchart

Description of Figure 3-2

A Start, dimension statements, call plot

B Input data, wheel geometry, speed, stagnation entrance properties

C Specify a flowrate

D Is gas velocity greater than wheel speed? No--turbine return to C, yes--compressor return to C.

E Isentropic converging section

F Specify increment in control volume analysis

G Perform control volume analysis by solving fundamental equations

H Calculate control volume exit properties (e.g. P(J+1) = P(J)+dP)

I Is flow choked? Yes--go to M

J Have 100 iterations been completed? No--return to F

K Isentropic diverging section. Calculate P_1-P_2, eff_T, eff_u, H_p, T_1-T_2

L Is maximum flowrate reached? No--return to C. Yes--read additional data if available

M Draw axis, plot data

N Stop. Data set, subroutine

Accumulative properties such as work and heat transfer are numerically integrated along the arc by the computer which adds the contributions of each increment. Choking will limit the mass flow through the rectangular cross section, in a manner similar to Fanno or Rayleigh flow. This is signified in the operation of the program by change of sign of the C3 term in the denominator of dV. When this occurs, attempts to run at higher flowrates are useless. Then program operation is passed to the plotter.

Following a successful march through the arc, without choking, isentropic relations are again used to determine stagnation properties of the gas leaving the disk. These, with the accumulated work term are used to calculate efficiencies, power and temperature and pressure differences. Higher flowrates are then attempted until choking occurs or in the case of the compressor, when inlet gas velocity exceeds wheel speed which results in zero pressure increase and an ineffective compressor.

3-2. Computer Analysis (Variable Area)

In the previous discussion, for constant cross sectional flow, dA was zero and took no part in turbine performance. When variable areas are incorporated into the analysis, two possibilities exist. First, dA could be specified as constant or as some function of arc position. Then the turbine performance could be determined for any particular

variable area geometry. The user would be left to randomly try geometries in an attempt to optimize performance.

A second technique, however, is a more direct method to optimize turbine performance. Since the fluid stresses vary as the square of gas velocity, the optimum velocity for turbine performance is first established. Then the area profile required to maintain that velocity is calculated. The maximum height to width ratio is arbitrarily limited to ten in order to remain within reasonable machining capabilities. Since the varying area maintains constant velocity through the turbine, exceeding height to width ratio of ten indicates flowrate too great for the turbine, and is equivalent to choking.

To maintain constant velocity through the turbine,

$$dV = 0 = \frac{C_4}{C_3}$$

Therefore,

$$C_4 = 0$$

$$\frac{C_1}{RT} - \frac{C_2 P}{RT^2} + \rho \frac{dA}{A} = 0$$

and

$$\frac{dA}{A} = \frac{1}{\rho}\left[\frac{C_2 P}{RT^2} - \frac{C_1}{RT}\right]$$

3-3. Friction Factor Subroutine

A subroutine has been written to calculate turbulent and laminar friction factors from Reynolds numbers. Using the empirical relations of Section 2-3 the subroutine (Appendix B) calculates the friction factor directly for Reynolds numbers less than 2000 from

$$f = 64/Re \qquad (7)$$

Reynolds numbers greater than 2000 require use of Prandtl's Law of Friction Factors,

$$\frac{1}{\sqrt{f}} = 2.0 \log_{10} (Re\sqrt{f}) - .8 \qquad (7)$$

In order to solve this equation, the subroutine is strictly a trial and error convergence routine. Beginning with $f = .05$ the program adds or subtracts $.025\ (\frac{1}{2})^n$, where n equals the number of prior attempts, depending on whether the previous guess was high or low. Using this technique the computer approaches the correct f for a given Re. Ten iterations result in accuracy within four percent.

CHAPTER IV

RESULTS OF ANALYSIS

4-1. Comparison of Theoretical and Experimental Data

Measurements are not available for actual high speed viscous turbine performance. However, a viscous compressor has been tested (references 1 and 2). Figures 4-1, 4-2 and 4-3 compare empirical data from these reports and theoretical data from the computer model discussed in Chapter III for a 6.6 inch diameter compressor at various rotational speeds. The correlation is remarkably good at low speeds with increasing disparity at higher speeds. This was expected due to the increased difficulty of sealing the test apparatus at higher speeds and pressures. Whereas, the computer model has assumed perfect seals with no leakage at any speed.

Logically speaking, sealing should not be as critical in a viscous turbine as in the compressor. In the compressor, air has the tendency to leak back from the high pressure outlet opposite to the flow to the atmosphere. However, all of the turbine gases exit and there is no tendency for low pressure air to leak back into the higher pressure inlet region. Therefore, correlation between theoretical and empirical turbine data is expected to be even better than that shown for the compressor.

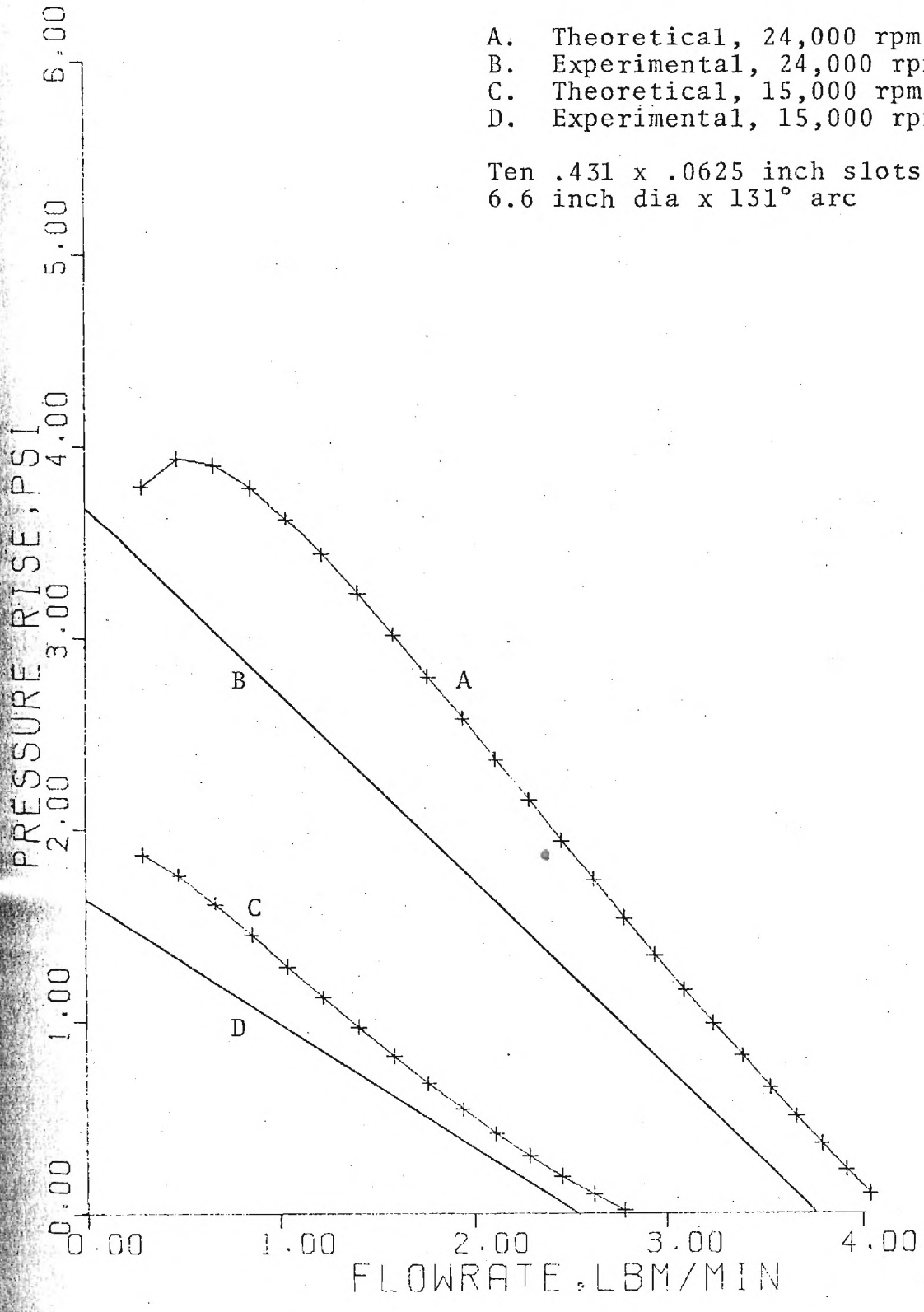

Figure 4-1. Experimental and Theoretical Data Correlation in Compressor

A. Theoretical, 30,000 rpm
B. Experimental, 30,000 rpm
C. Theoretical, 15,000 rpm
D. Experimental, 15,000 rpm

Ten .431 x .0625 inch slots
6.6 inch dia x 131° arc

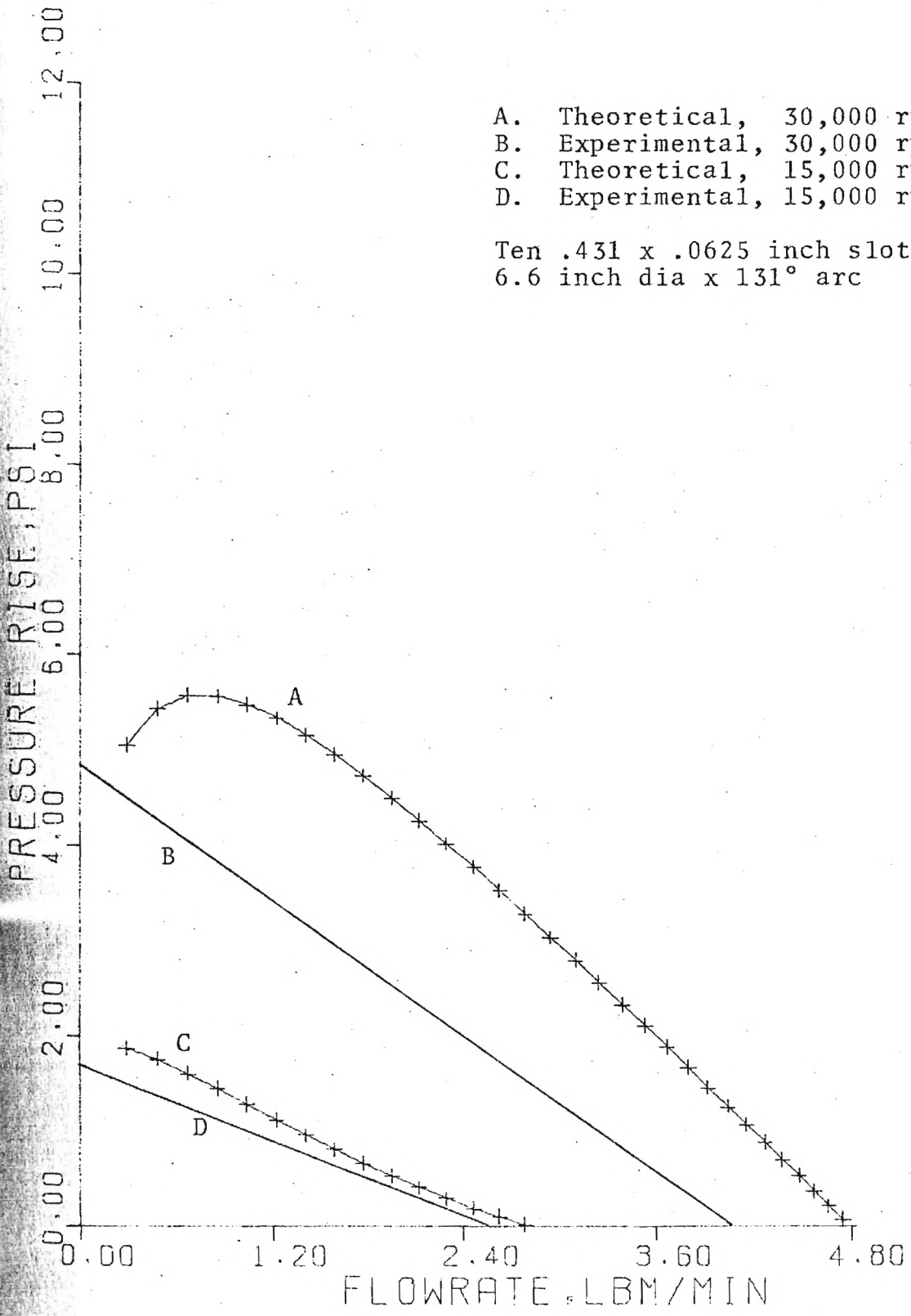

Figure 4-2. Experimental and Theoretical Data Correlation in Compressor

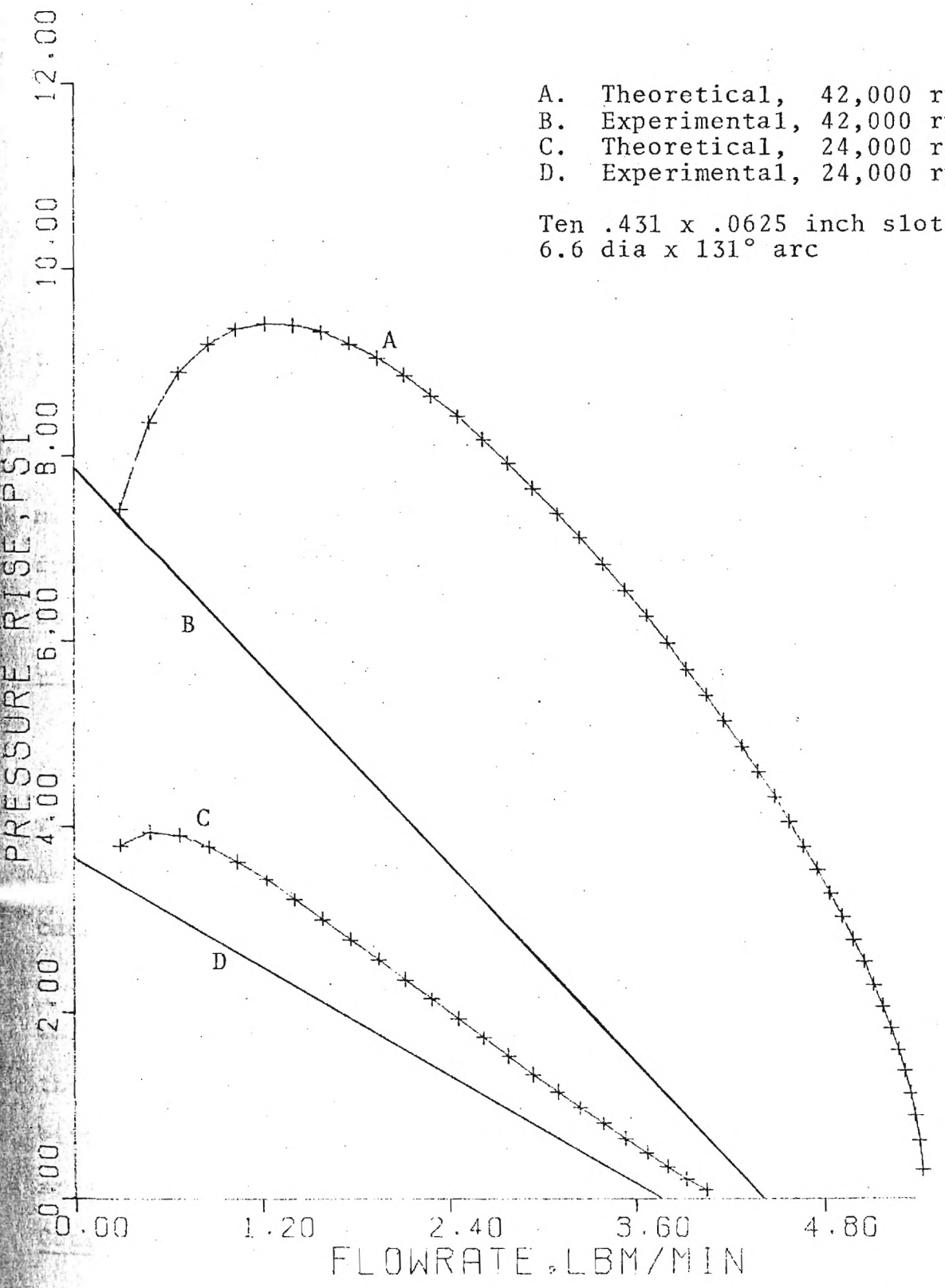

Figure 4-3. Experimental and Theoretical Data Correlation in Compressor

4-2. Limiting Cases and Outer Wall Losses

In order that the analysis be valid, it must correctly evaluate the limiting cases where solutions are known.

Zero Wheel Speed

The first such case is adiabatic flow when the wheel is static. These computer predictions are the same as well tabulated Fanno flow. For a 60 inch diameter turbine with 1.5 x .15 inch slots and a flowrate of 33.7 lb_m/min at an entrance pressure of 50 psia and temperature of 3960°R, the model predicts a total pressure drop of 28.2 psi Fanno flow for the same arc length and conditions predicts a 28.4 psia total pressure drop.

Gas Velocity Relative to Wheel Speed

Neglecting the outer wall drag, the computer model indicates net work in for wheel speed greater than gas velocity and work out for wheel speed less than gas velocity as expected. However, addition of the static wall stress causes negative pressure rise at gas velocity equal to and slightly lower than wheel speed due to the losses along the wall. In Figure 4-4 the curve without wall stress crosses the axis at the flowrate where velocity equals wheel speed. With the wall stress, zero pressure differential is found at slightly lower velocities.

Converging-Diverging Section Without Friction

Air flow without heat transfer or friction is isentropic. Under these conditions, the program was found to agree with

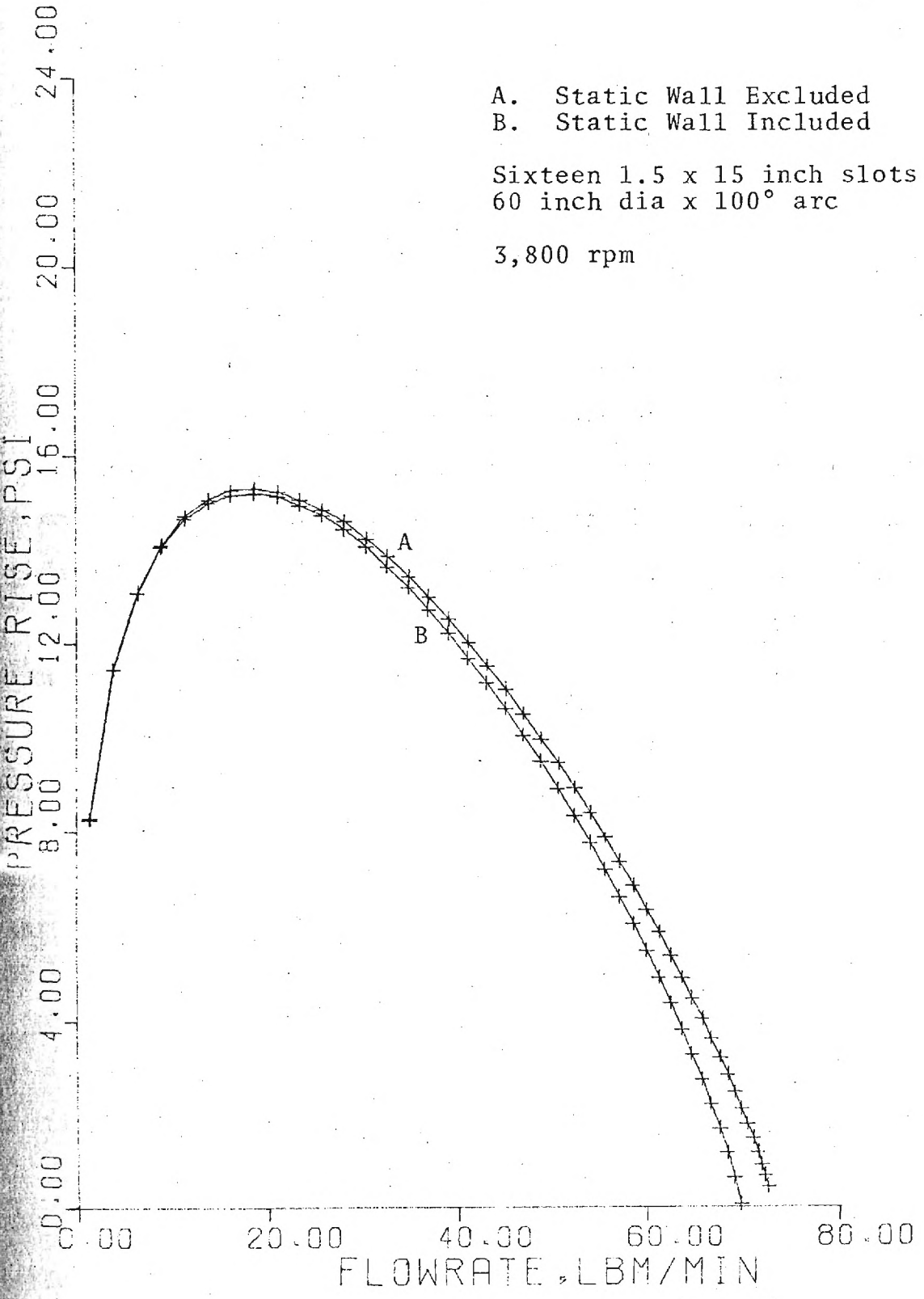

Figure 4-4. Compressor Performance

isentropic tables within 2 percent except for mach numbers between .95 and 1.05. The finite difference method breaks down in this range due to the rapid change in velocity over a small distance as choked flow is approached.

Effect of Outer Wall Drag on Efficiency

Figures 4-5 and 4-6 show the effects of the outer wall on compressor and turbine efficiency. As was expected, the static losses reduce both compressor and turbine efficiency. The effects are most pronounced as gas velocities approach wheel speed. This is because the static wall losses become relatively larger compared to the small pressure differences created by a very small relative speed between the gas and rotor. Figure 4-7 shows the disparity in efficiency increasing as the pressure differential approaches zero.

4-3. Turbine Optimization

Allowing a maximum slot height to width ratio of ten to facilitate manufacture of the disks, optimum turbine efficiency as shown in Figure 4-8 has been determined to be 44 percent. Figure 4-8 also clearly illustrates the transition between laminar and turbulent flow through the rotor slots. The effects of other parameters on turbine performance are demonstrated in Figures 4-9 through 4-14. Variable arc length produces the same effects as variable diameter at equivalent rim speed and is not included.

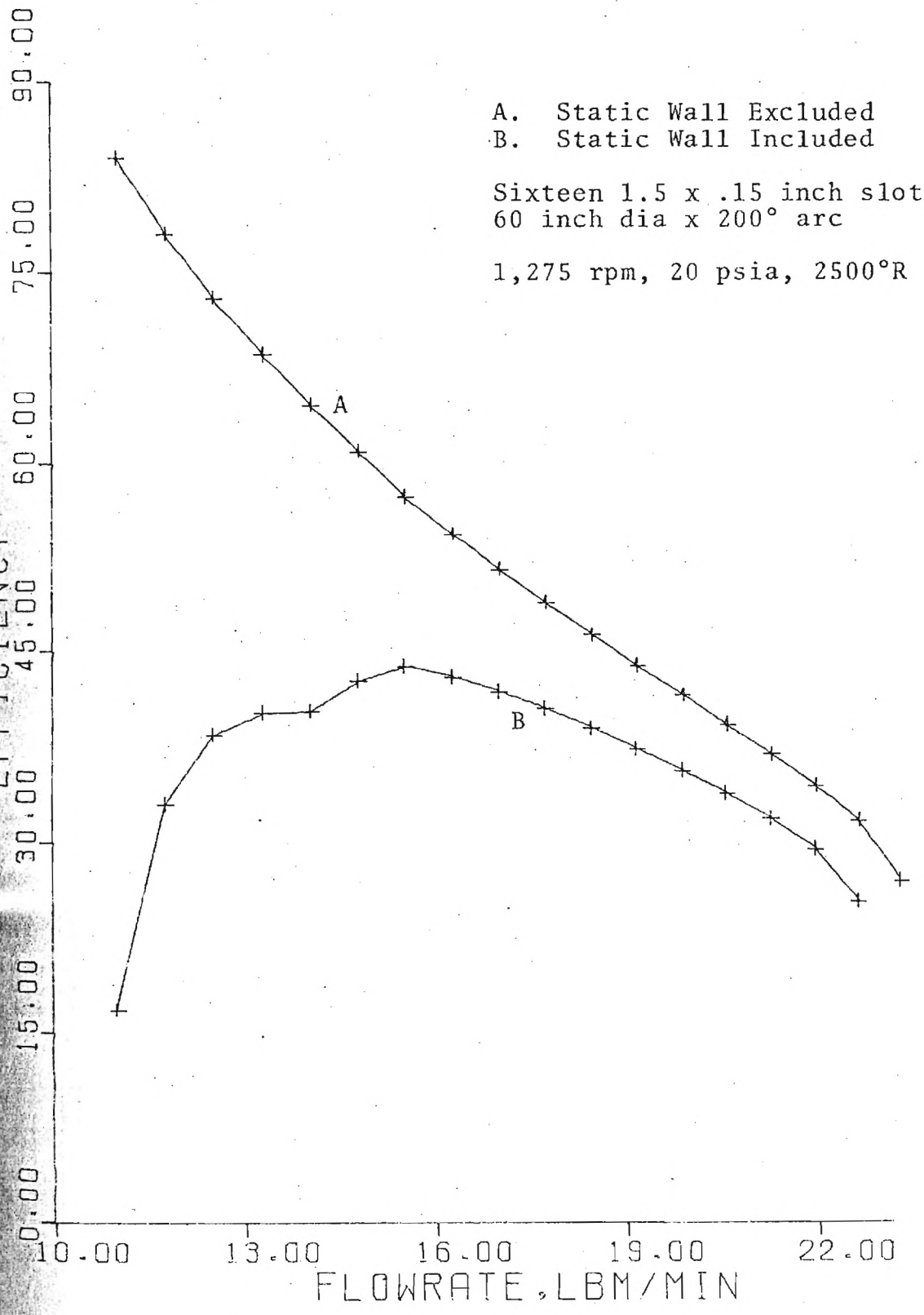

Figure 4-5. Turbine Performance

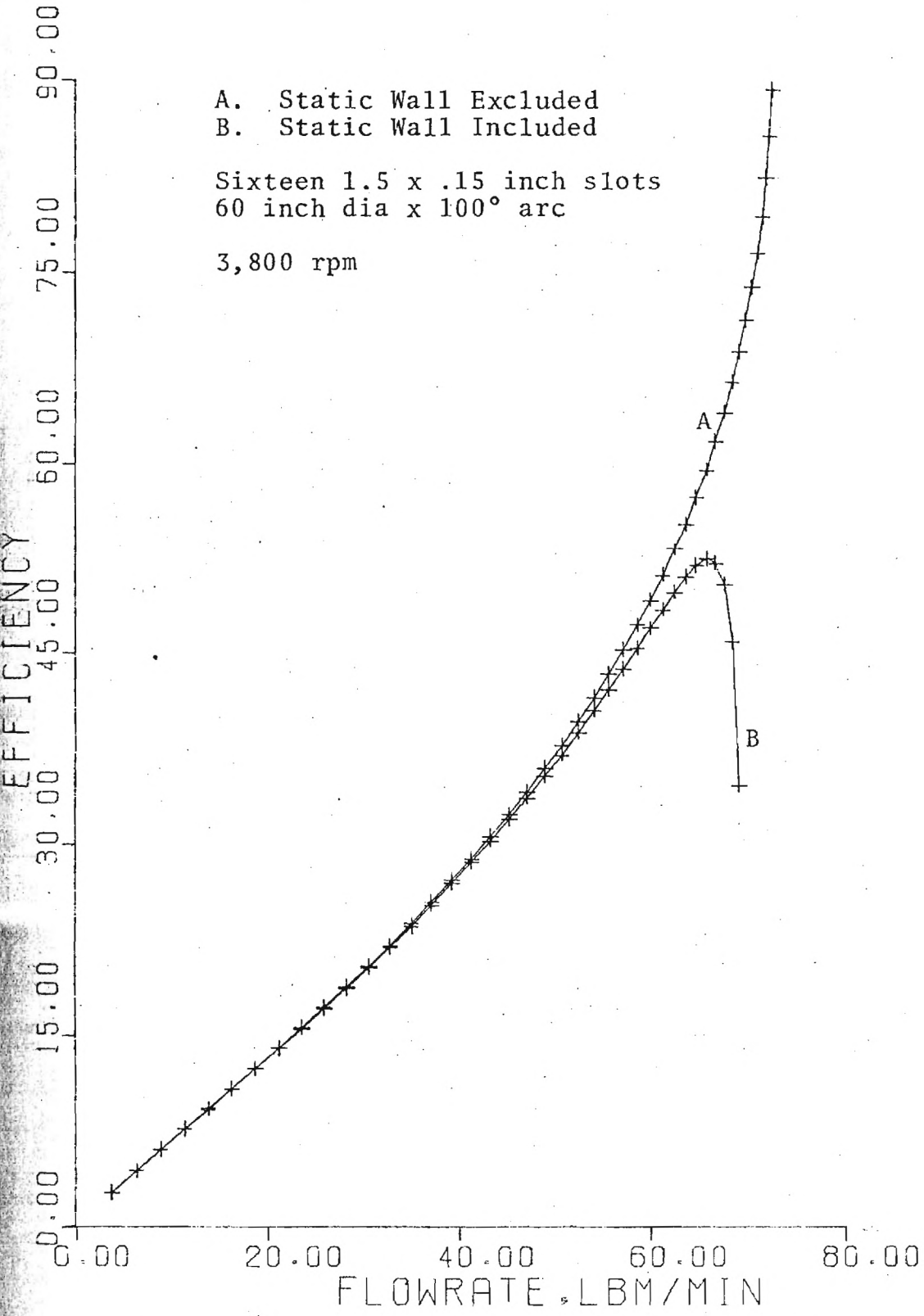

Figure 4-6. Compressor Performance

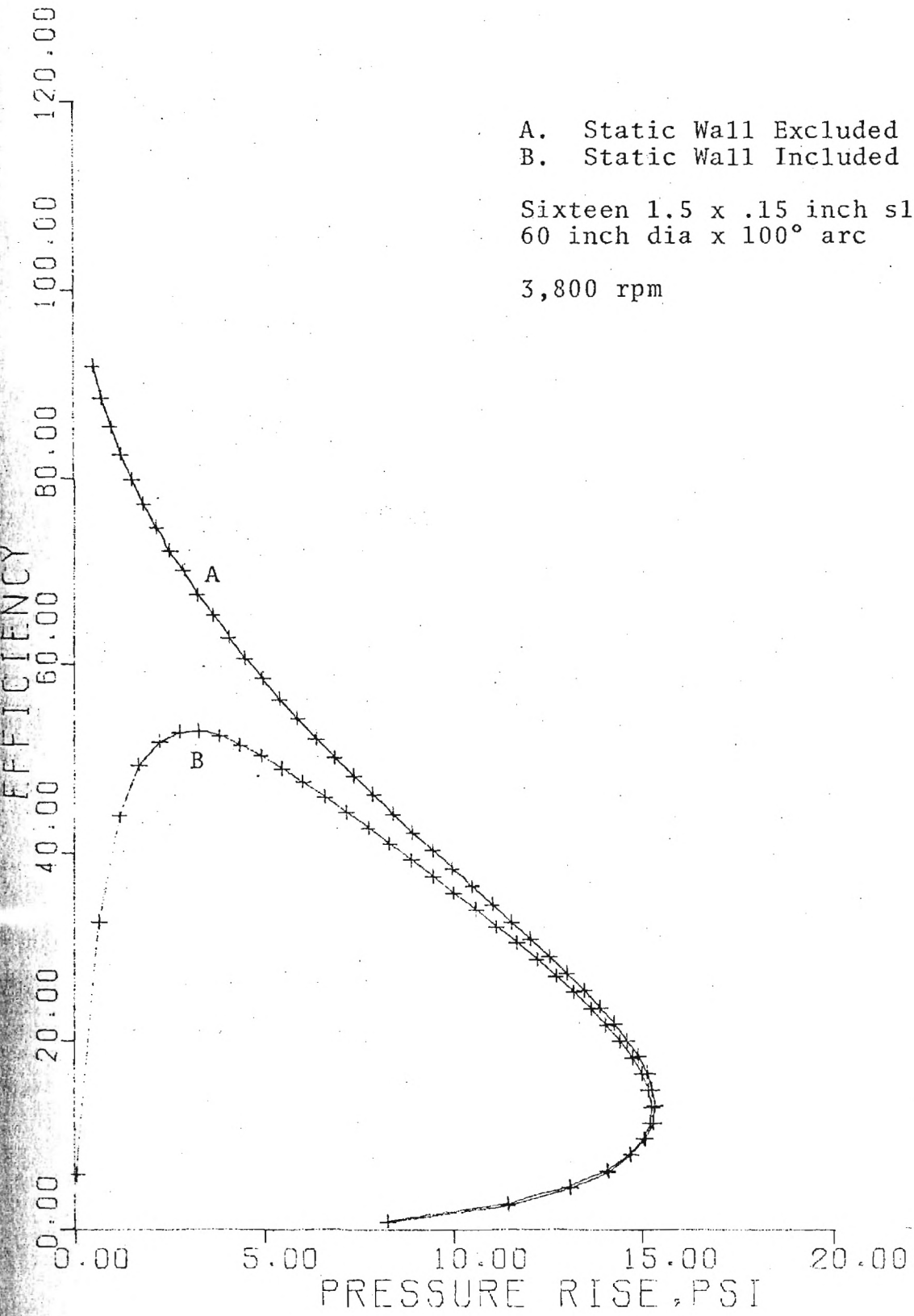

Figure 4-7. Compressor Performance

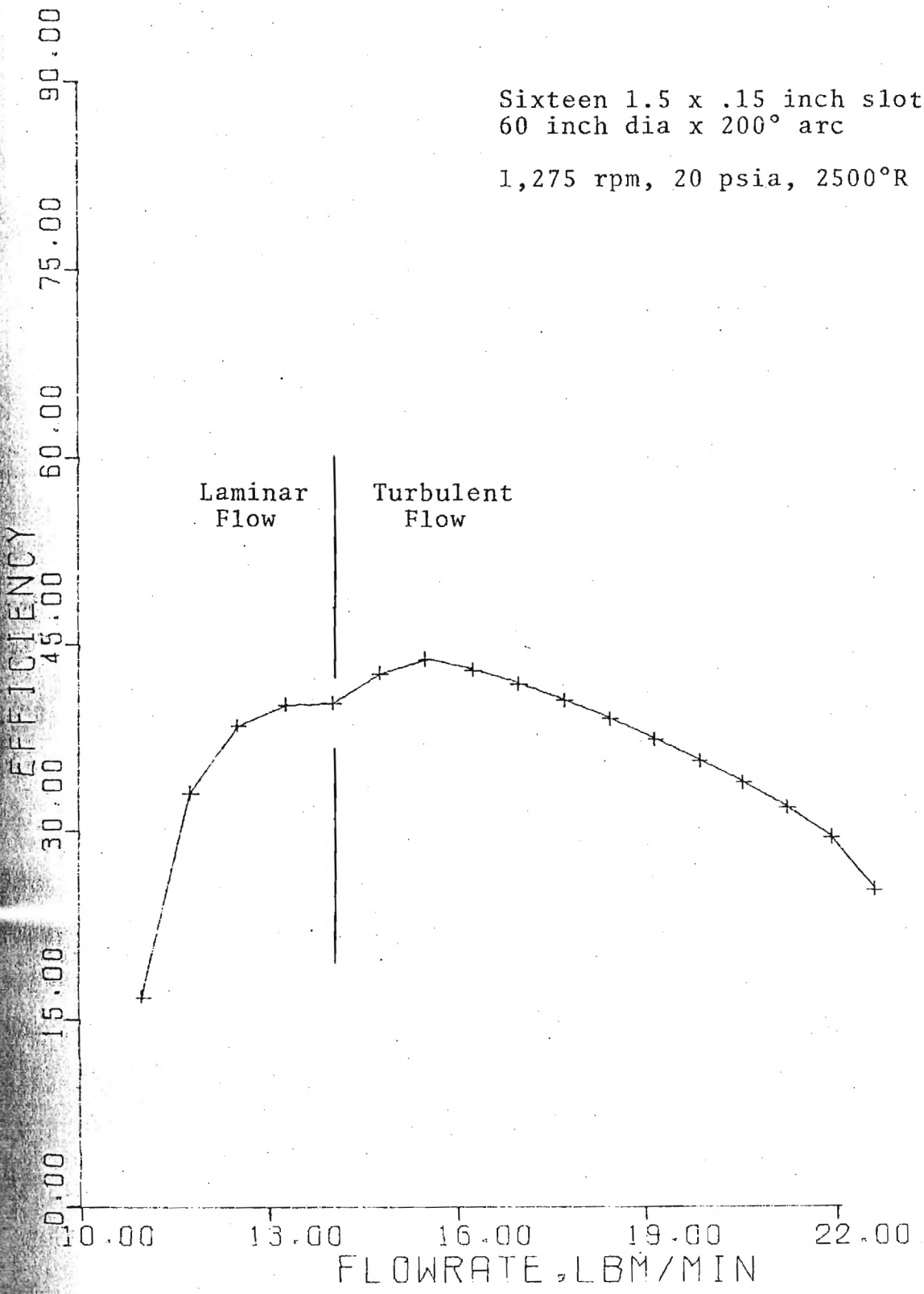

Figure 4-8. Turbine Performance

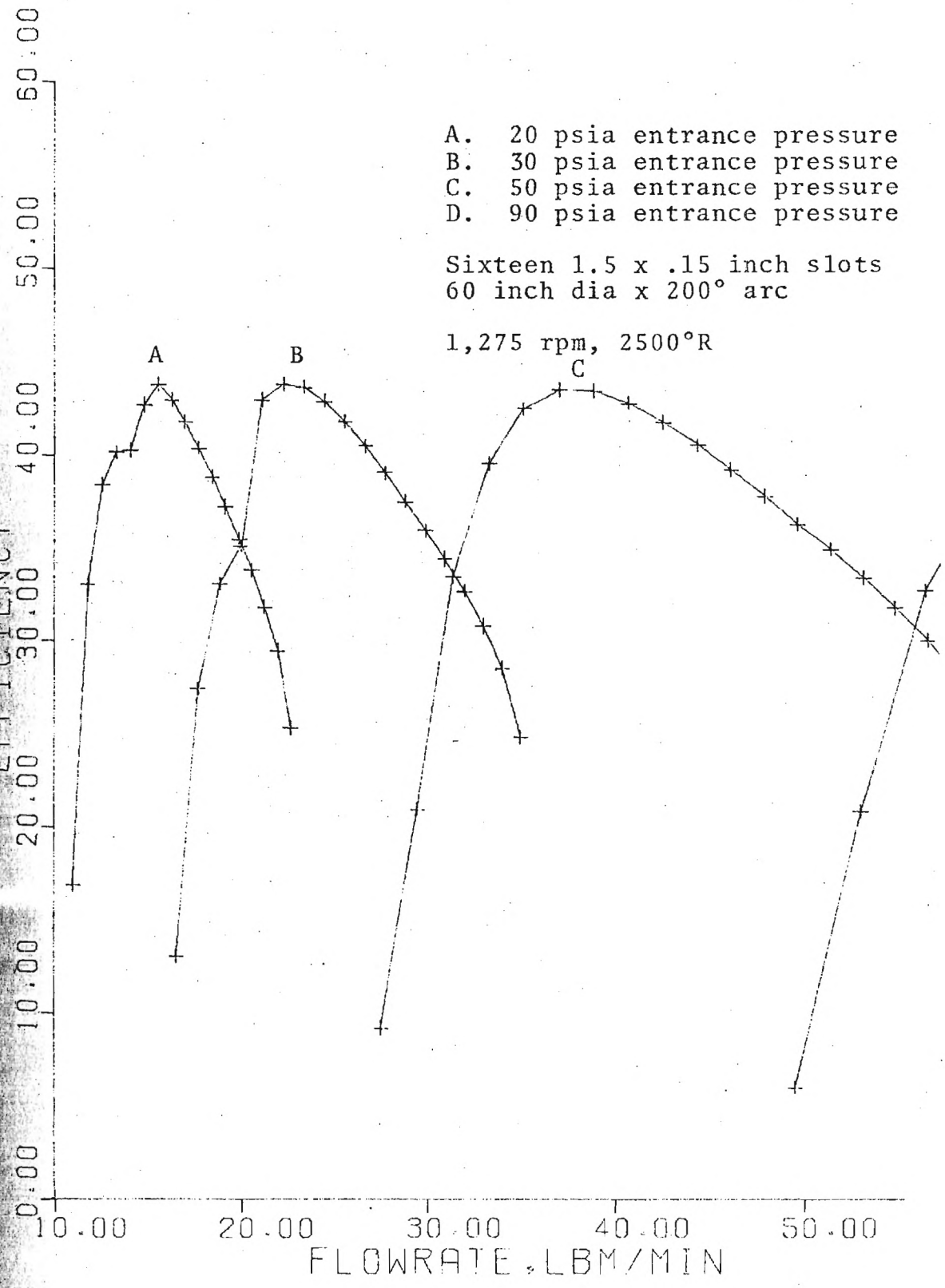

Figure 4-9. Turbine Performance

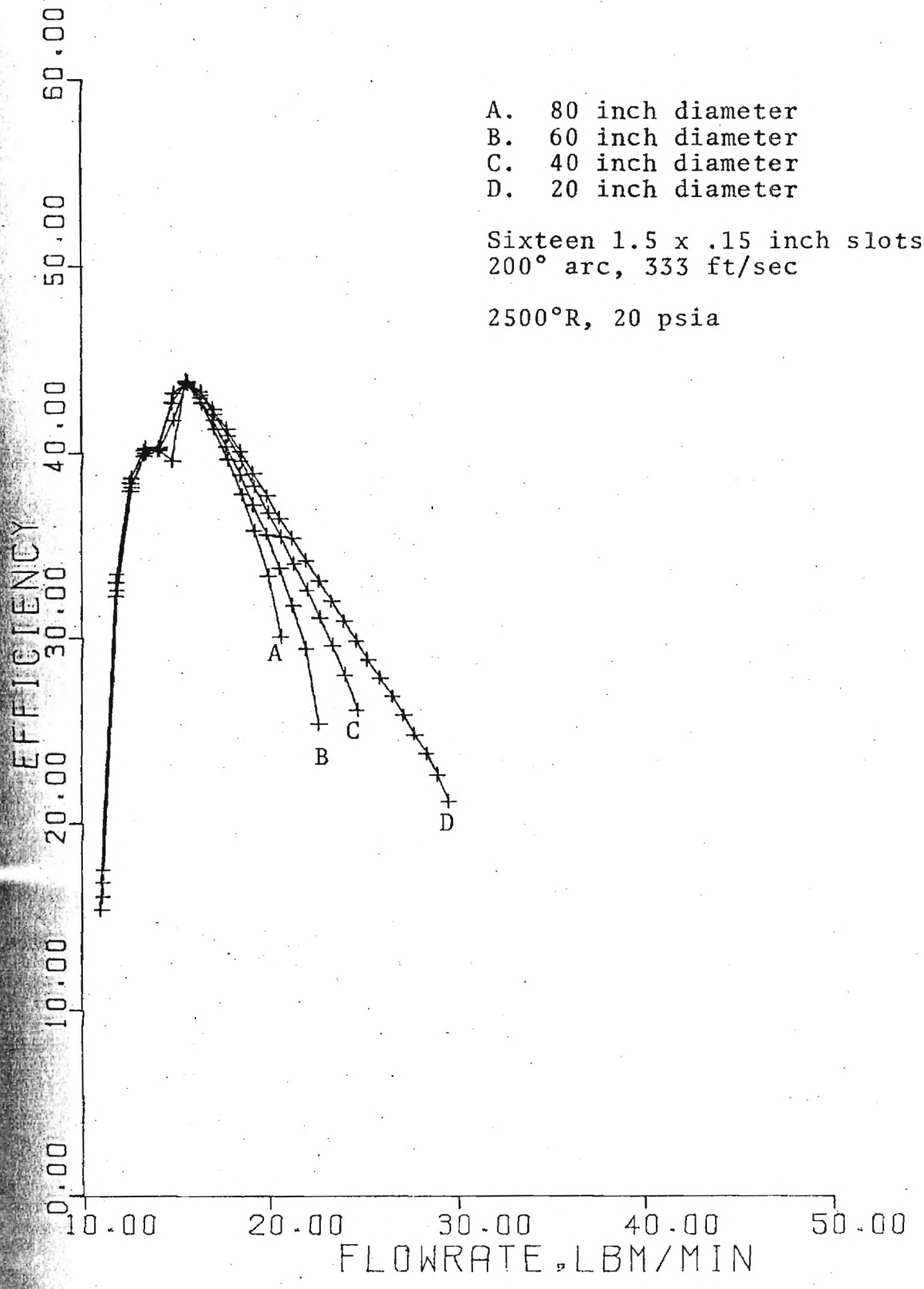

Figure 4-10. Turbine Performance

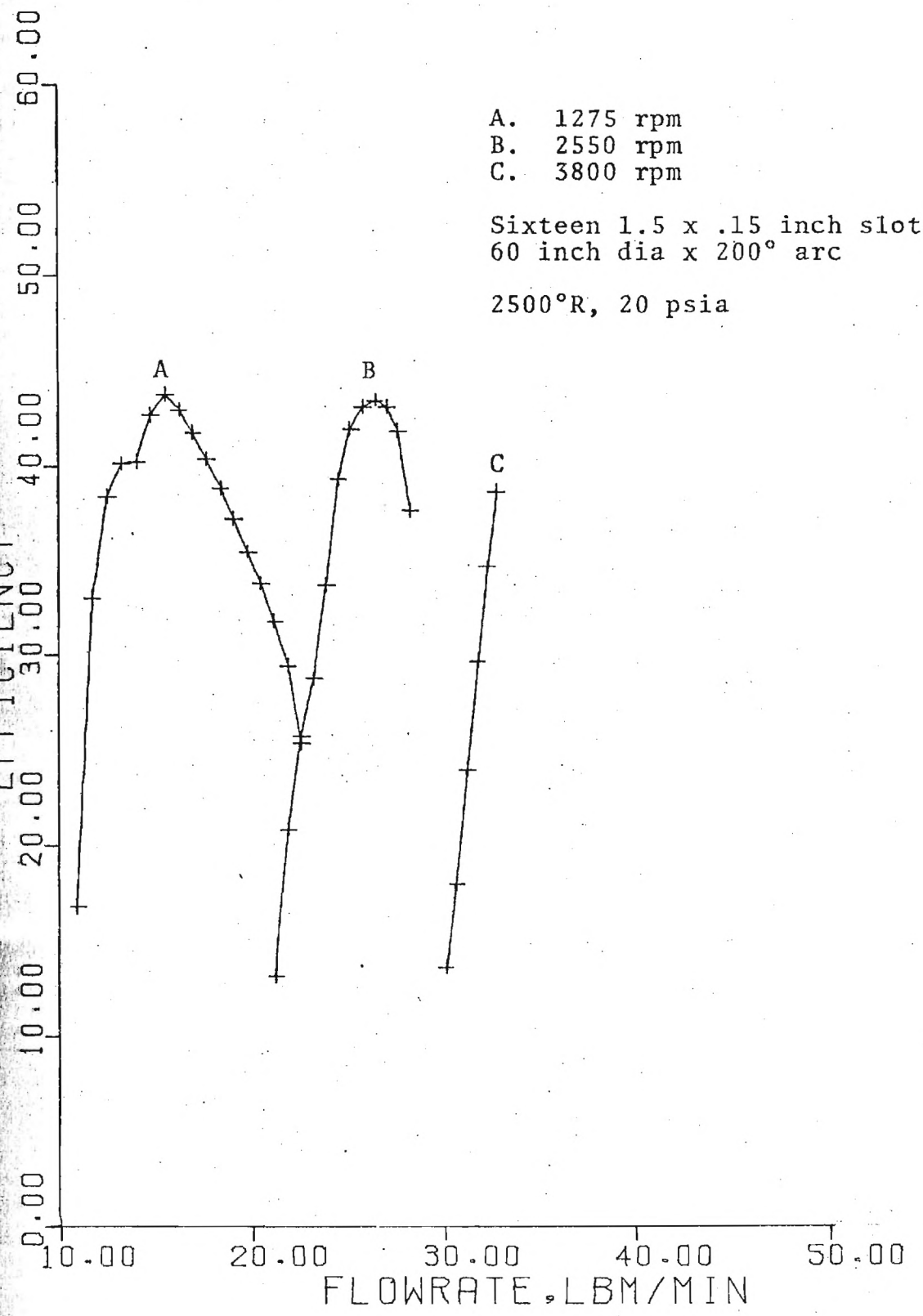

Figure 4-11. Turbine Performance

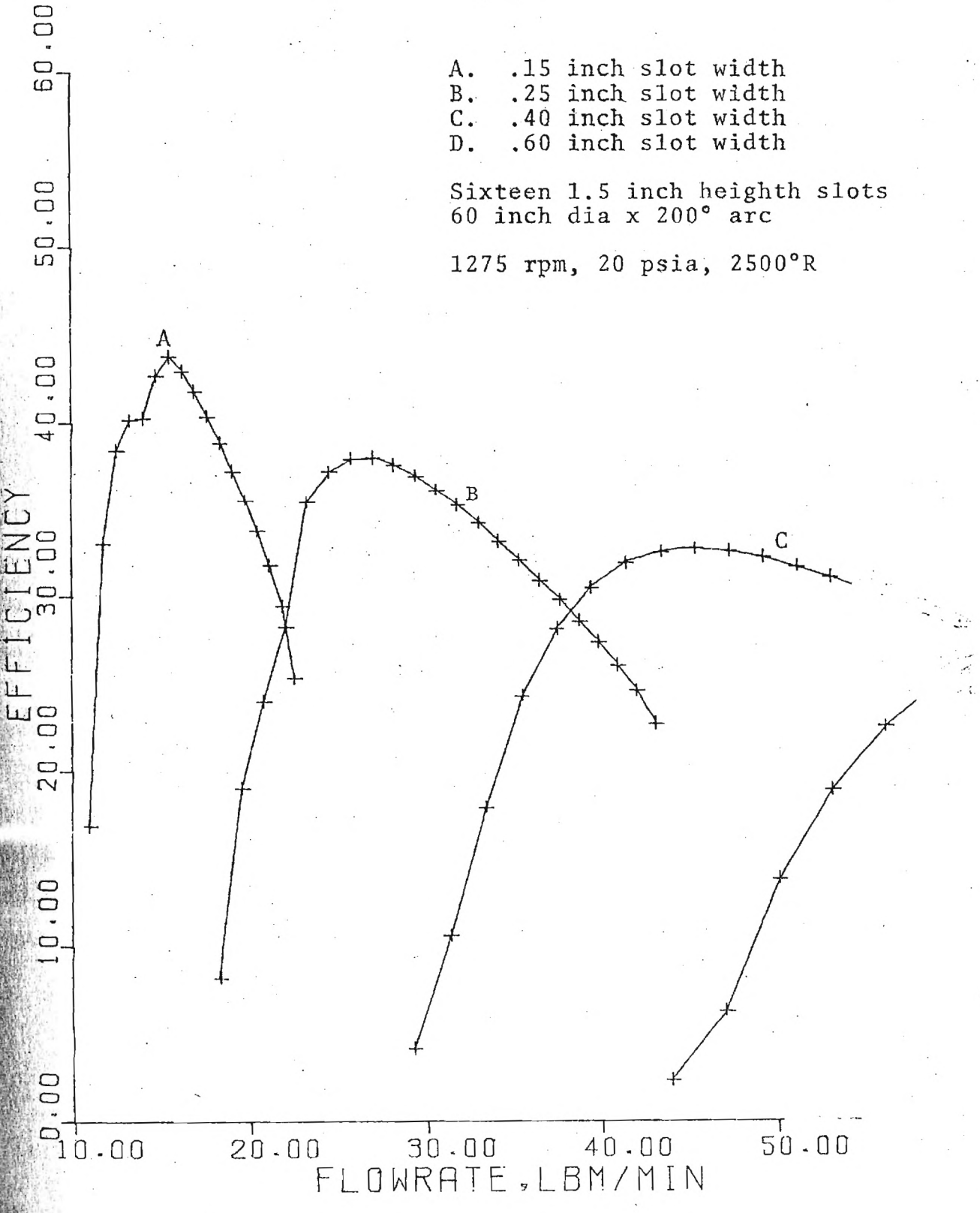

Figure 4-12. Turbine Performance

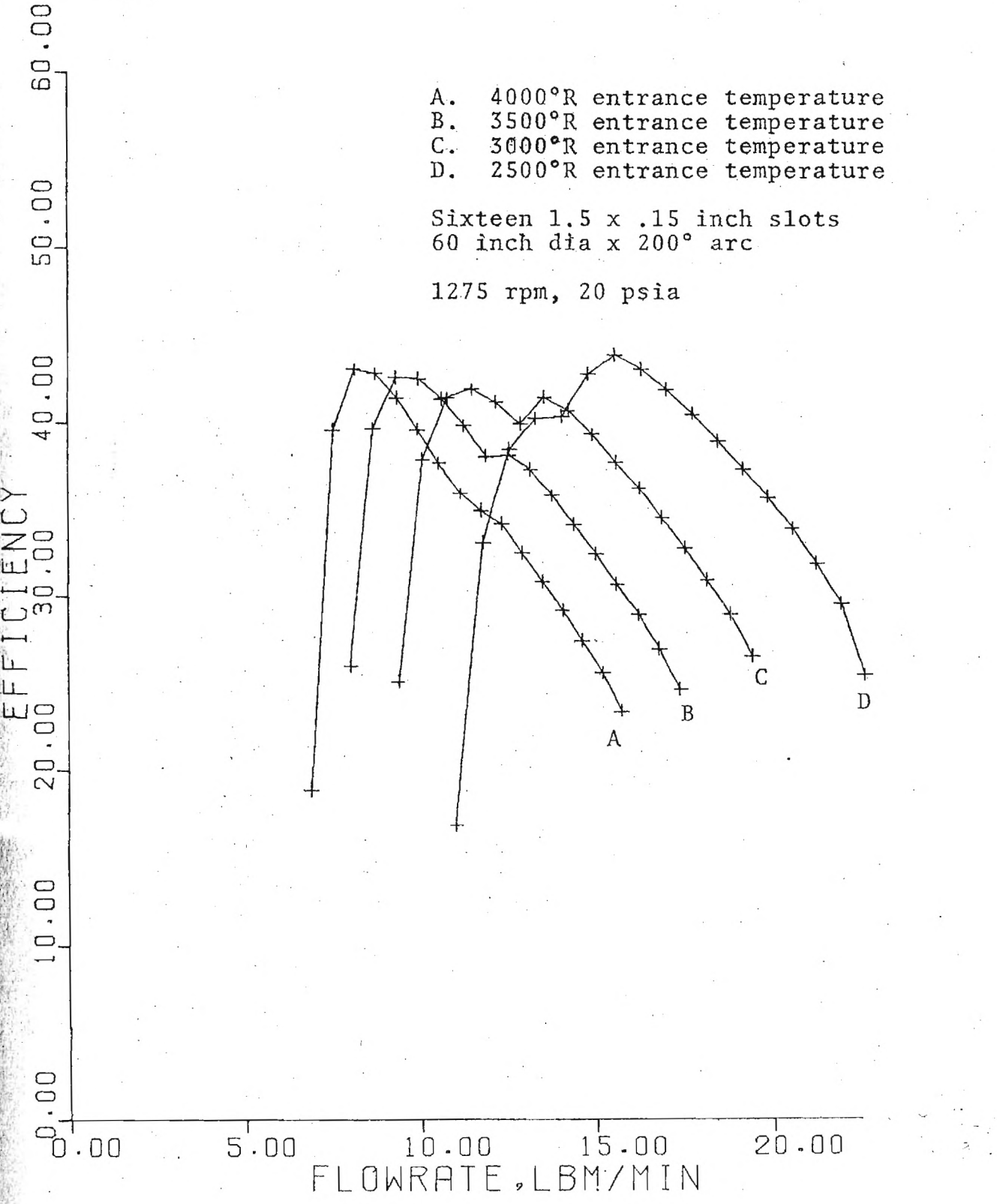

Figure 4-13. Turbine Performance

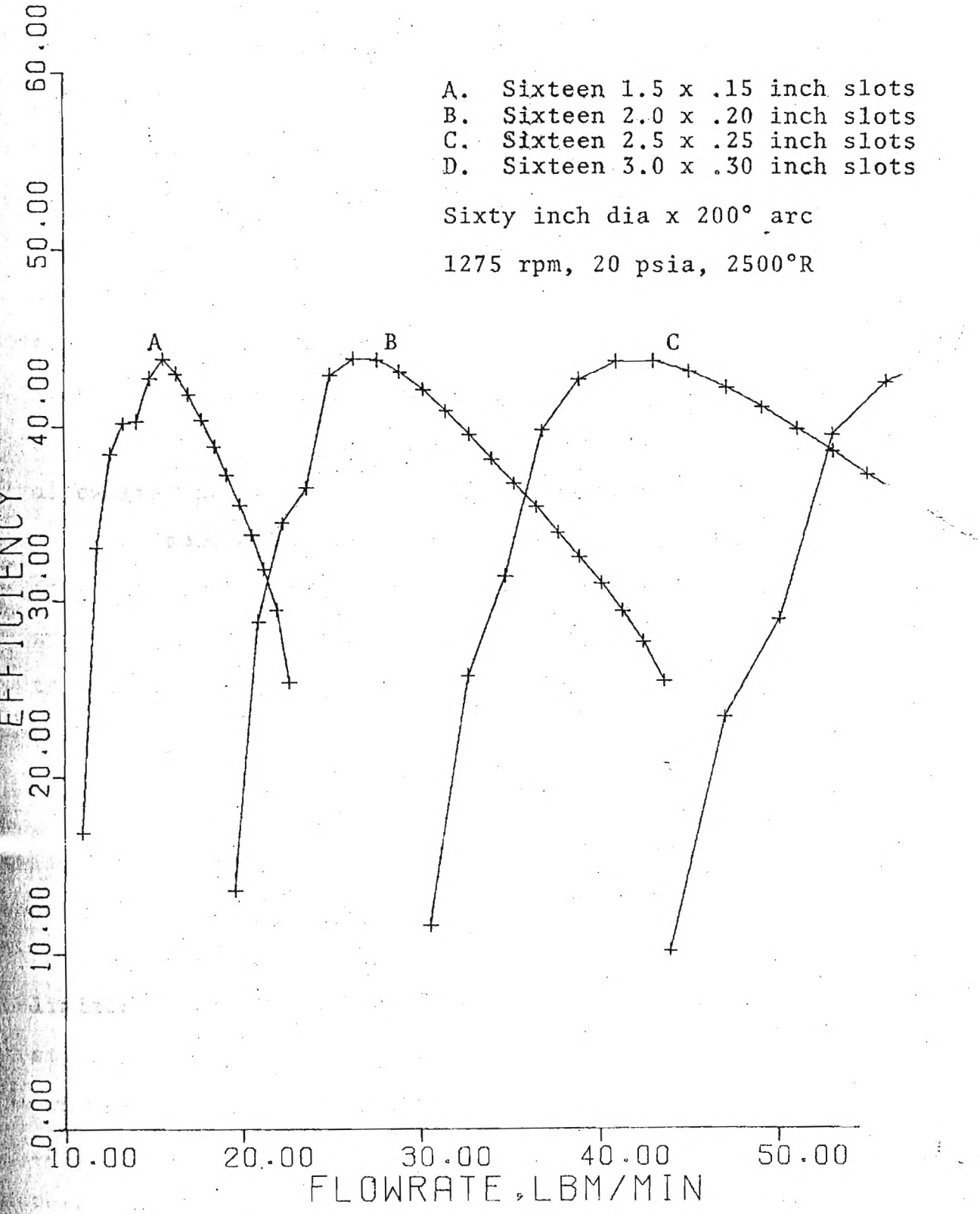

Figure 4-14. Turbine Performance

With exception of the slot width (Figure 4-12), the parameters have only minor effect on peak efficiency. Henceforth a minimum slot width of 1/10 the slot height will be considered. Geometry and rotational speed of the turbine do have significant effect on the output as reflected in the pressure drop (Figures 4-15 and 4-17). Even more meaningful are Figures 4-16, 4-18 and 4-19 which reveal a tradeoff between pressure ratio and efficiency. The inverse relationship was expected, considering that greater pressure ratios allow greater deviation from the ideal isentropic case.

Figure 4-18 shows combined efficiency and output increasing with turbine size or diameter for a given rim speed. Hence, the efficiency, output, and size (cost) of the turbine are all mutual tradeoffs. The same tradeoffs apply to a viscous rotating compressor. Figures 4-20 through 4-25 show a maximum compressor efficiency of 58 percent and a maximum pressure increase of 25 psi.

4-4. Variable Area Turbine

The pressure ratios of the viscous turbines are limited by choking. A concept of including a comb in the static housing to vary turbine flow area as a function of arc position has potential for increasing turbine pressure ratios. Increasing flow area, decreases gas velocity retarding choking and allowing greater entrance mach numbers and therefore greater relative velocity between the gas and

A. 1275 rpm
B. 2550 rpm
C. 3800 rpm

Sixteen 1.5 x .15 inch slots
60 inch dia x 200° arc

2500°R, 20 psia

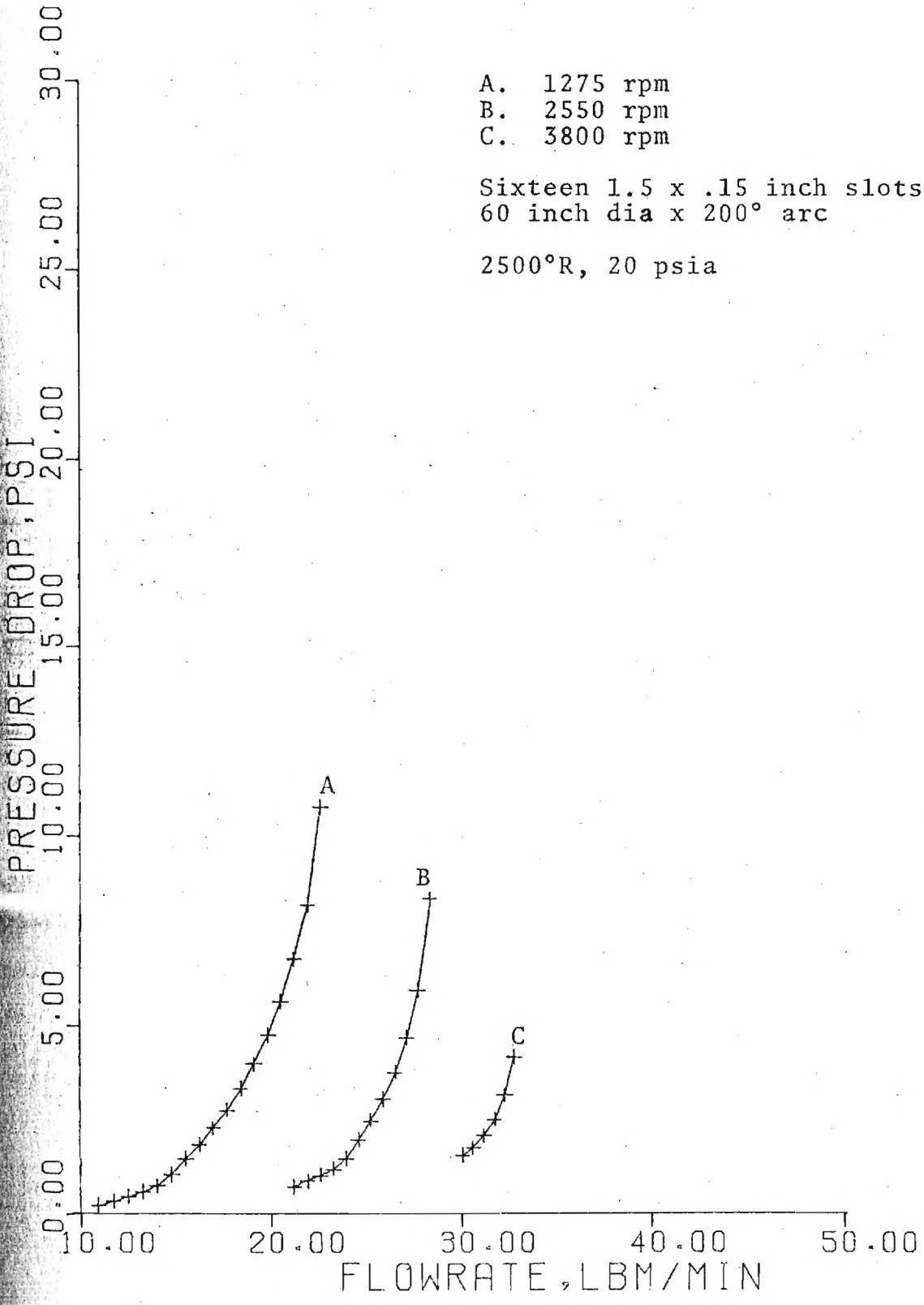

Figure 4-15. Turbine Performance

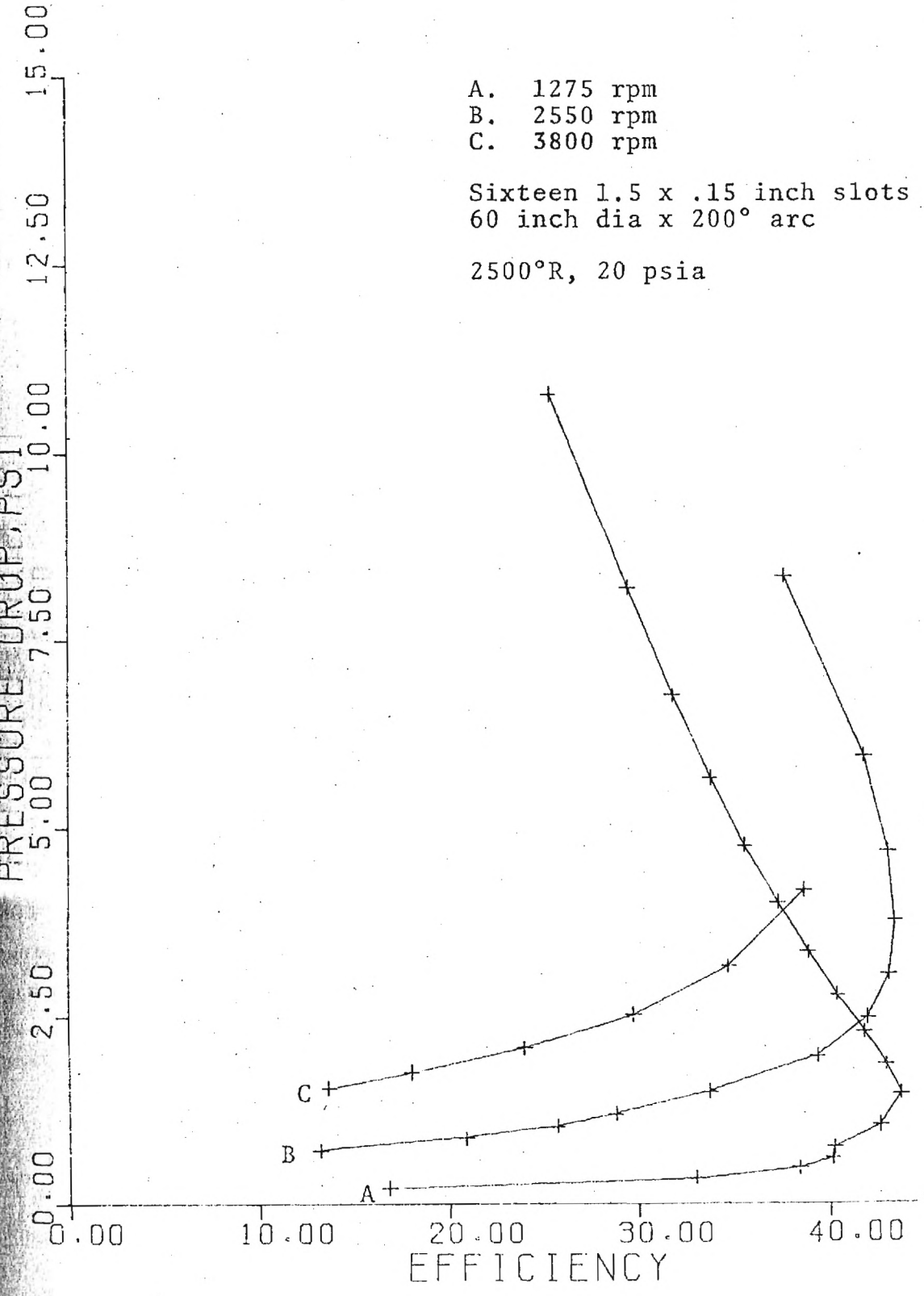

Figure 4-16. Turbine Performance

A. 80 inch diameter
B. 60 inch diameter
C. 40 inch diameter
D. 20 inch diameter

Sixteen 1.5 x .15 inch slots

200° arc, 333 ft/sec, 2500°R,

20 psia

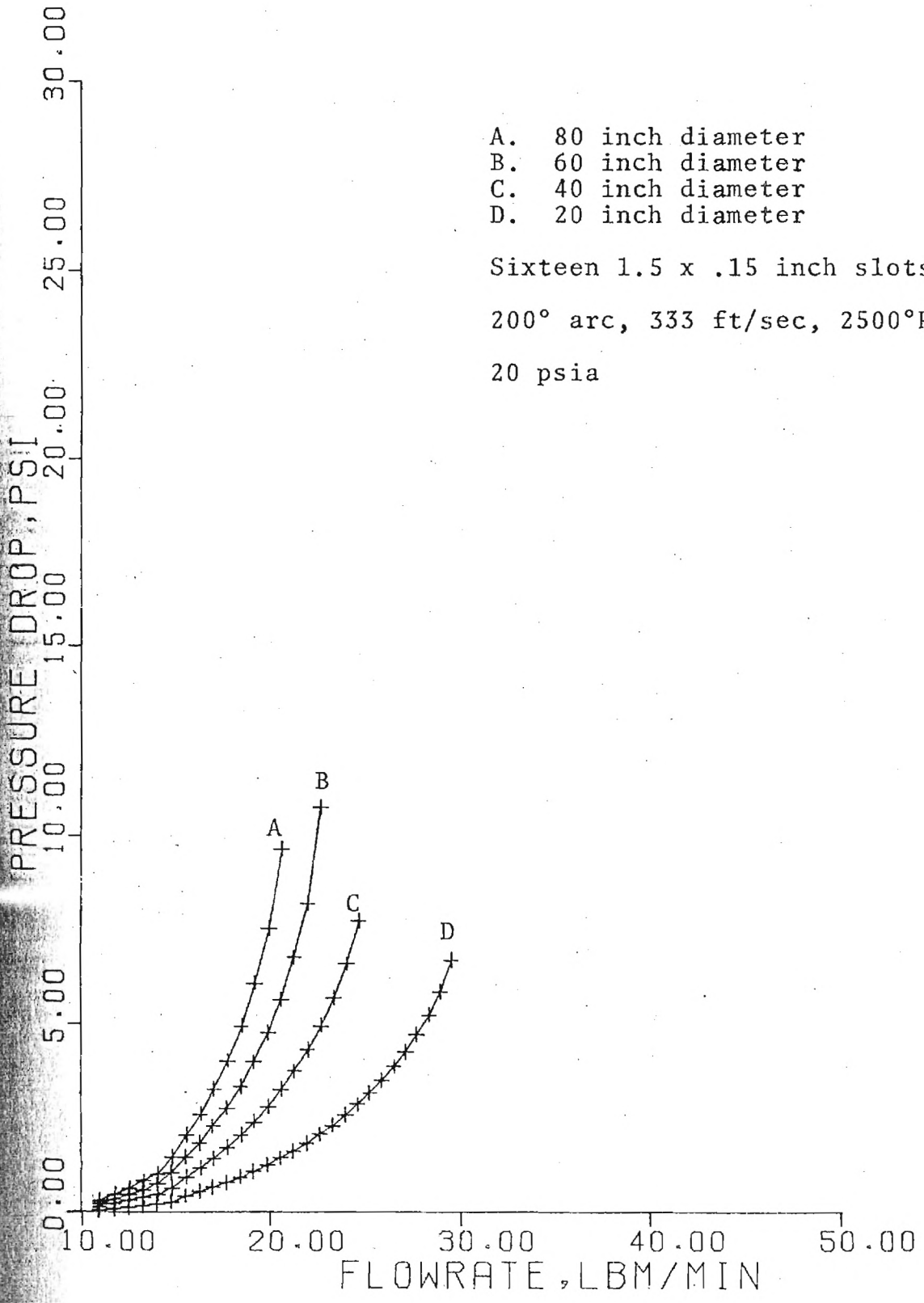

Figure 4-17. Turbine Performance

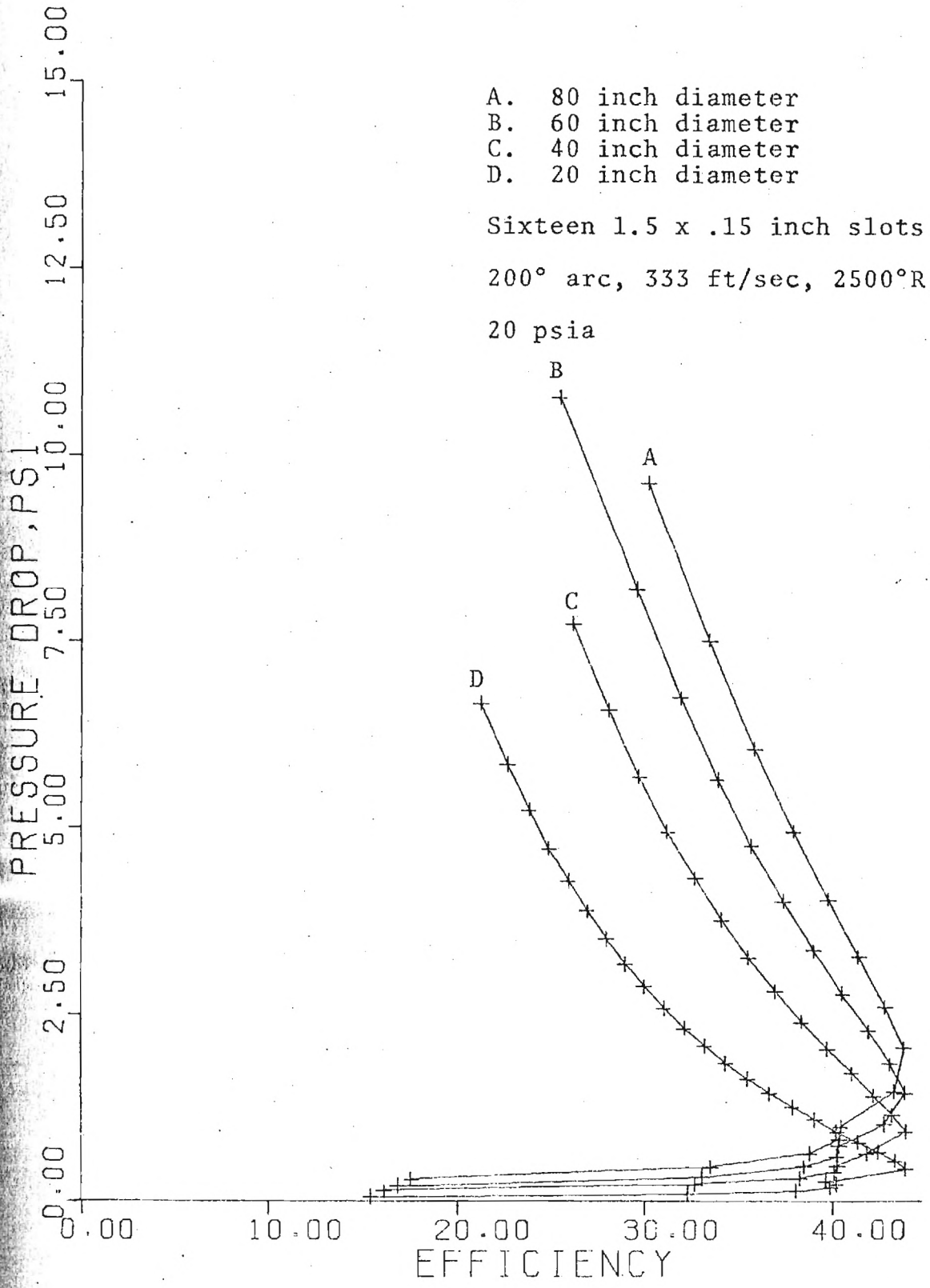

Figure 4-18. Turbine Performance

A. Sixteen 1.5 x .15 inch slots
B. Sixteen 2.0 x .20 inch slots
C. Sixteen 2.5 x .25 inch slots

60 inch dia x 200° arc

1275 rpm, 20 psia, 2500°R

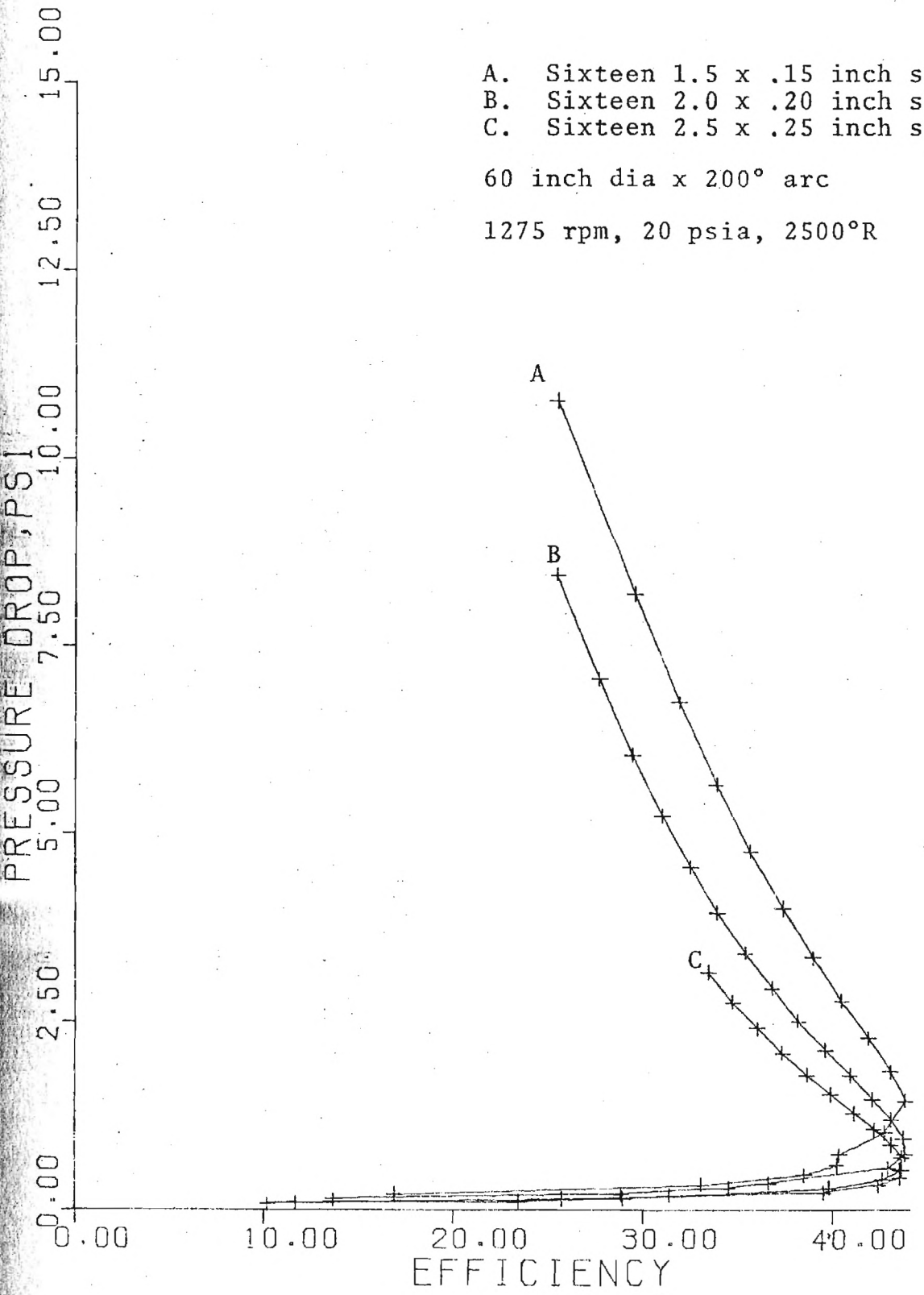

Figure 4-19. Turbine Performance

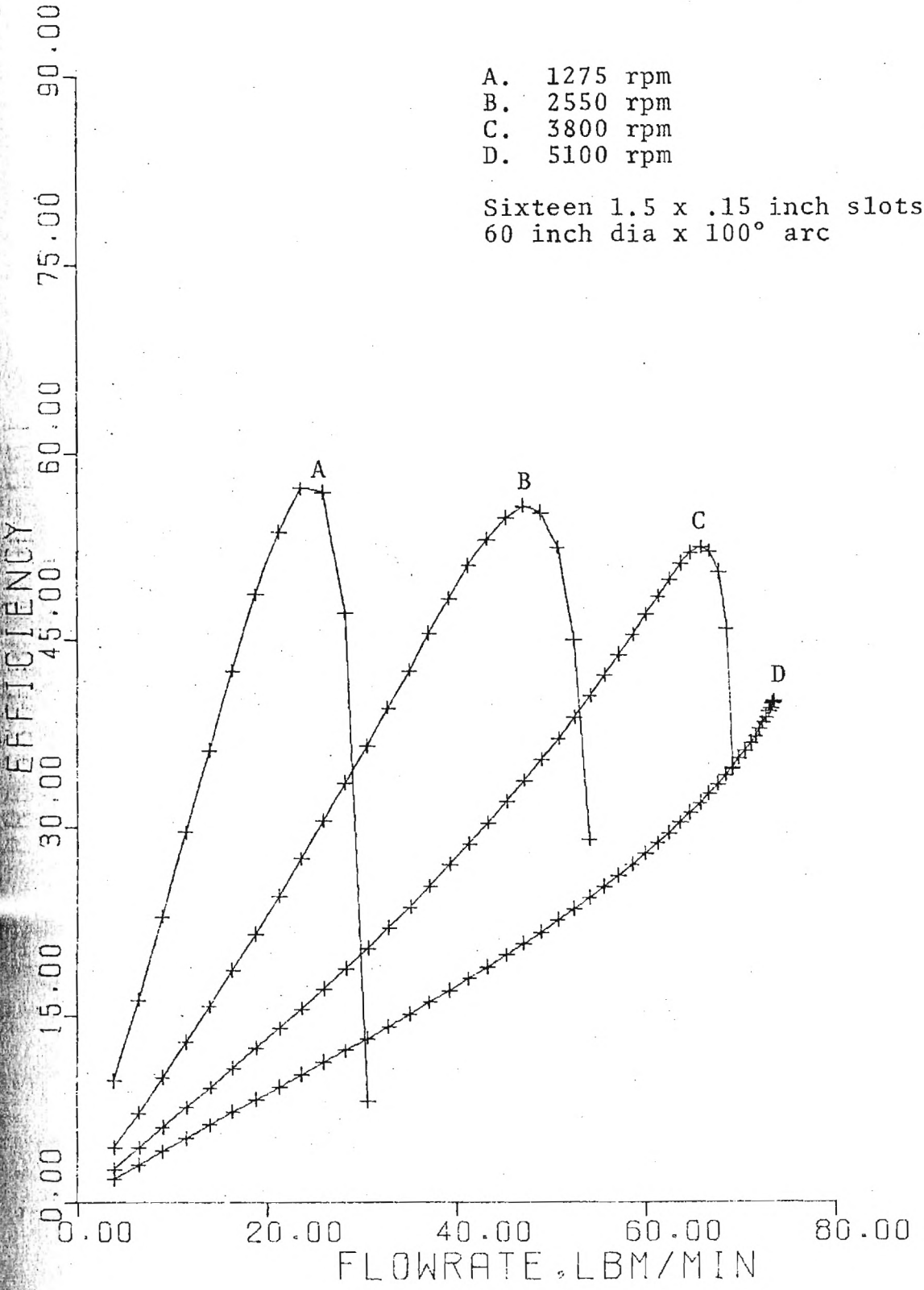

Figure 4-20. Compressor Performance

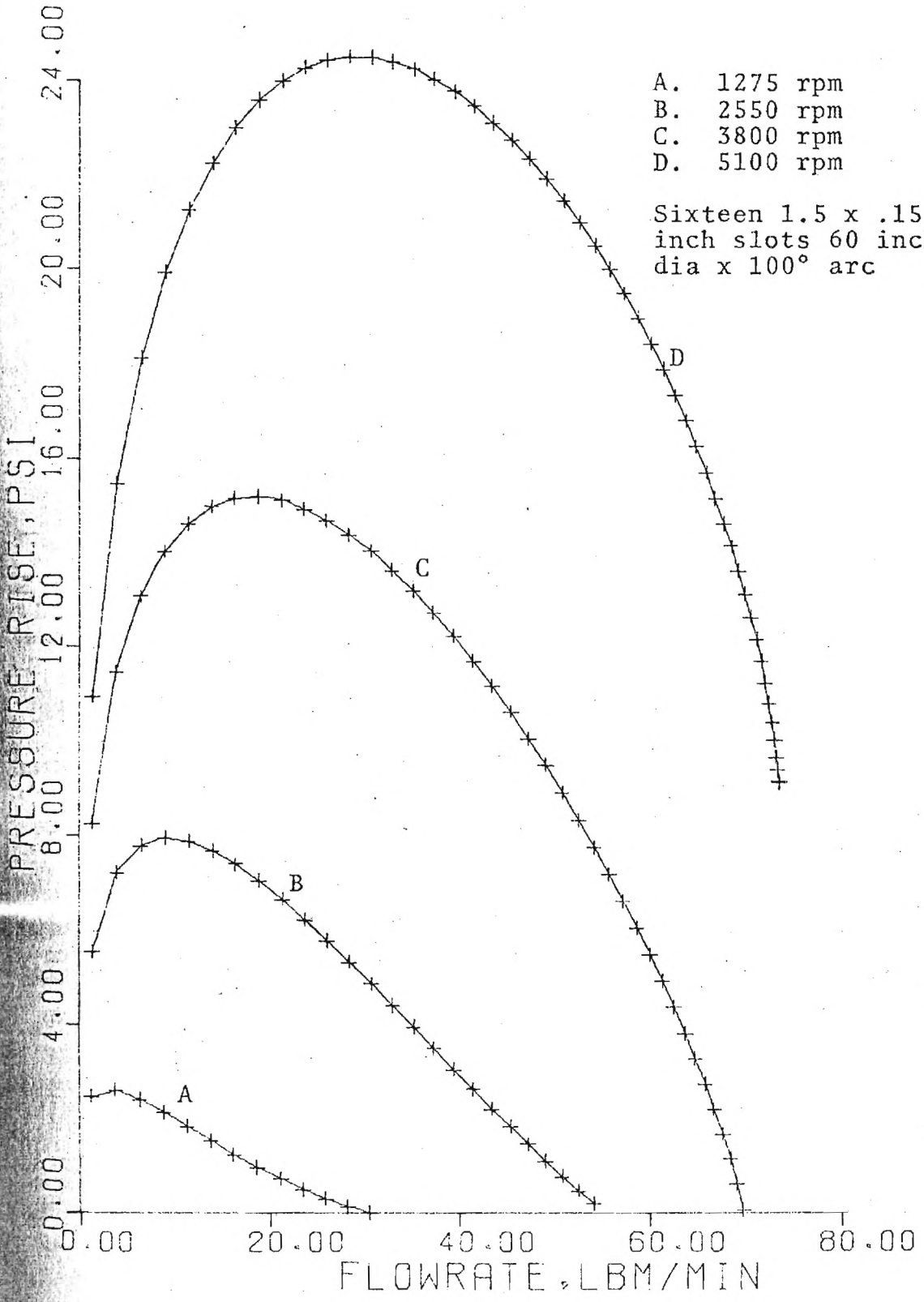

Figure 4-21. Compressor Performance

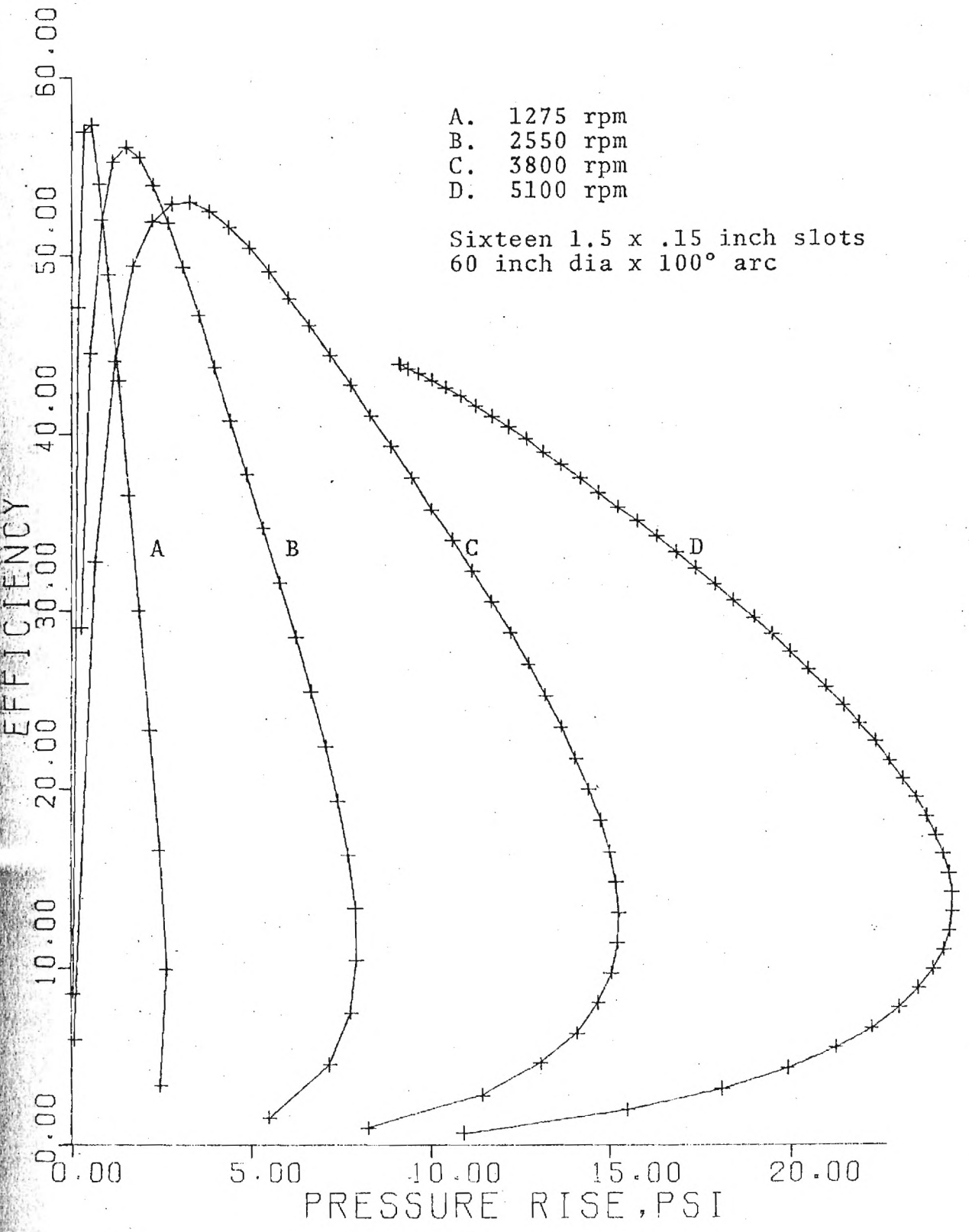

Figure 4-22. Compressor Performance

A. 80 inch diameter
B. 60 inch diameter
C. 40 inch diameter
D. 20 inch diameter

Sixteen 1.5 x .15 inch slots

100° arc, 1000 ft/sec

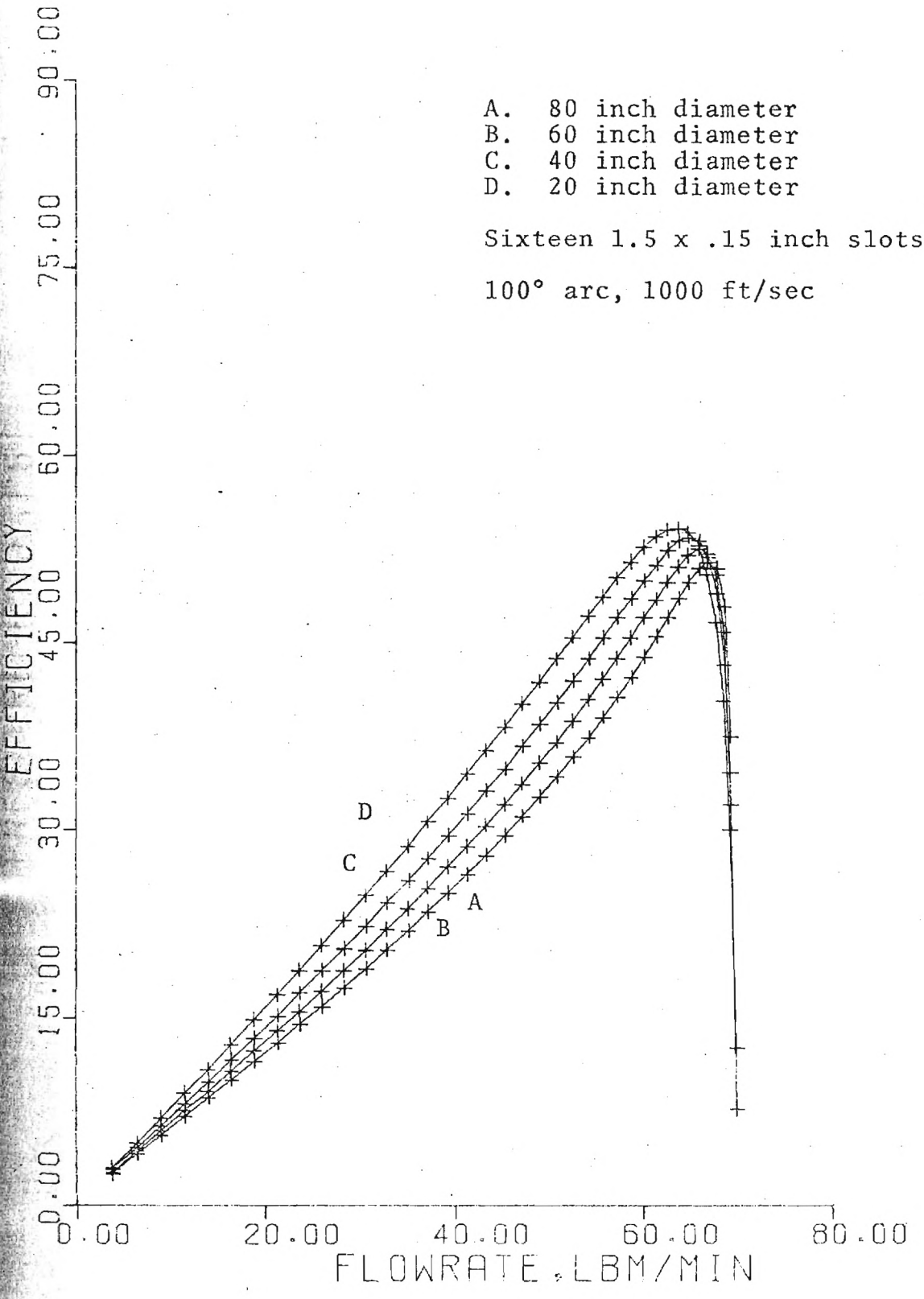

Figure 4-23. Compressor Performance

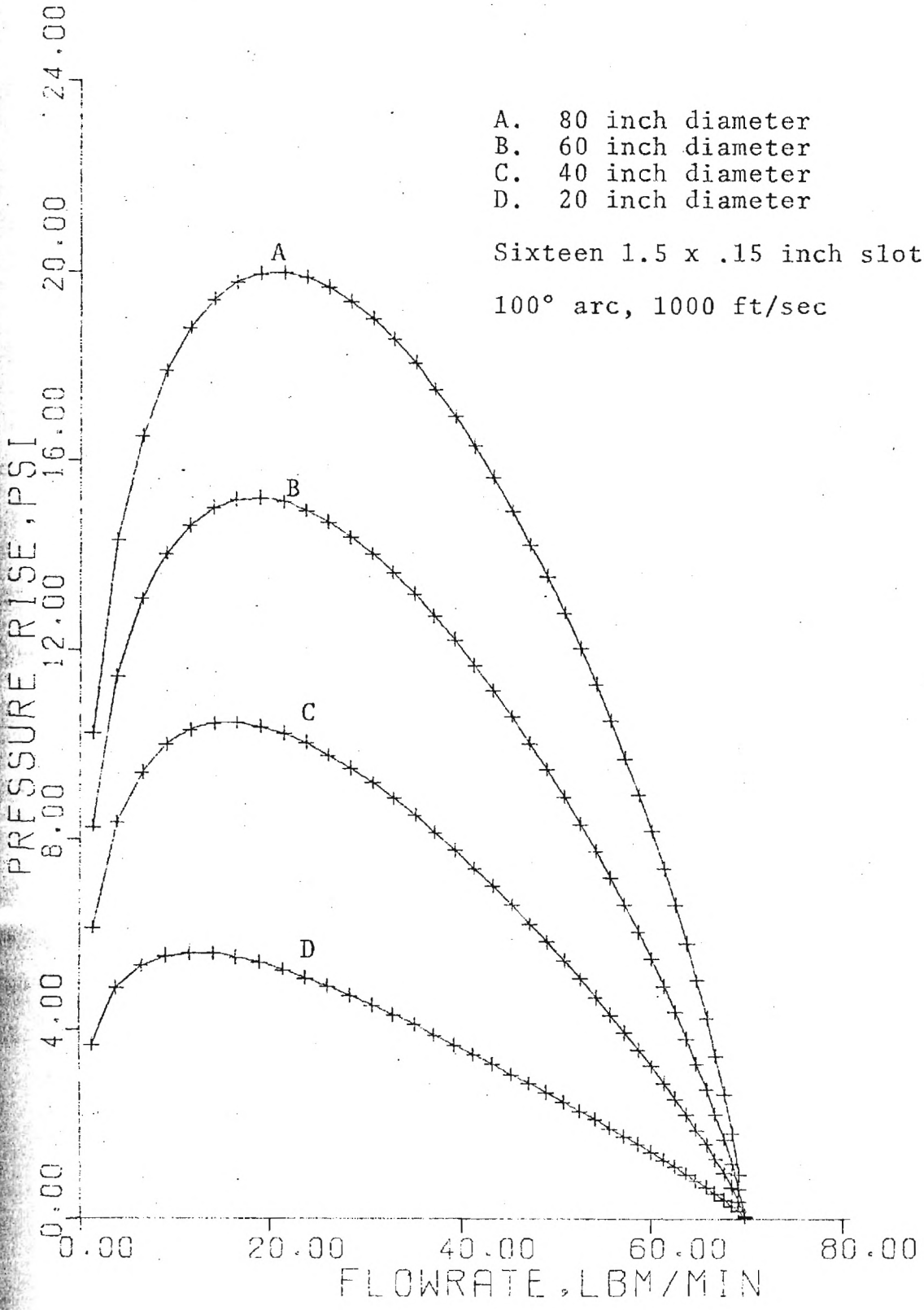

Figure 4-24. Compressor Performance

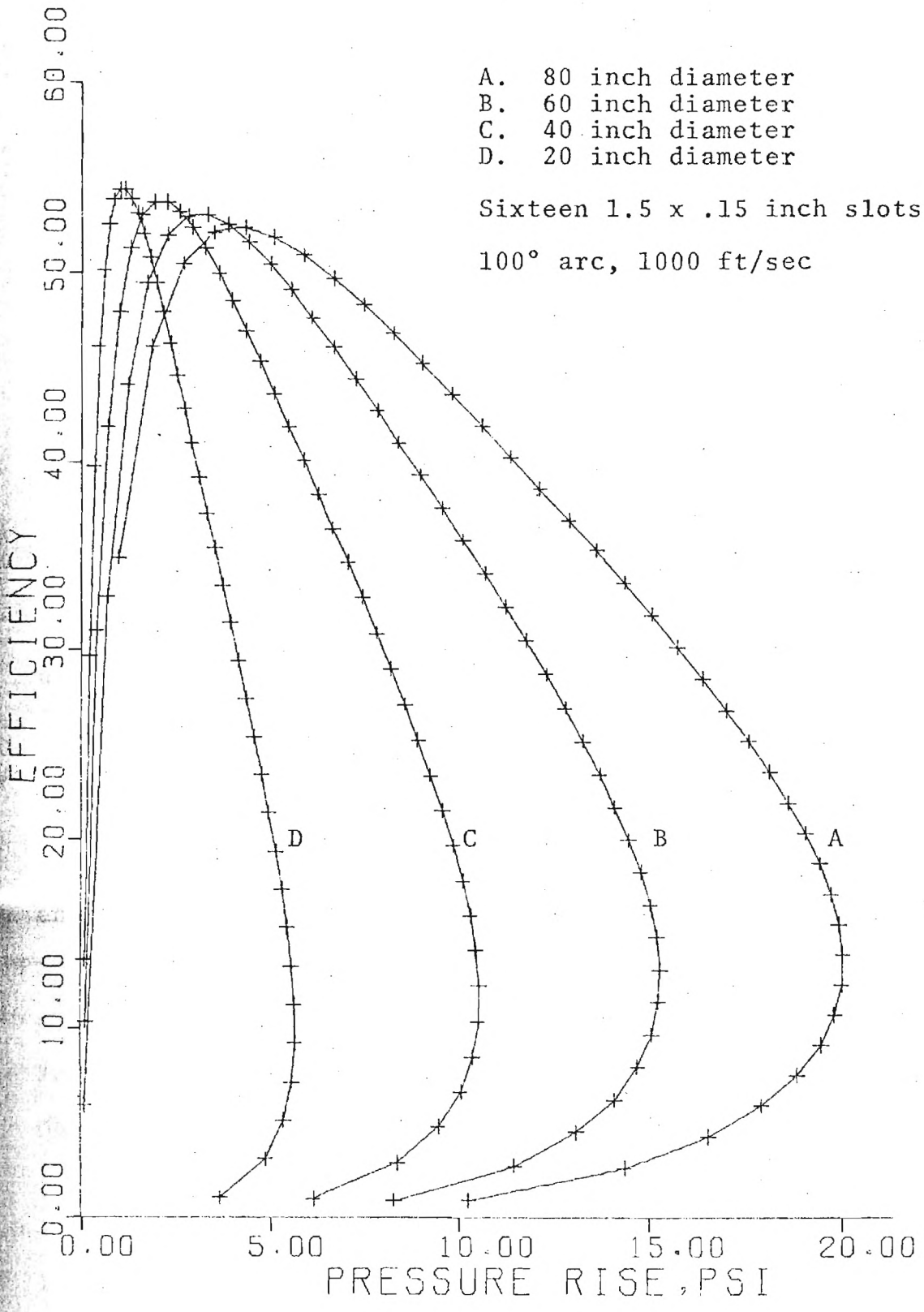

Figure 4-25. Compressor Performance

rotor. Figure 4-26 shows a 60 inch diameter turbine with 1.5 x .15 inch slots operated with and without the comb. The variable area greatly increases pressure ratio, with however a loss of efficiency as indicated in Figure 4-27. The efficiency decrease is largely due to reduction of the effective height to width ratio of the slots. Because the comb takes up a portion of the slot height.

Further construction of the entrance area results in even greater pressure ratios (Figures 4-28). Virtually any pressure ratio desired is attainable, however, with a corresponding decrease in turbine efficiency (Figure 4-29). Of even greater importance, the restricted entrance drastically reduces flowrate which is proportional to unit horsepower output for a given pressure ratio.

4-5. Single Stage Unit Efficiencies

Taking the turbine in conjunction with a compressor and heat source forms a Brayton cycle engine as discussed in Section 2-5. Such an engine utilizing a viscous compressor and turbine (see Figure 4-30) was evaluated. Due to combined low turbine and compressor efficiencies and difficulty in matching performance parameters, unit efficiencies were very low. The maximum discovered was .51 percent at .53 horsepower. Attempts to increase output resulted in negative efficiency. The program is included in Appendix C.

More promising is the possibility of connecting the

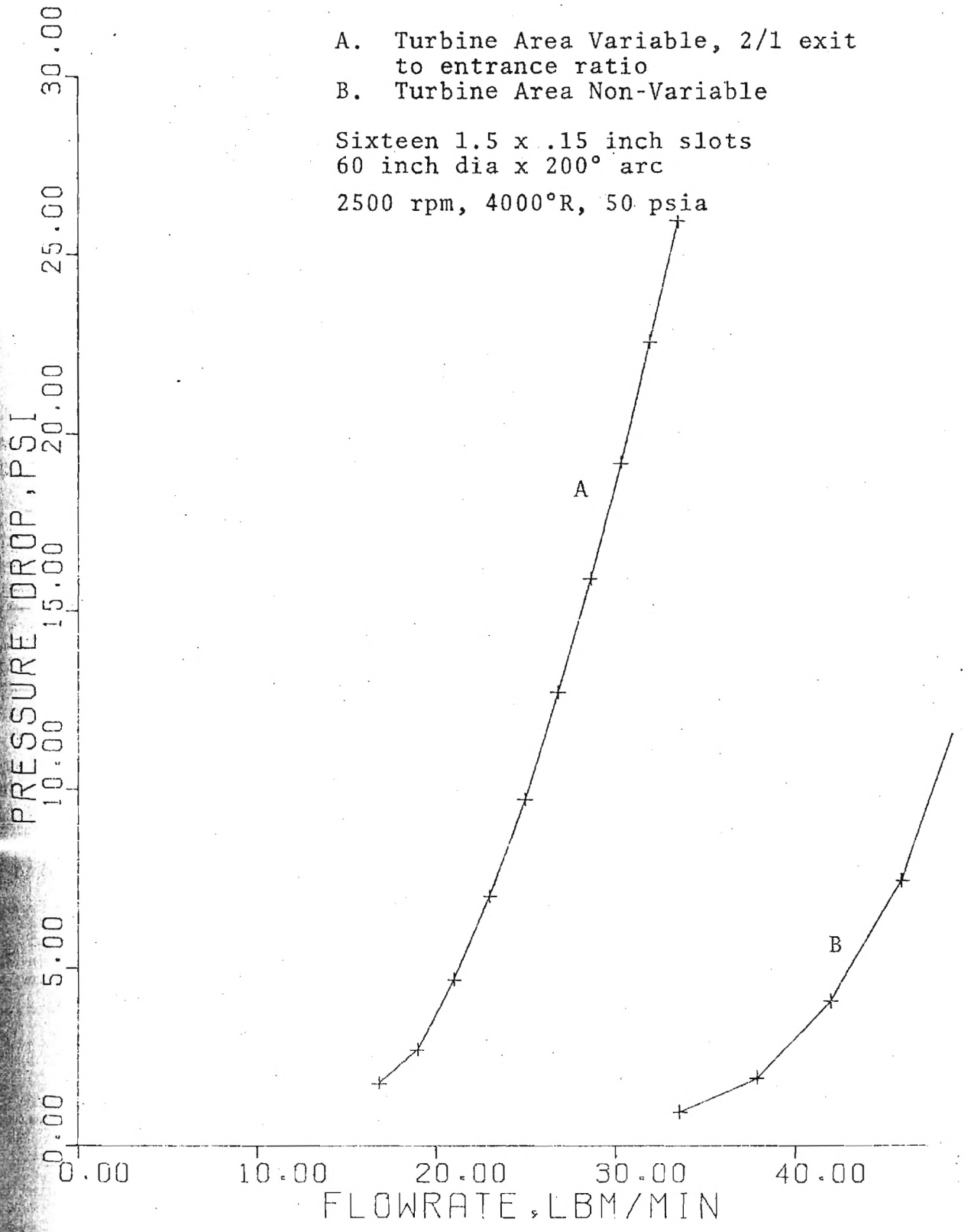

Figure 4-26. Comparison of Variable Area and Regular Turbines

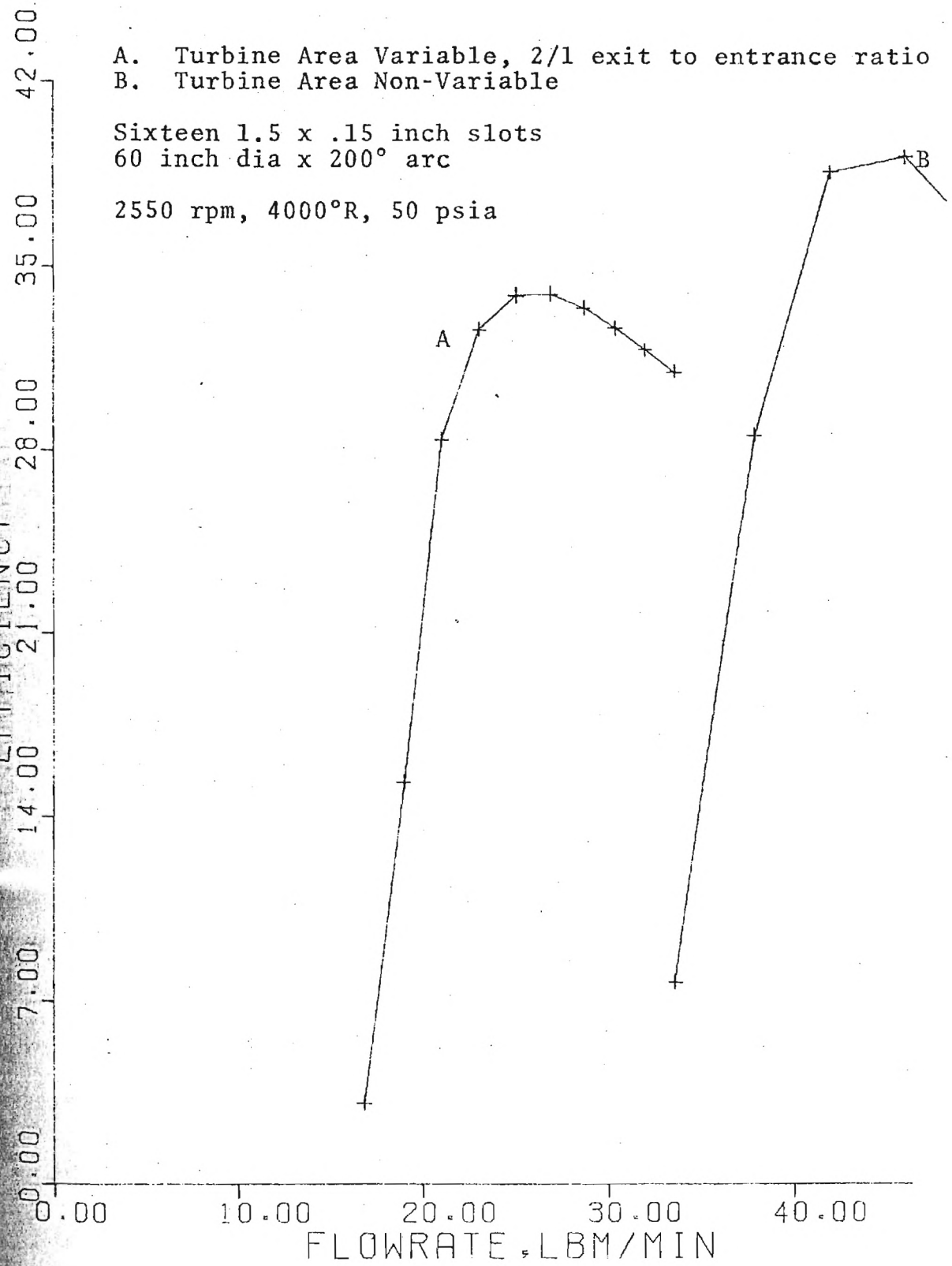

Figure 4-27. Comparison of Variable Area and Regular Turbines

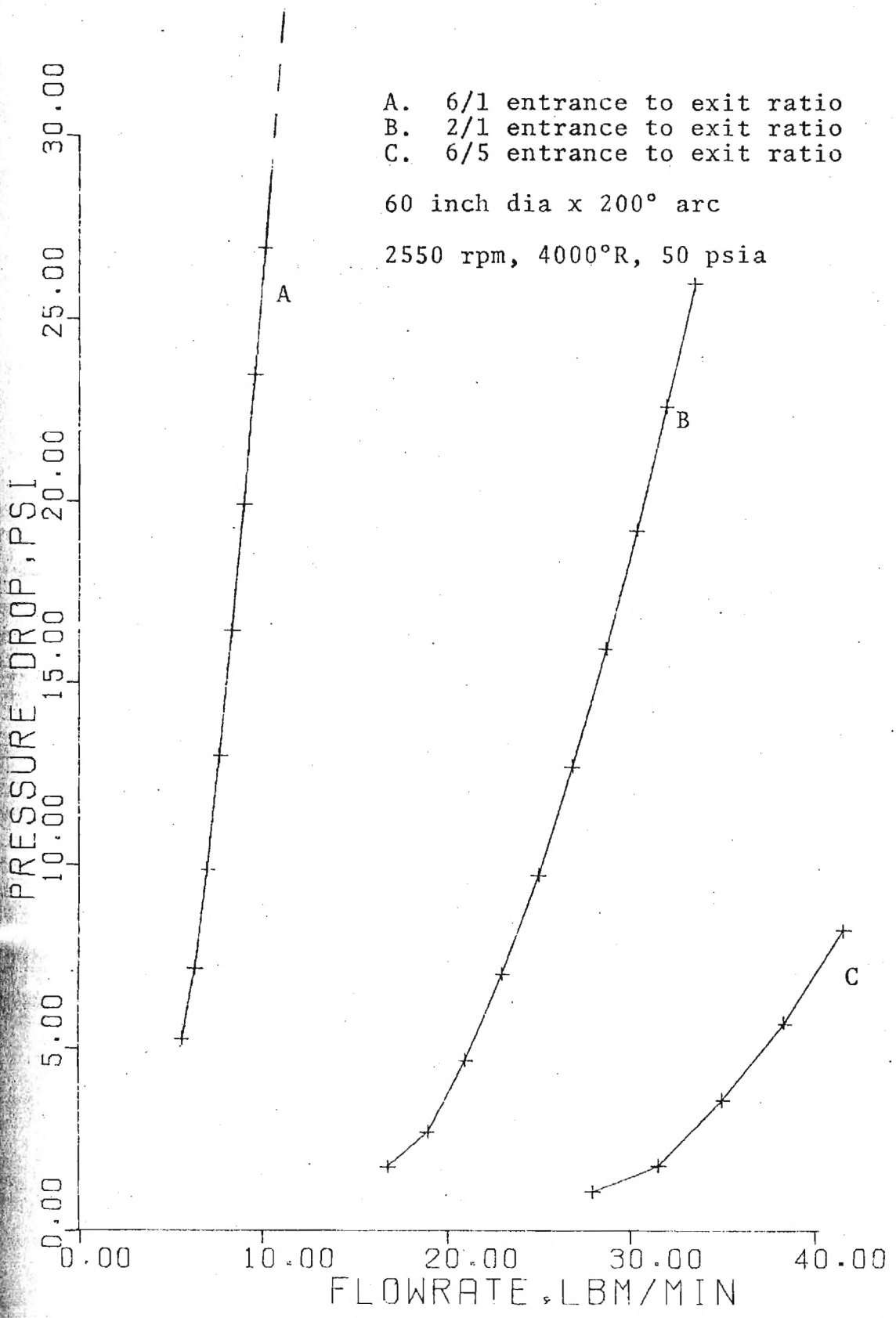

Figure 4-28. Variable Area Turbine Performance

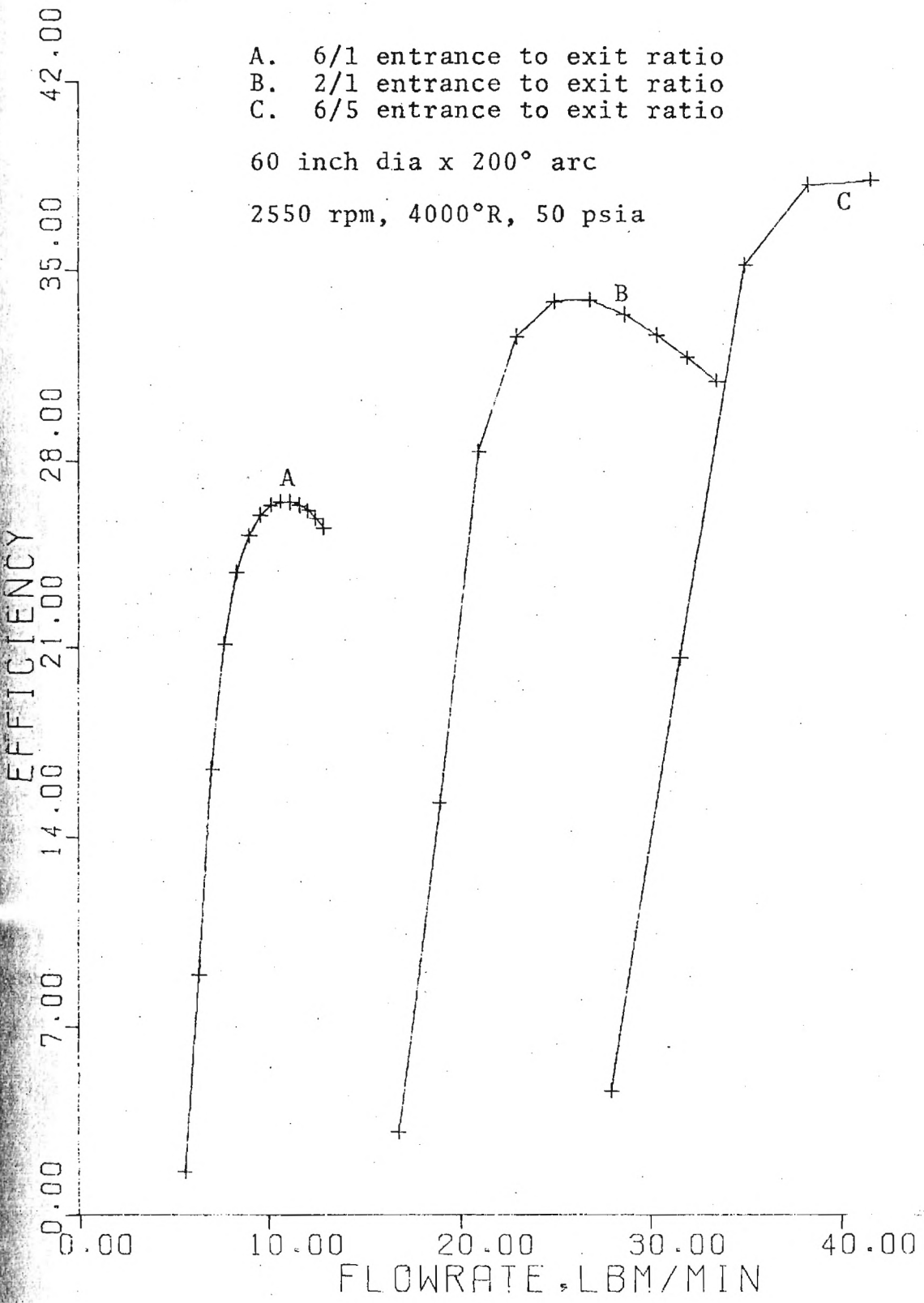

Figure 4-29. Variable Area Turbine Performance

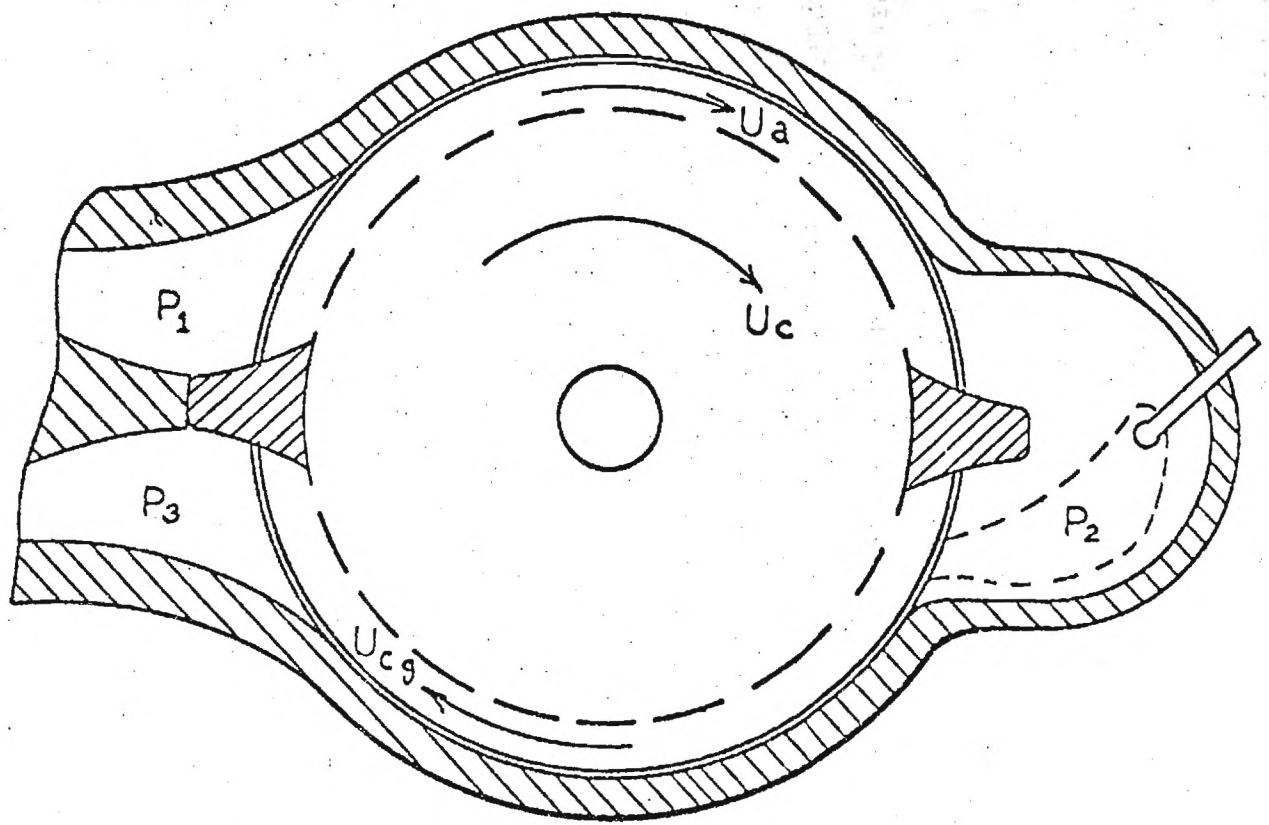

Figure 4-30. Viscous Engine

viscous turbine with a conventional axial flow compressor. Eighty percent was assumed for the efficiency of the conventional compressor. Figure 4-31 shows the effect of turbine efficiency on unit efficiency at various pressure ratios at an entrance temperature of 4000°R. Unfortunately, as previously discussed, pressure ratio is inversely related to turbine efficiency.

Single stage unit efficiencies are calculated with compressor work based on the turbine pressure ratio. For example, a turbine from 90 psia to 60 psia requires a compressor operating on a 1.5 compression ratio. Compressor inlet temperature is taken to be 530°R. Single turbine unit efficiencies with an 80 percent axial compressor are shown in Figures 4-32 and 4-33. These curves turn back on themselves as turbine efficiency decreases. Eventually compressor work exceeds turbine output resulting in negative net horsepower and efficiency.

Increasing maximum temperature to 4000°R and attempting various rotational speeds yields greater overall efficiency and output. Figures 4-34 and 4-35 indicate a potential of 14 hp at 3.2 percent unit efficiency and 56 hp at 2.6 percent unit efficiency.

Greater pressure ratios, therefore, larger unit efficiencies are possible using the variable area turbine discussed in Section 4-4. Comparison of single unit efficiencies with variable and non-variable turbines is given in

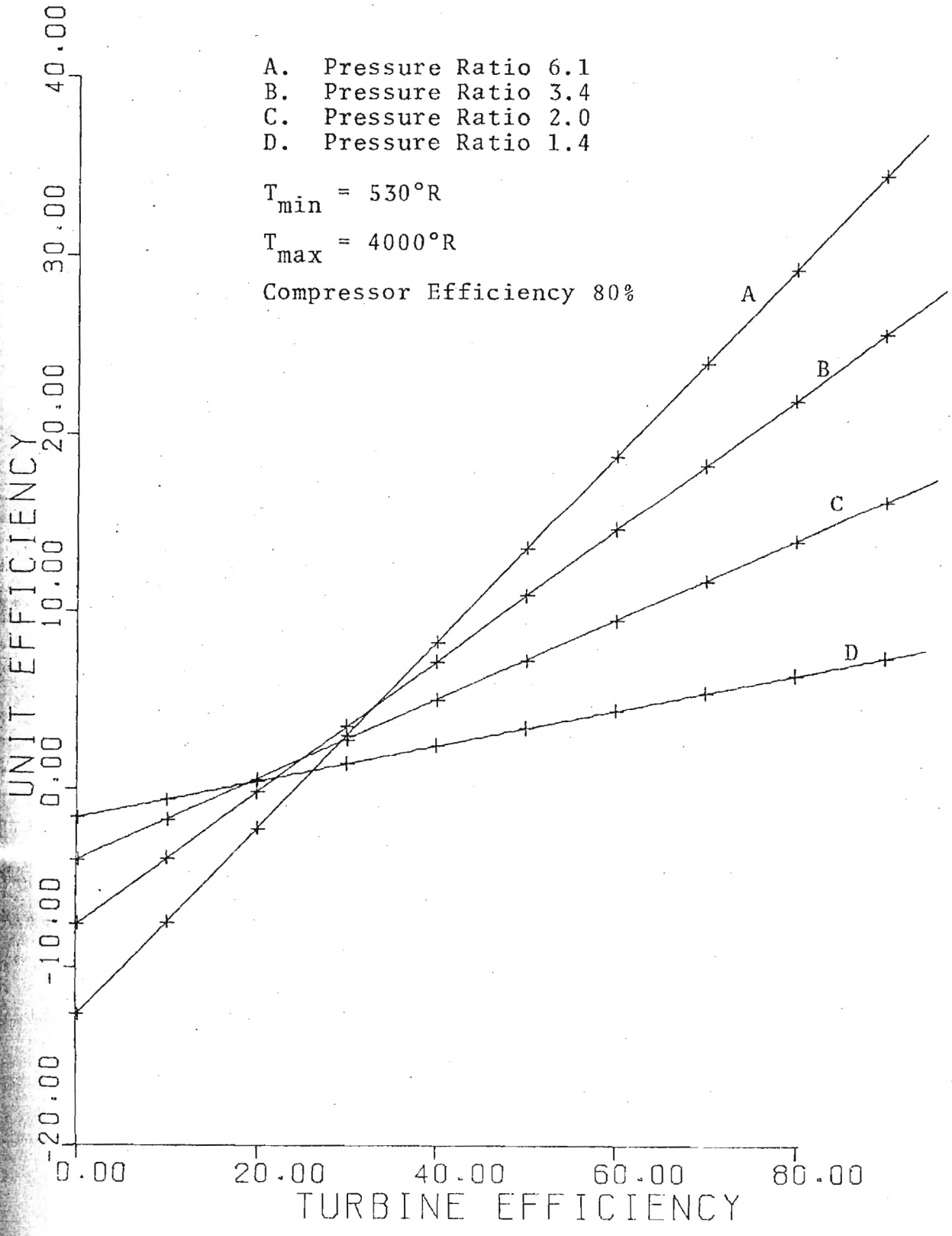

Figure 4-31. Brayton Cycle Efficiencies

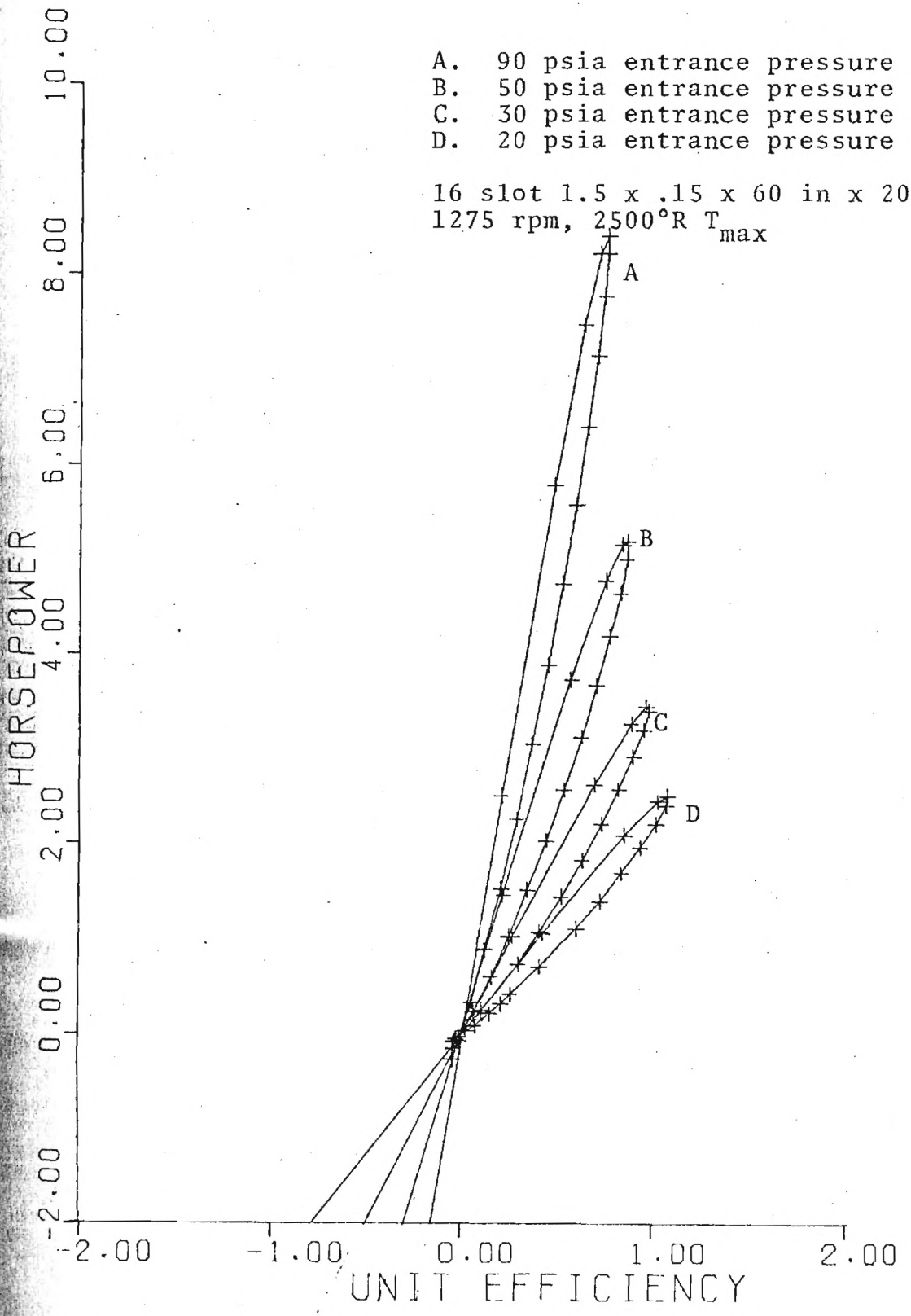

Figure 4-32. Single Stage Unit Efficiency

A. Sixteen 3.0 x .3 inch slots
B. Sixteen 2.5 x .25 inch slots
C. Sixteen 2.0 x .20 inch slots
D. Sixteen 1.5 x .15 inch slots

60 inch dia x 200° arc

1275 rpm, 2500°R T_{max}, 20 psia

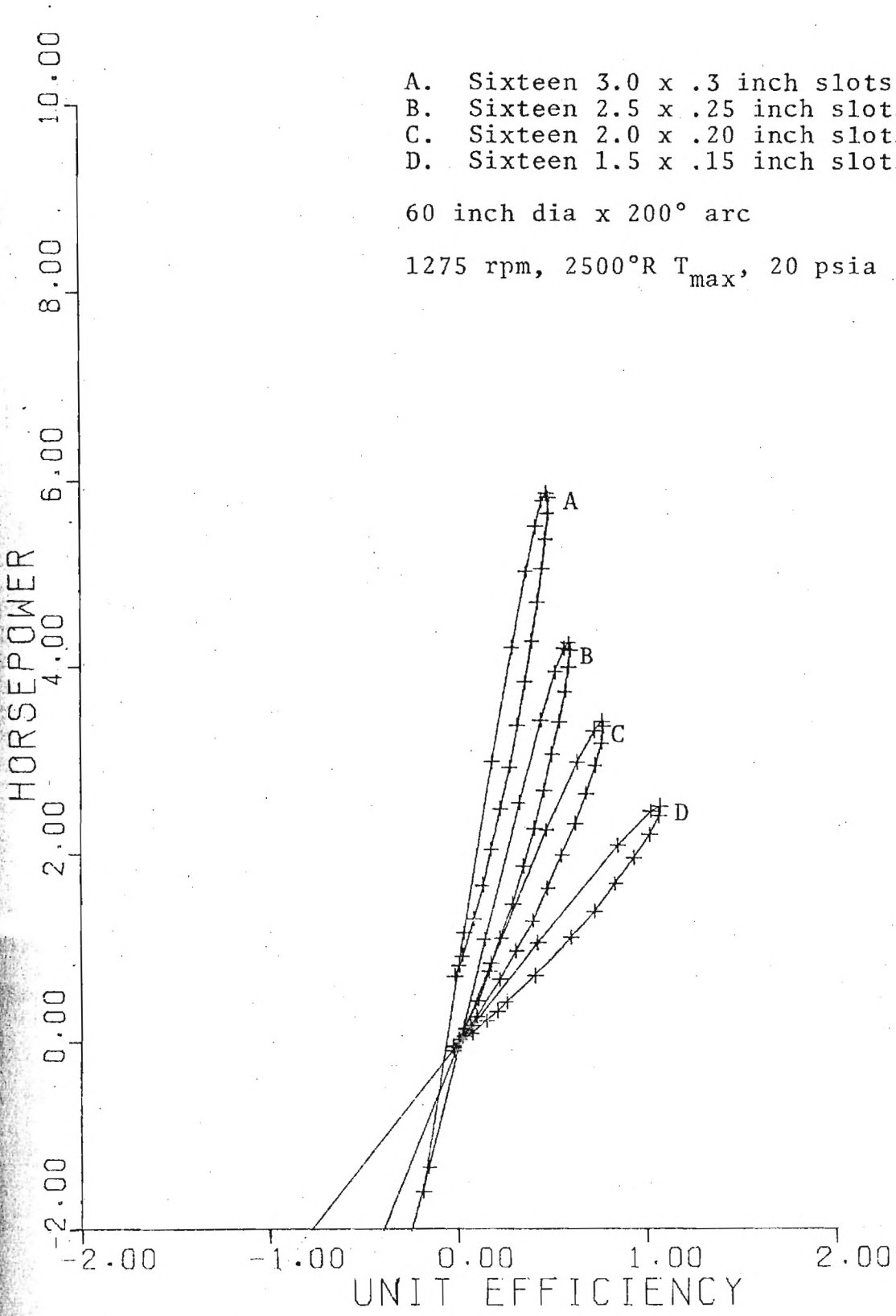

Figure 4-33. Single Stage Unit Efficiency

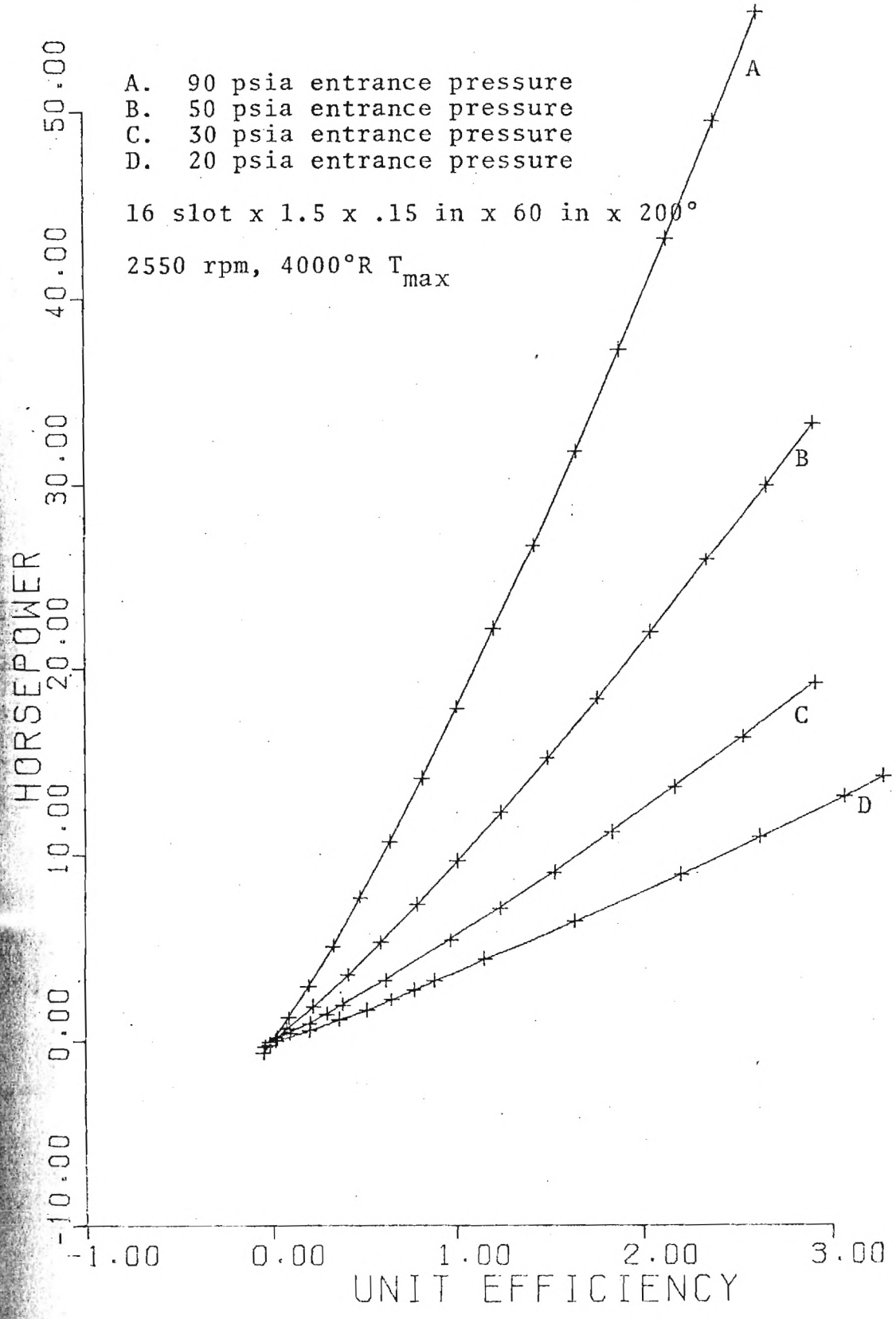

Figure 4-34. Single Stage Unit Efficiency

A. 3,175 rpm
B. 2,550 rpm
C. 1,900 rpm
D. 1,275 rpm

Sixteen 1.5 x .15 inch slots
60 inch dia x 200° arc

4000°R T_{max}, 20 psia

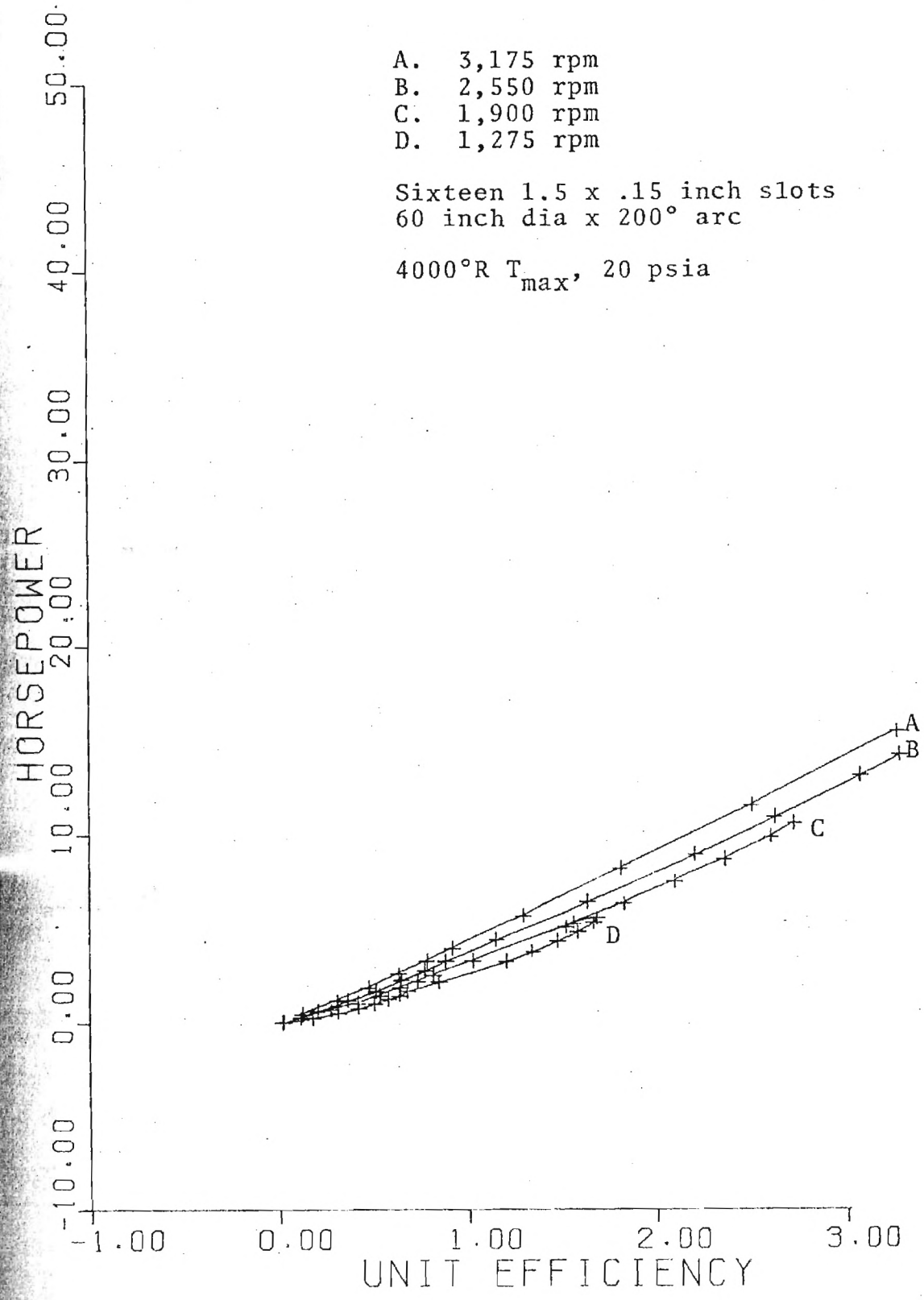

Figure 4-35. Single Stage Unit Efficiency

Figure 4-36. The variable area turbine sacrifices horsepower due to decrease in flowrate for greater unit efficiency. Figure 4-37 shows other degrees of area variation in the turbine. Maximum attainable efficiency for the variable area single stage turbine is 4.5 percent thermal efficiency with 22.2 net horsepower output.

4-6. Multiple Stage Turbine Arrangement

In order to achieve greater unit efficiencies by operating at greater pressure ratios, a concept of operating the viscous turbine in a series has been developed. Figure 4-38 shows a possible arrangement including heat exchangers for cooling the turbine disks.

Five adiabatic multiple stage units have been evaluated for overall performance. In each case, succeeding turbines must have ever increasing numbers of slots to pass the expanding gas and operate at optimum conditions. Variable area turbines have the potential to reduce the equipment requirements (number of turbines) for a given overall pressure ratio. However, they cannot increase either efficiency or horsepower of the multiple stage unit due to decrease in efficiency and flowrate of the individual turbines.

The following cases represent the calculations performed:

Case 1. Eight 1.5 x .15 x 60 x 200° turbines entrance

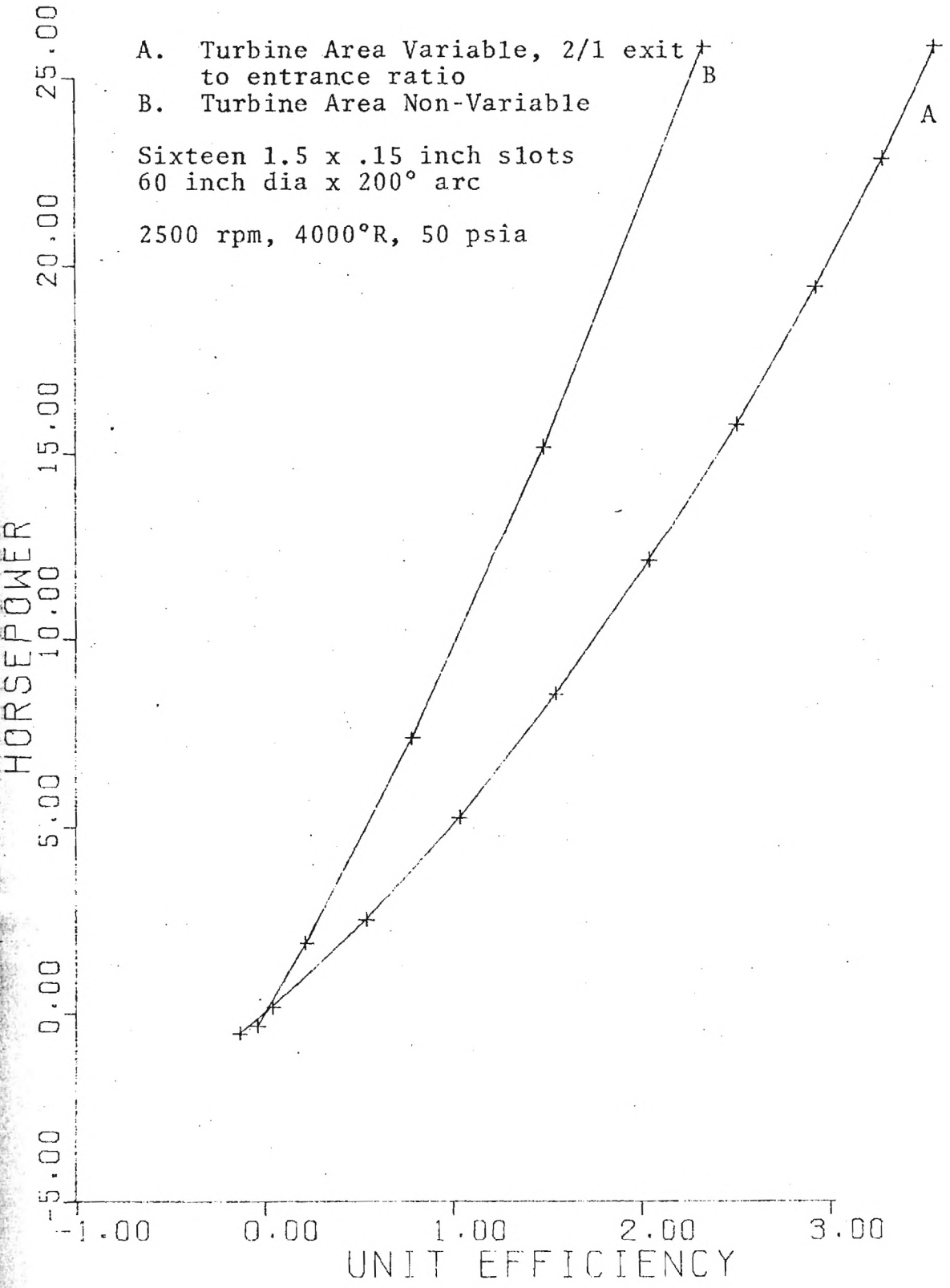

Figure 4-36. Comparison of Variable Area and Regular Turbines for Single Unit Efficiencies

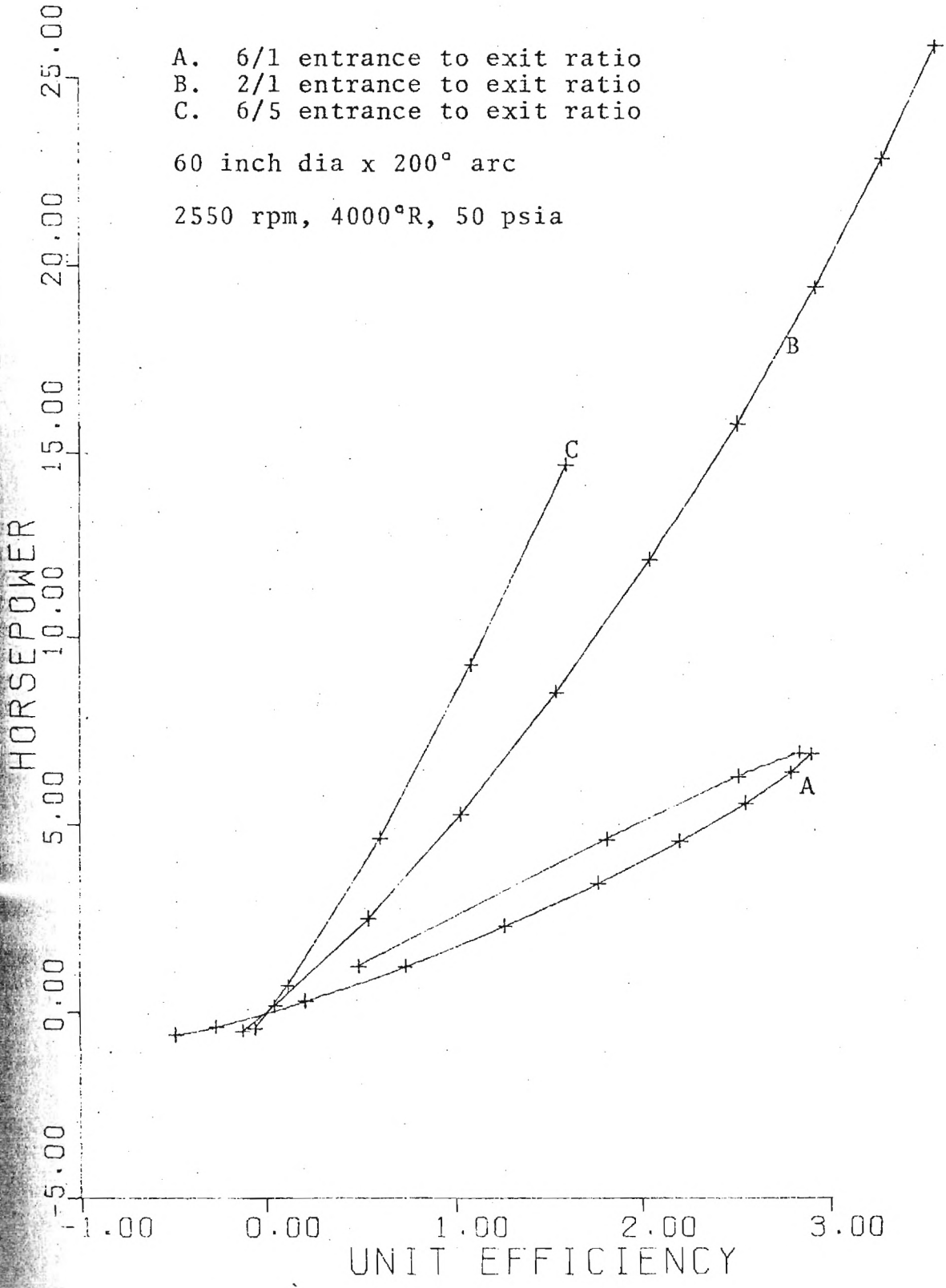

Figure 4-37. Single Unit Efficiency with Variable Area Turbine

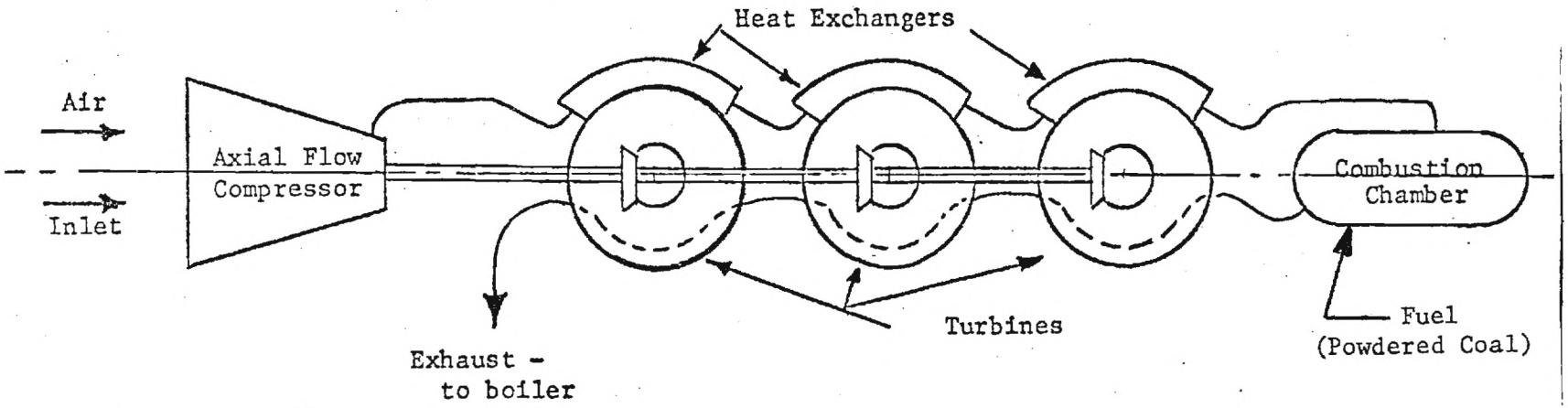

Figure 4-38. Axial Flow Compressor and Viscous Turbines in Series
Schematic of Possible Topping Cycle

conditions, 4000°F at 147 psia 80 percent axial compressor at 168.1 lb_m/min 399 total slots, 8.3 ft approximate total length. Unit efficiency 13.9 percent at 440 hp.

Case 2. Eight 1.5 x .15 x 60 x 200° turbines with reheat to max temperature. Entrance conditions, 4000°F at 147 psia, 80 percent axial compressor at 168.1 lb_m/min, 462 total slots, 9.6 ft approximate total length. Unit efficiency 13.3 percent at 557 hp.

Case 3. Eight 1.5 x .15 x 60 x 200° turbines. Entrance conditions, 2500°F at 147 psia, 80 percent axial compressor at 225.3 lb_m/min, 411 total slots, 8.6 ft approximate total length. Unit efficiency 1.3 percent at 25.6 hp.

Case 4. Eight 3.0 x .30 x 60 x 200° turbines entrance conditions, 4000°F at 147 psia, 80 percent axial compressor at 798.0 lb_m/min, 429 total slots, 14.3 ft approximate total length. Unit efficiency 9.3 percent at 1392 hp.

Case 5. Eleven 1.5 x .15 x 60 x 200° turbines entrance conditions, 4000°R at 367.5 psia, 80 percent axial compressor at 420.0 lb_m/min, 1111 total slots, 23.1 approximate total length. Unit efficiency 14.1 percent at 935 hp.

Performance data for each of the eight turbines comprising Cases 1 and 2 are included in Section 4-9, Figures 4-51 through 4-58.

Case 4 of those considered is the most interesting

since it deals with a slot width of .3 inch, which is quite practical. It also combines a relatively high horsepower output with a fair efficiency.

4-7. Heat Transfer Effects

Heat transfer in the turbine or compressor analysis is easily included by defining the average wheel temperature, T_w. Assigning an arbitrary temperature T_w of 2500°R, Case 1 of Section 4-6 was reevaluated to obtain an overall thermal efficiency of 5.7 percent with an output of 219.5 hp.

The decrease in efficiency was caused by high heat losses into the disk due to high forced convection factors. This reduced the gas temperature after the first turbine to 2827°R compared to 3889°R without heat transfer. In subsequent turbines, the gas temperature approaches the wheel temperature reducing the Brayton cycle efficiency greatly. In the last four turbines, the constant wheel temperature actually serves as a source of regeneration by maintaining gas temperature at 2500°F.

Now, in Case 1, with and without heat transfer, two extremes are represented. The first assumes zero heat transfer. The second neglects internal resistance of the disk fins and assumes an average wheel surface temperature. Neither assumption may be valid. Probable operation of the multiple stage unit falls between the 13.9 percent at 440 hp without heat transfer and the 5.7 percent at 219.5 hp with

constant surface temperature.

The possibility of operating at lower gas temperatures to negate heat transfer was investigated in Case 3 of Section 4-6. The lower gas velocities produced by lower temperatures resulted in very low thermal efficiency and output.

4-8. Supersonic Turbine

The mathematical model derived in Chapter II in no way precluded the possibility of supersonic flow in the viscous turbine. By placing a converging-diverging nozzle prior to the turbine entrance supersonic velocities could be introduced into the turbine. Data have been generated and displayed per Figures 4-39 through 4-44. Subsonic data were generated for the same general conditions for comparison and is given per Figures 4-45 through 4-50.

Generally, supersonic turbines have lower peak efficiencies due to greater losses at the static wall. Output in the supersonic turbine is greater with the higher relative velocity between the gas and rotor. However the supersonic turbines have an advantage in respect that much smaller diameters produce equivalent efficiency and output. (See Table 1.) Both supersonic and subsonic turbines are limited by choking.

4-9. General Turbine Performance Data

Performance data for each of the Case 1 and Case 2

A. 6.0 inch diameter
B. 12.0 inch diameter
C. 18.0 inch diameter
D. 24.0 inch diameter

Sixteen 1.5 x .15 inch slots

200° arc, 2080 ft/sec

2500°R, 50.0 psia

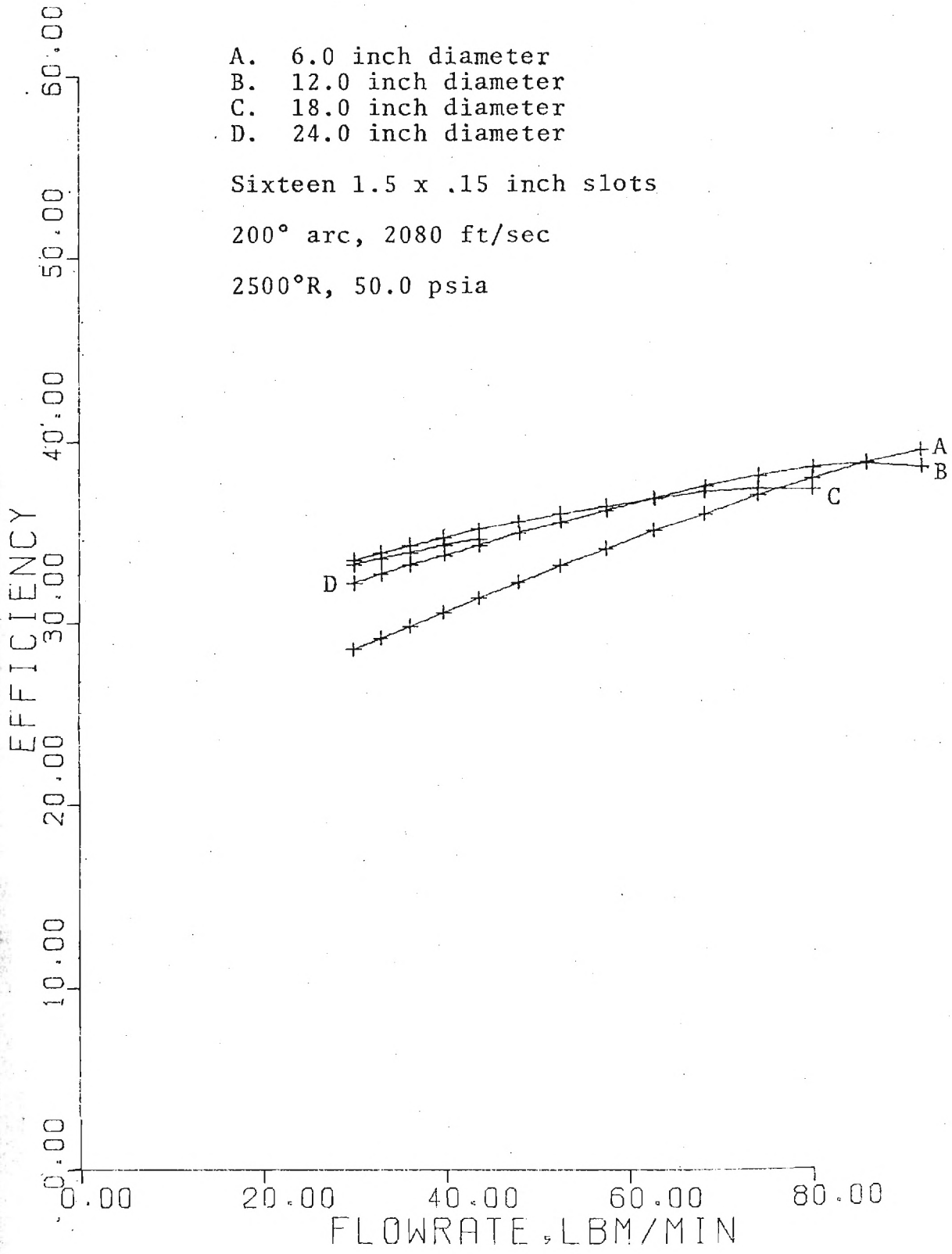

Figure 4-39. Supersonic Turbine Performance

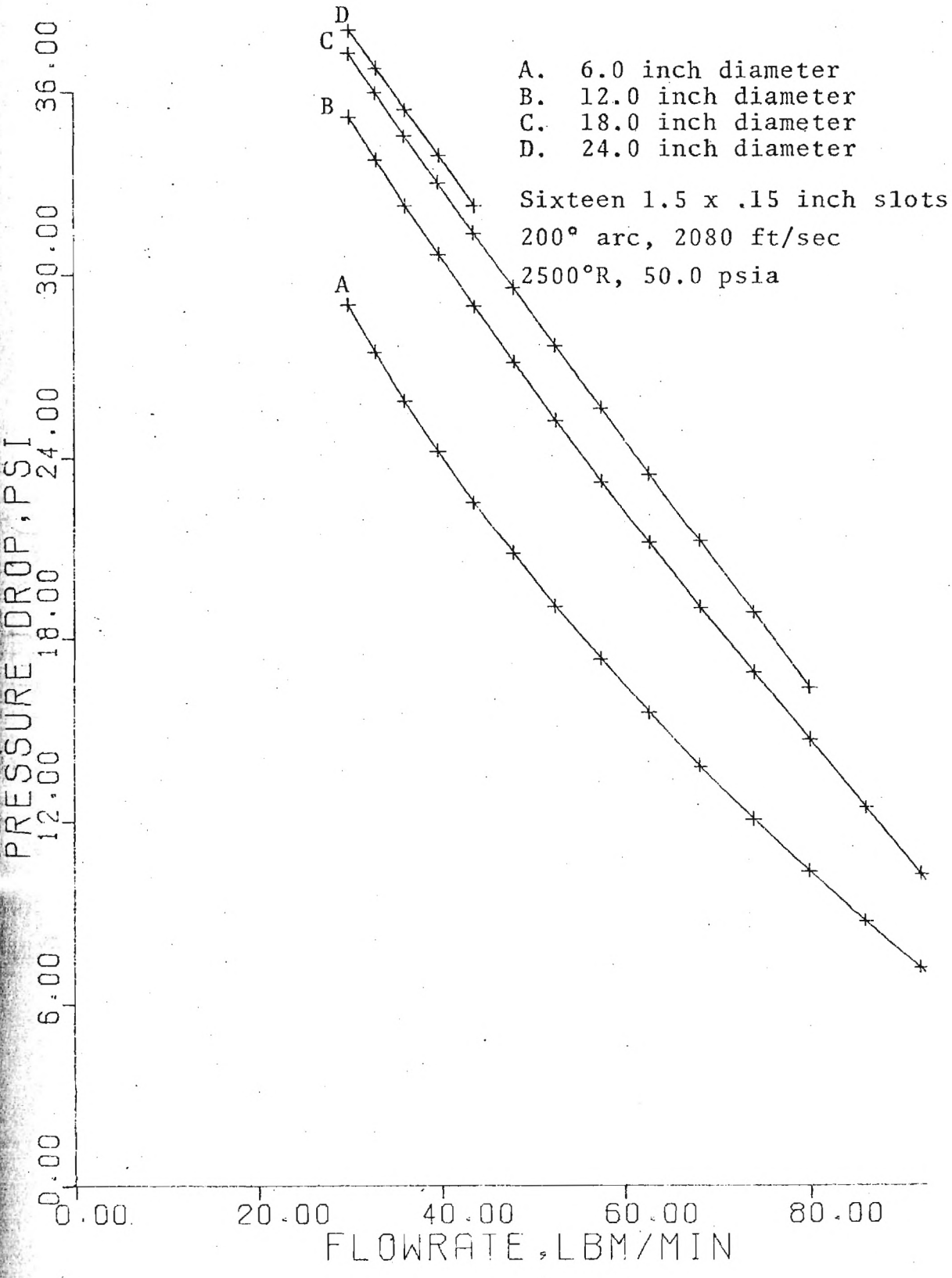

Figure 4-40. Supersonic Turbine Performance

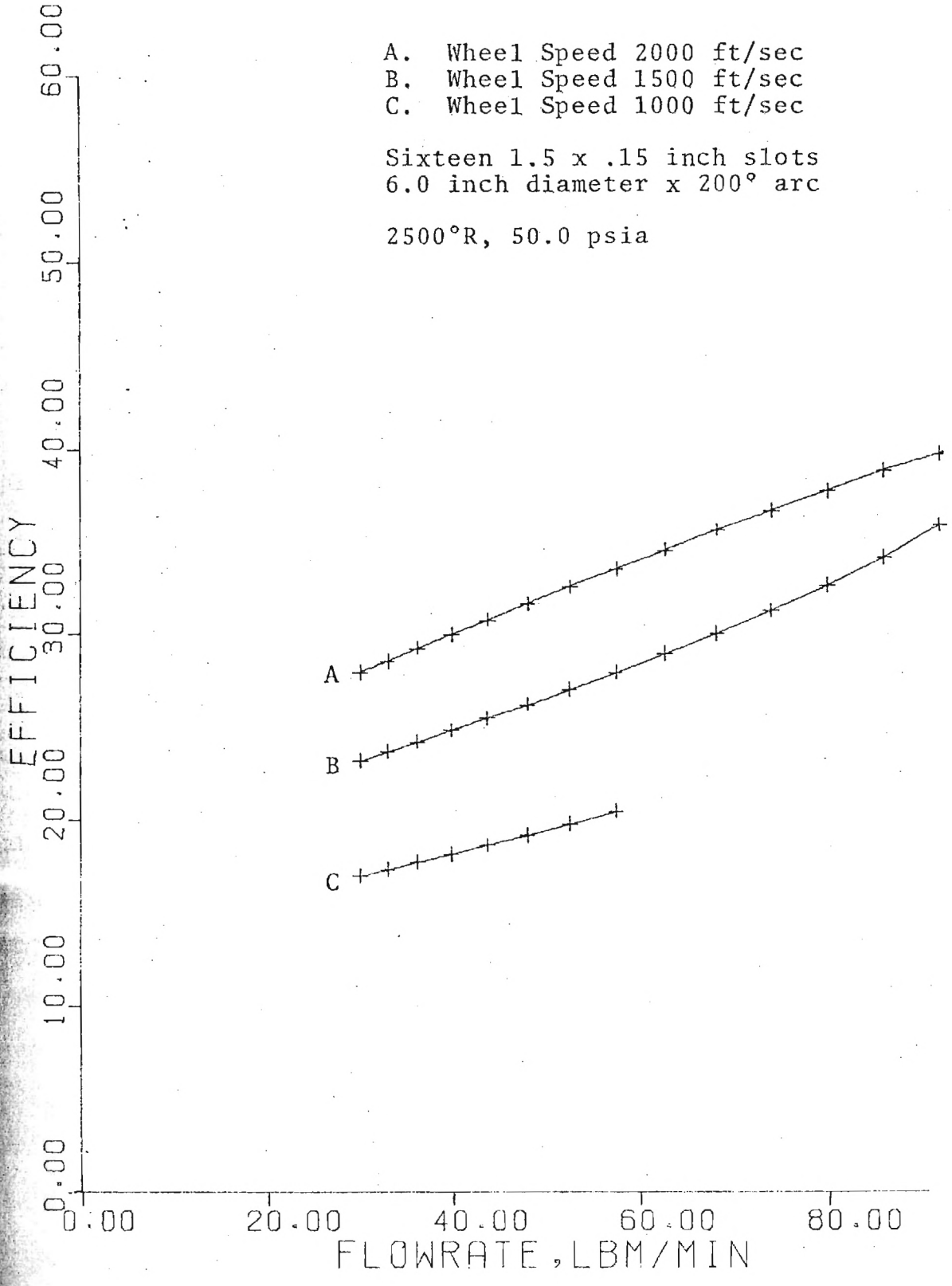

Figure 4-41. Supersonic Turbine Performance

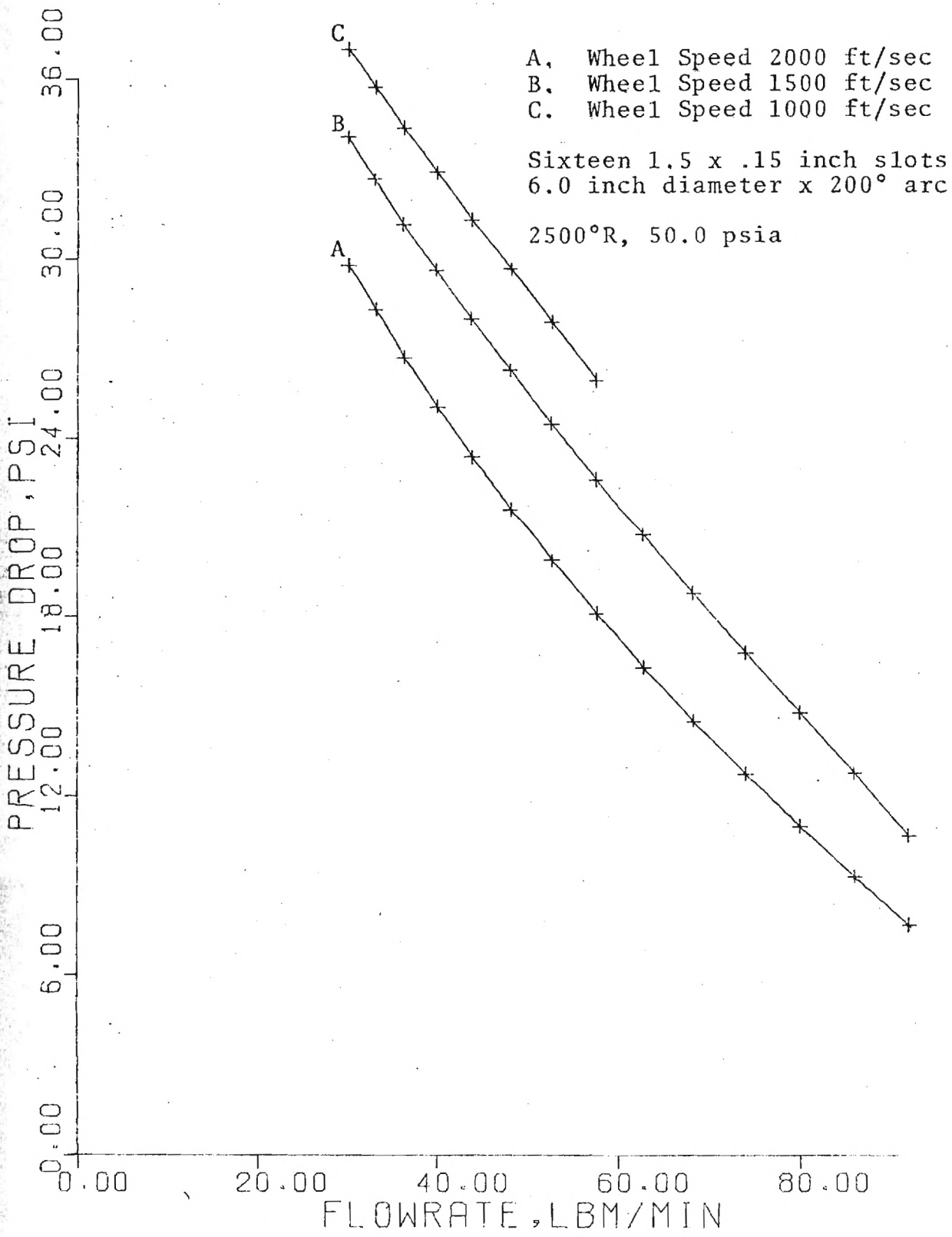

Figure 4-42. Supersonic Turbine Performance

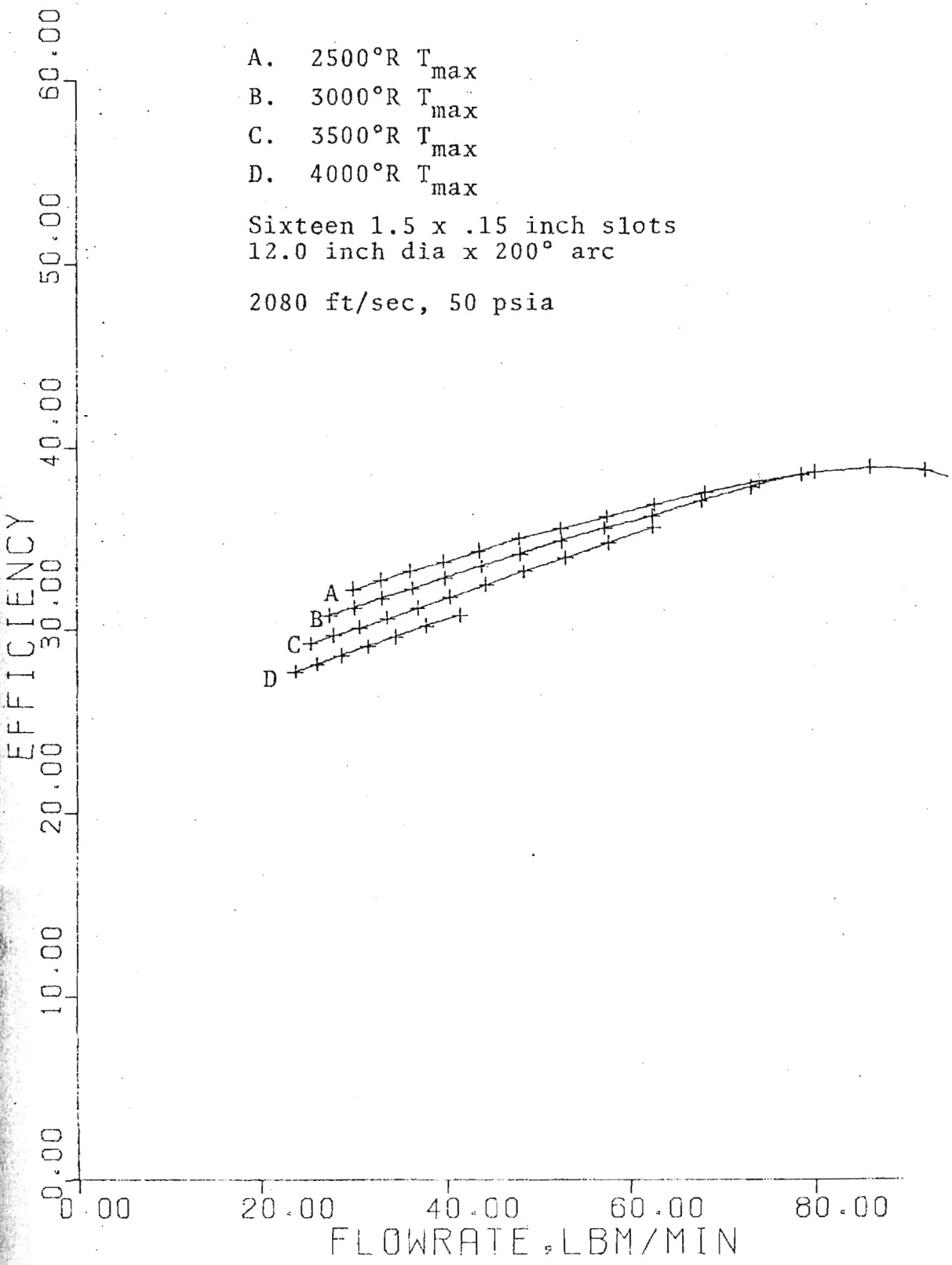

Figure 4-43. Supersonic Turbine Performance

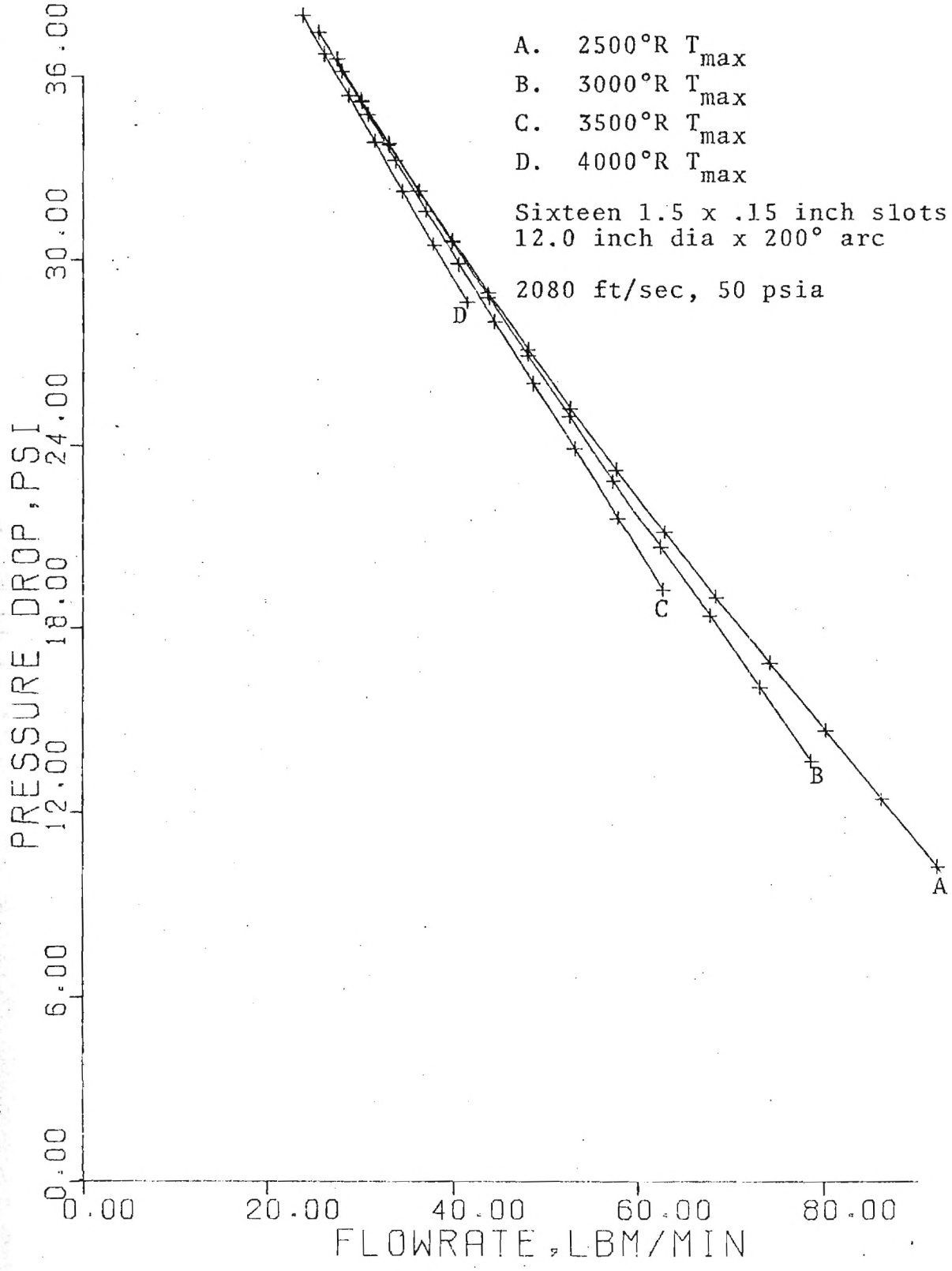

Figure 4-44. Supersonic Turbine Performance

A. 60 inch diameter
B. 40 inch diameter
C. 20 inch diameter

Sixteen 1.5 x .15 inch slots
200° arc, 666 ft/sec, 2500°R, 50.0 psia

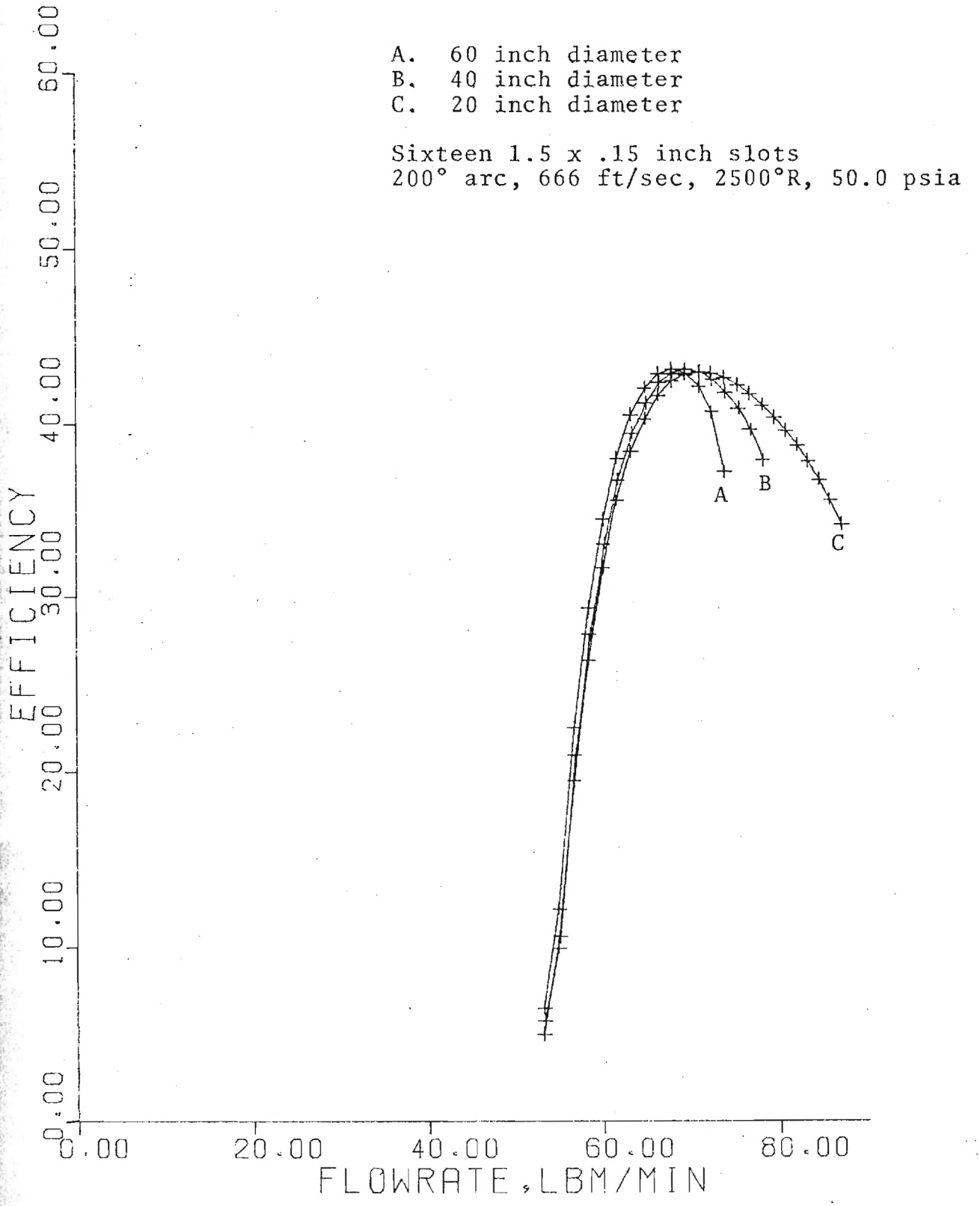

Figure 4-45. Turbine Performance

A. 60 inch diameter
B. 40 inch diameter
C. 20 inch diameter

Sixteen 1.5 x .15 inch slots
200° arc, 666 ft/sec, 2500°R, 50.0 psia

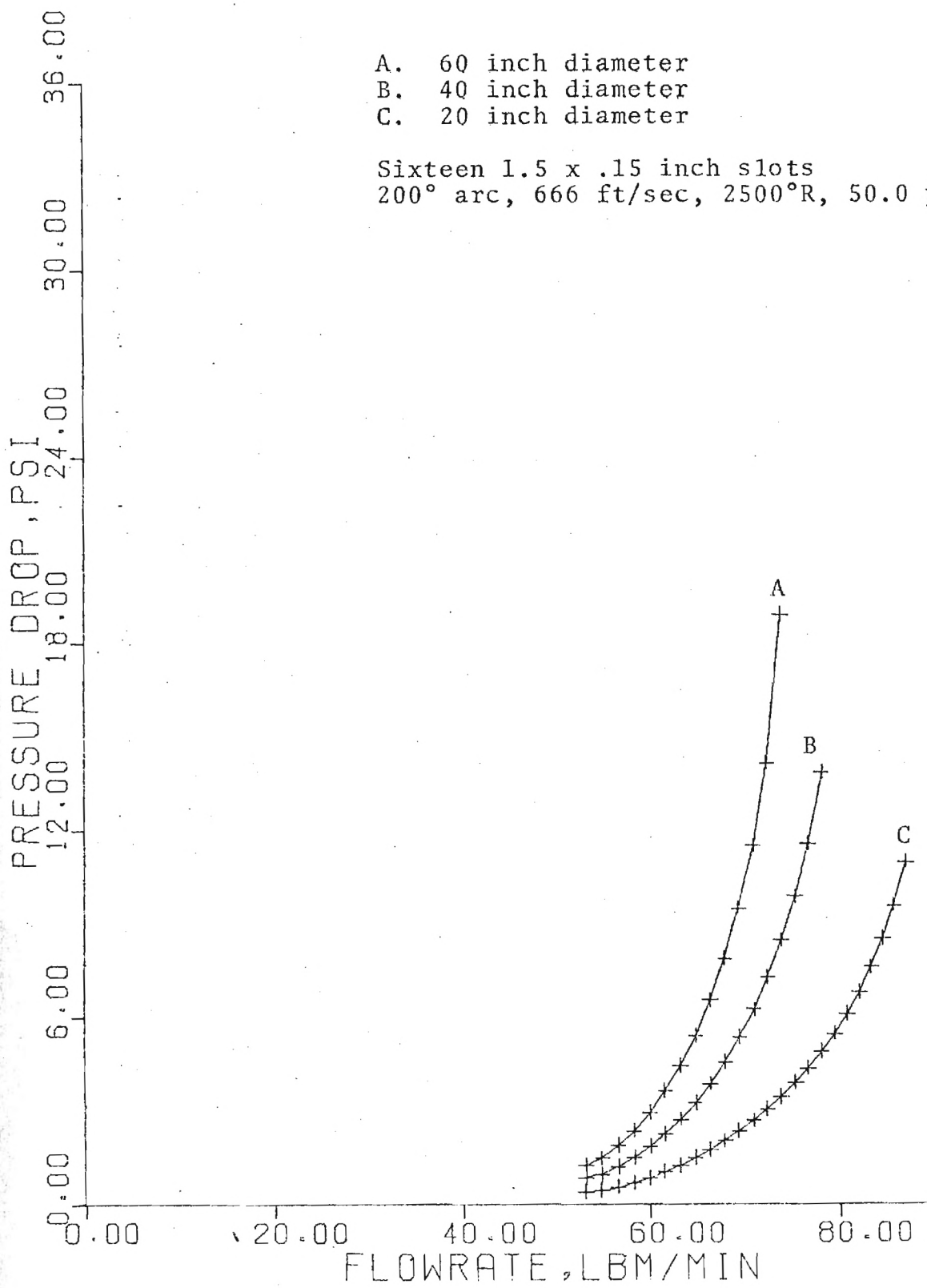

Figure 4-46. Turbine Performance

A. 333 ft/sec wheel speed
B. 666 ft/sec wheel speed
C. 1000 ft/sec wheel speed

Sixteen 1.5 x .15 inch slots
60 inch dia x 200° arc

2500°R, 50 psia

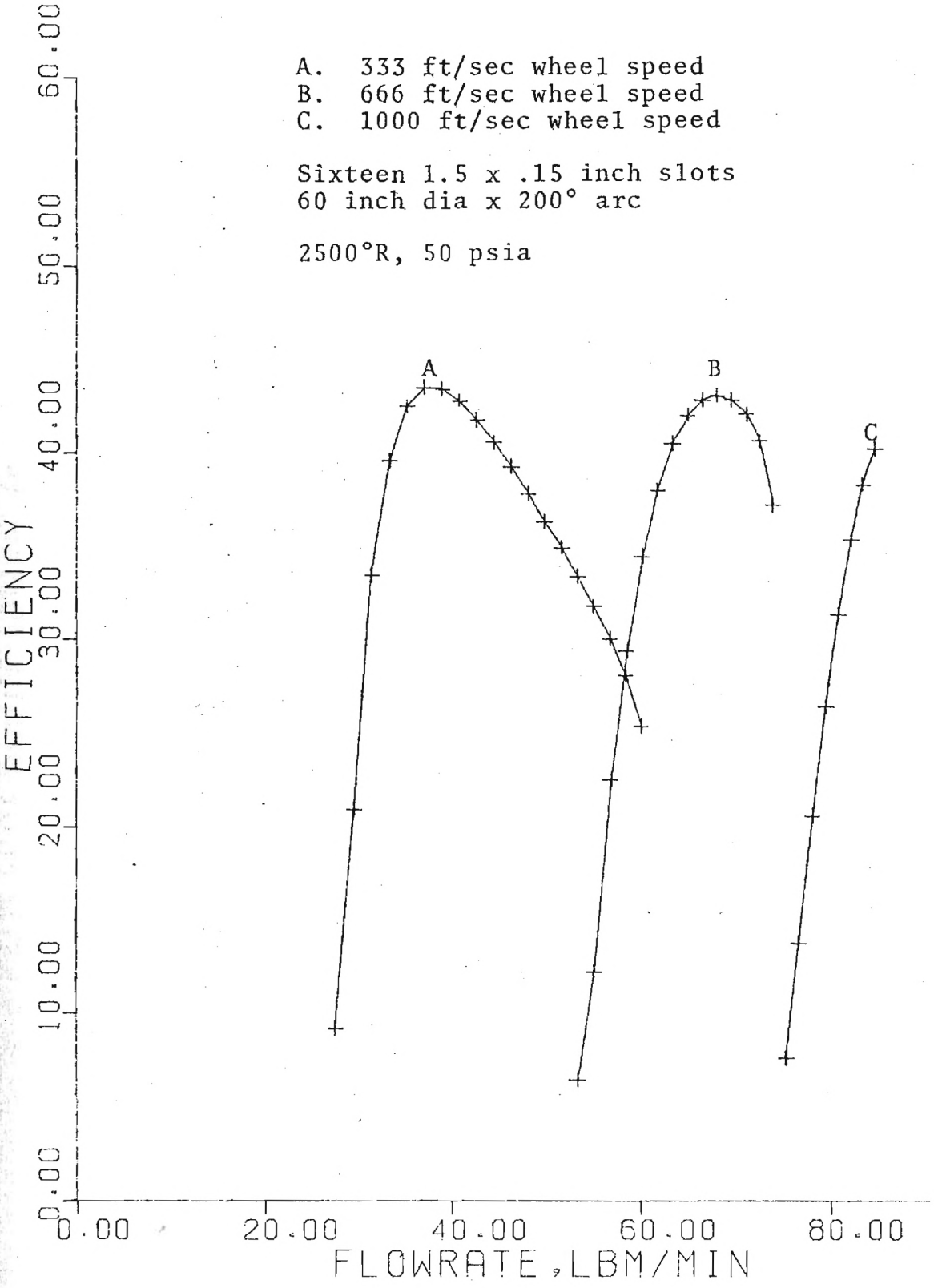

Figure 4-47. Turbine Performance

A. 333 ft/sec wheel speed
B. 666 ft/sec wheel speed
C. 1000 ft/sec wheel speed

Sixteen 1.5 x .15 inch slots
60 inch dia x 200° arc

2500°R, 50 psia

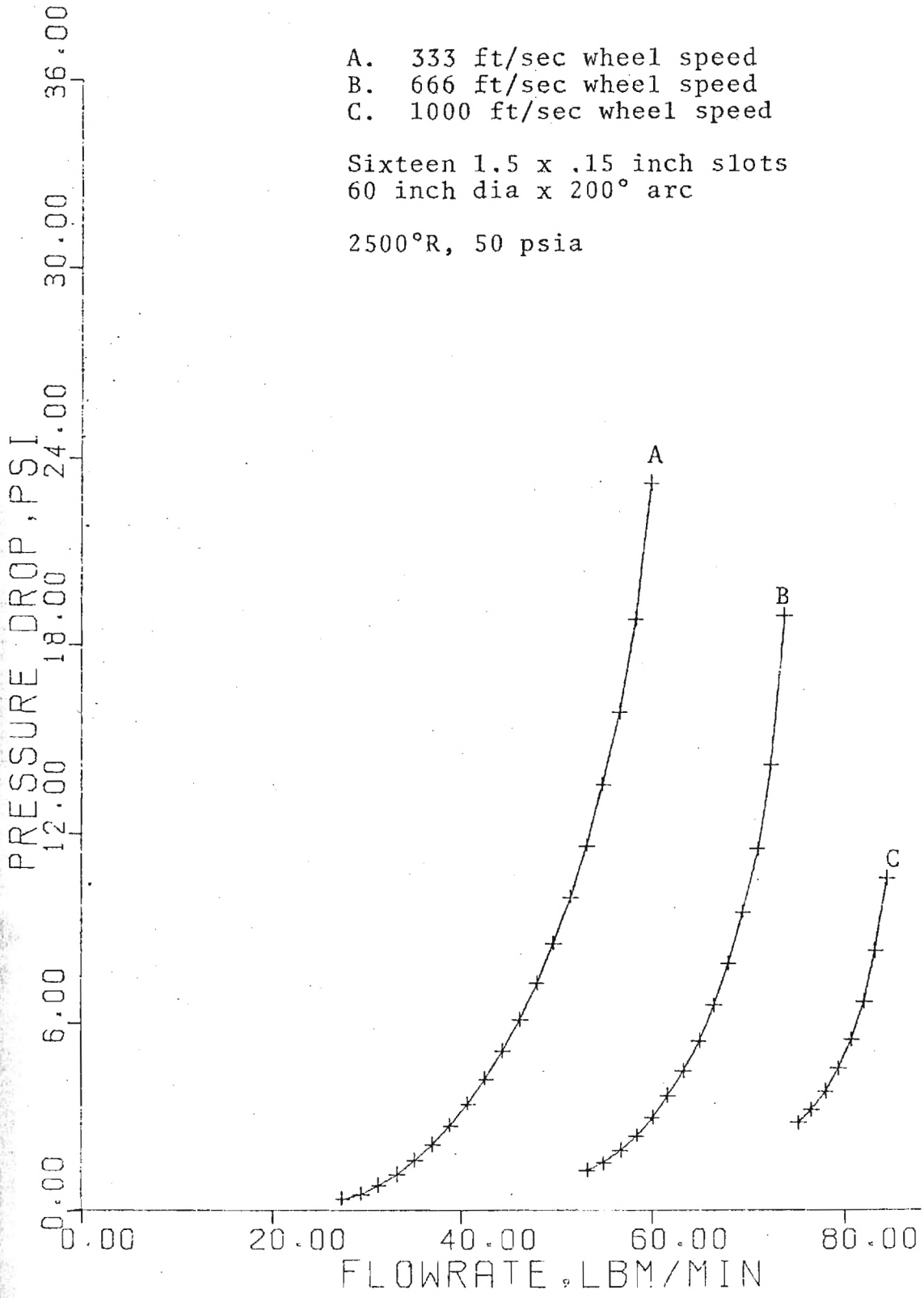

Figure 4-48. Turbine Performance

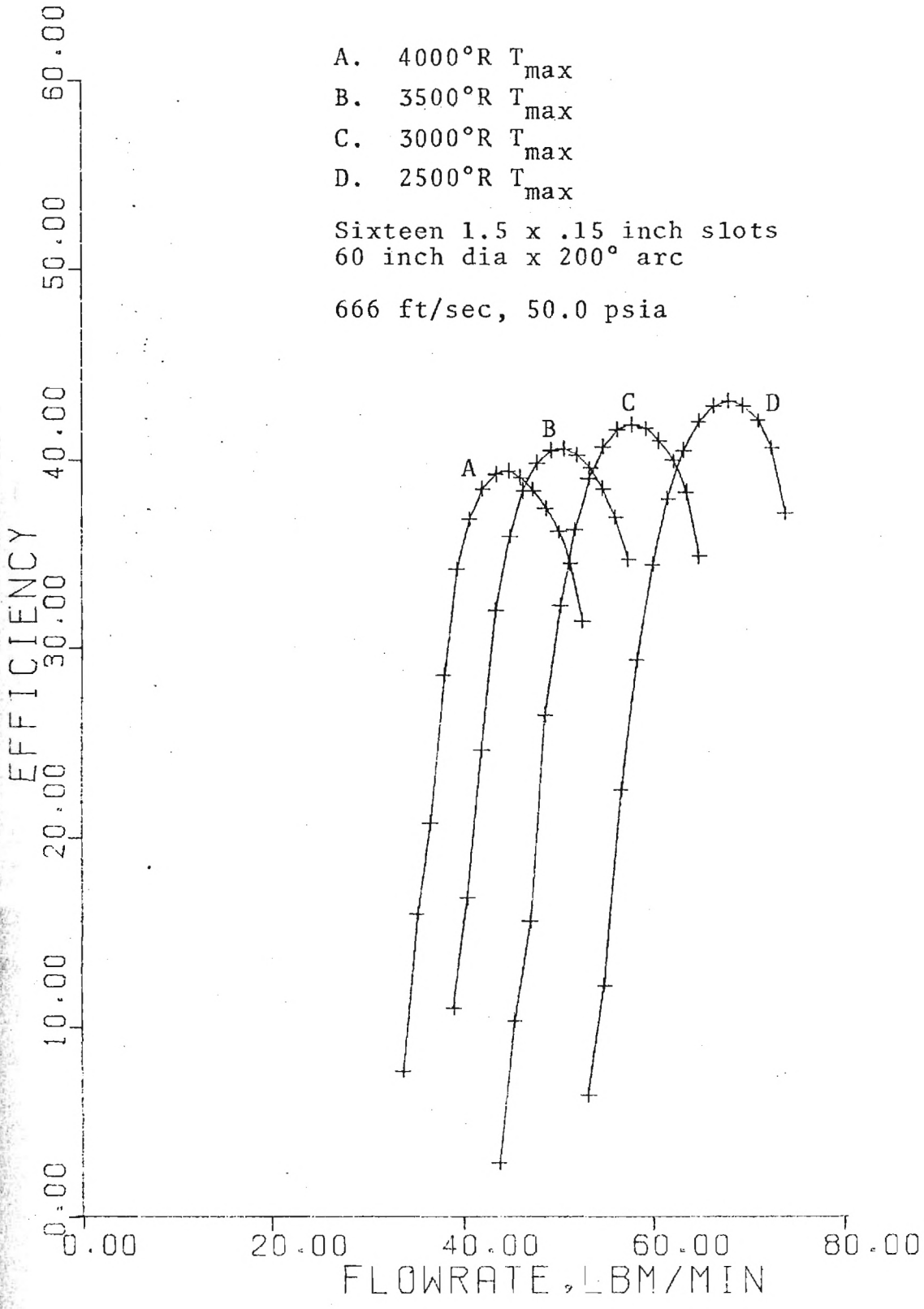

Figure 4-49. Turbine Performance

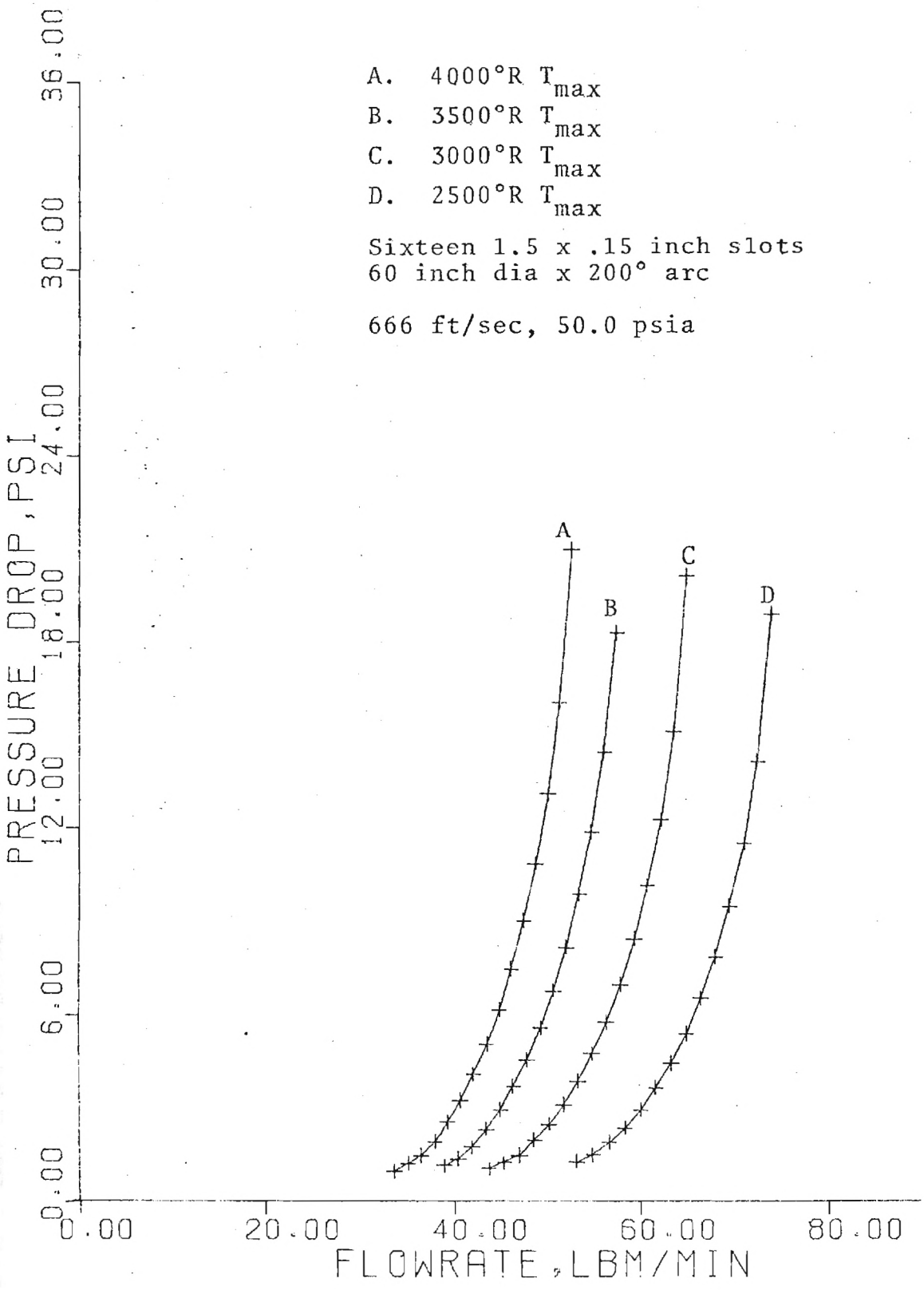

Figure 4-50. Turbine Performance

Table 1. Optimum Cases

Supersonic	Subsonic
18 inch diameter	60 inch diameter
26,500 rpm	3,800 rpm
2500°F	2500°F
Efficiency--37.3%	Efficiency--37.3%
58.2 hp	55.8 hp

turbines of Section 4-6 are given in Figures 4-51 through 4-58. This data, though generated for multiple staged Cases 1 and 2, is generally applicable for 1.5 x .15 x 60 x 200° turbines when the entrance conditions are identical. Interpolation for other cases is recommended. The following ledger (Table 2) defines the entrance conditions for each of the turbines evaluated in Figures 4-51 through 4-58.

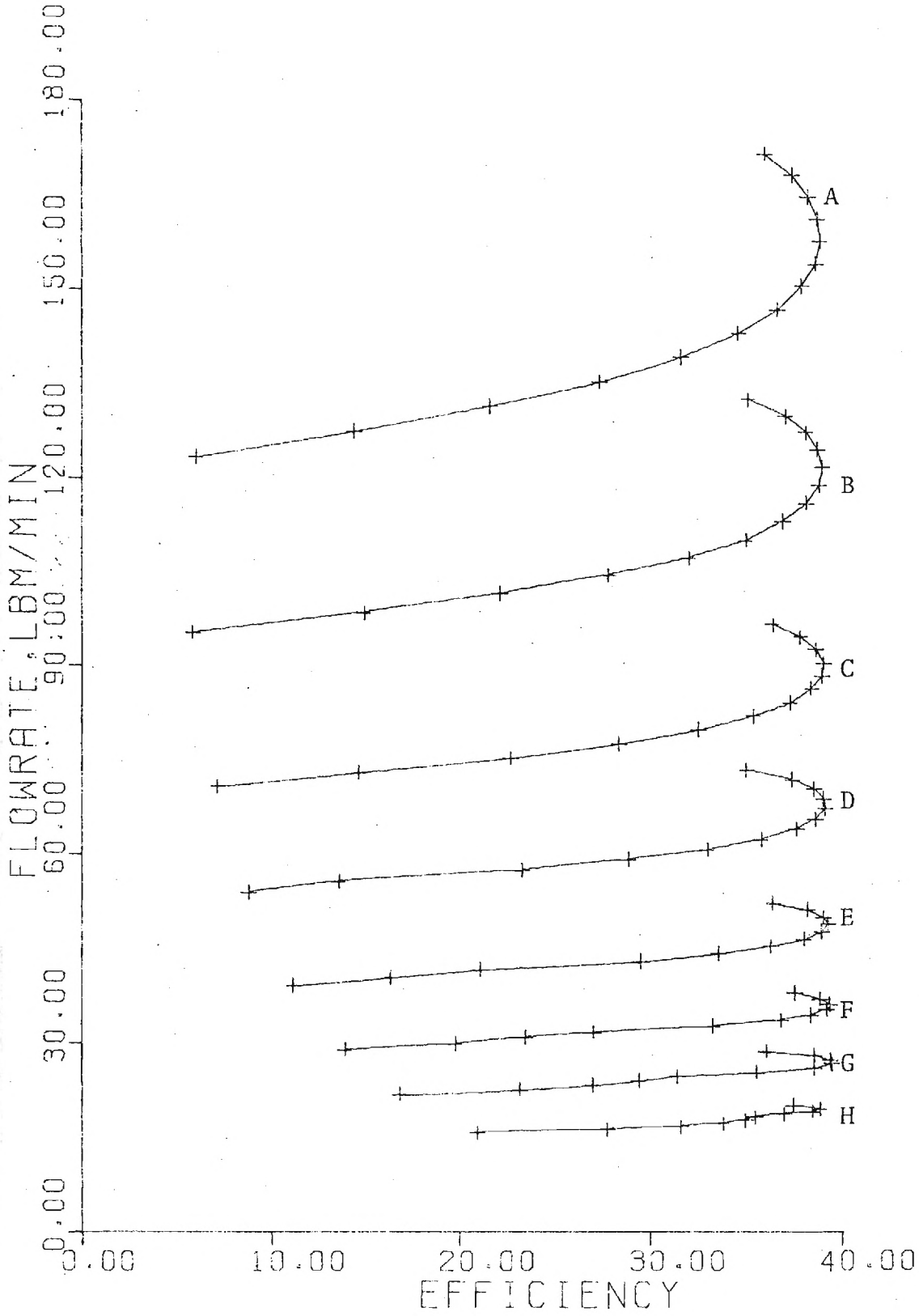

Figure 4-51. Case 1 Turbine Performance

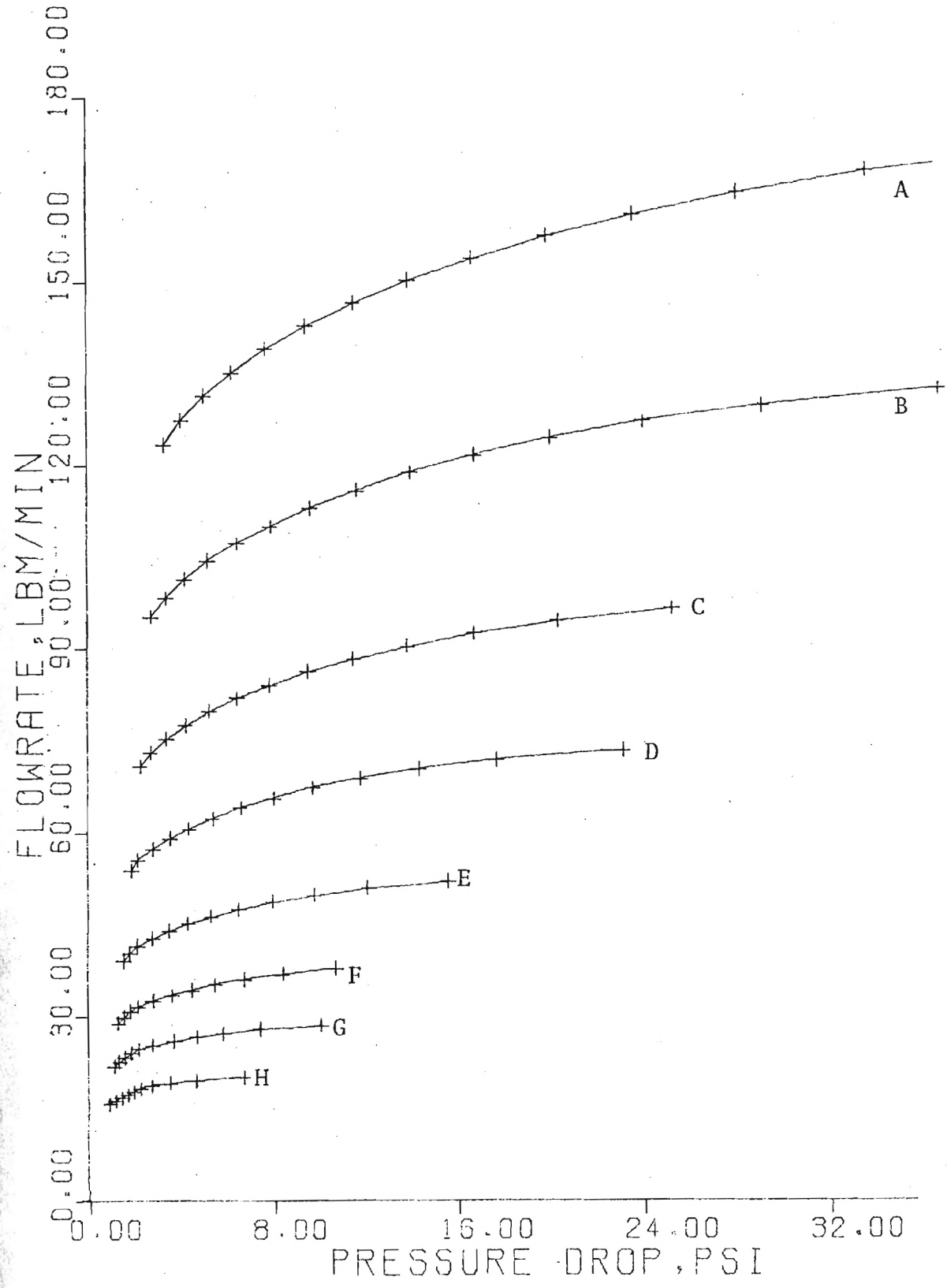

Figure 4-52. Case I Turbine Performance

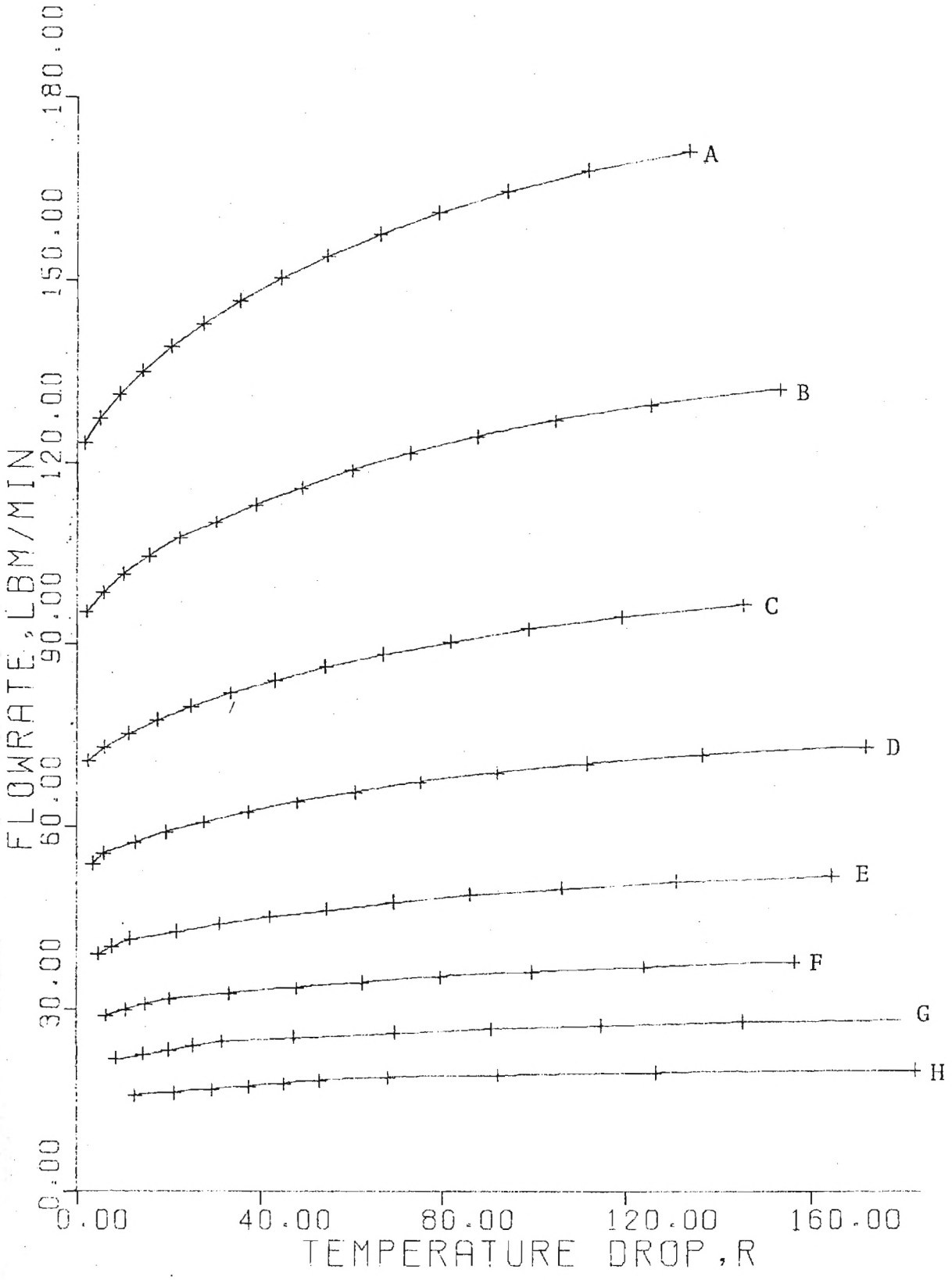

Figure 4-53. Case 1 Turbine Performance

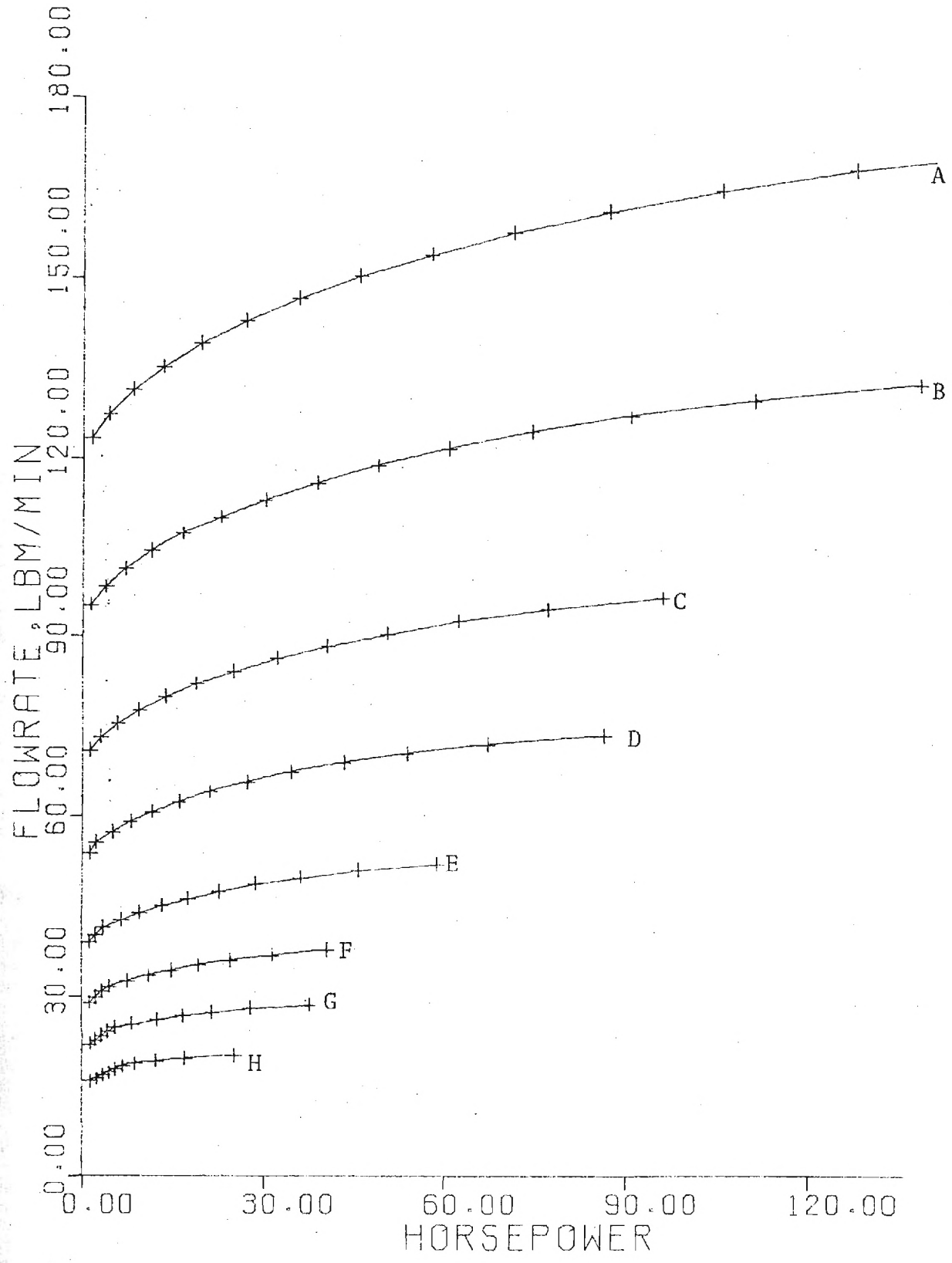

Figure 4-54. Case 1 Turbine Performance

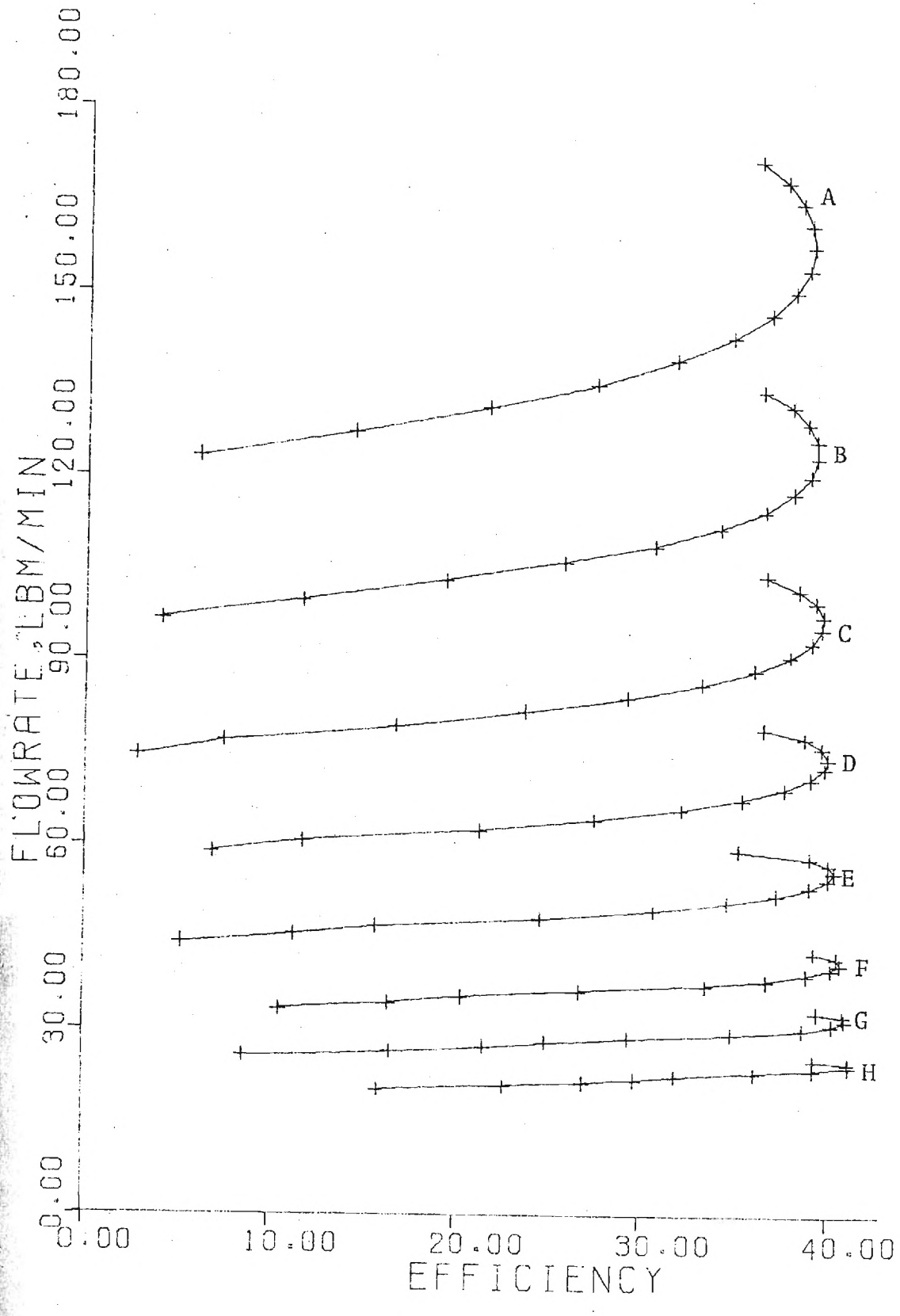

Figure 4-55. Case 2 Turbine Performance

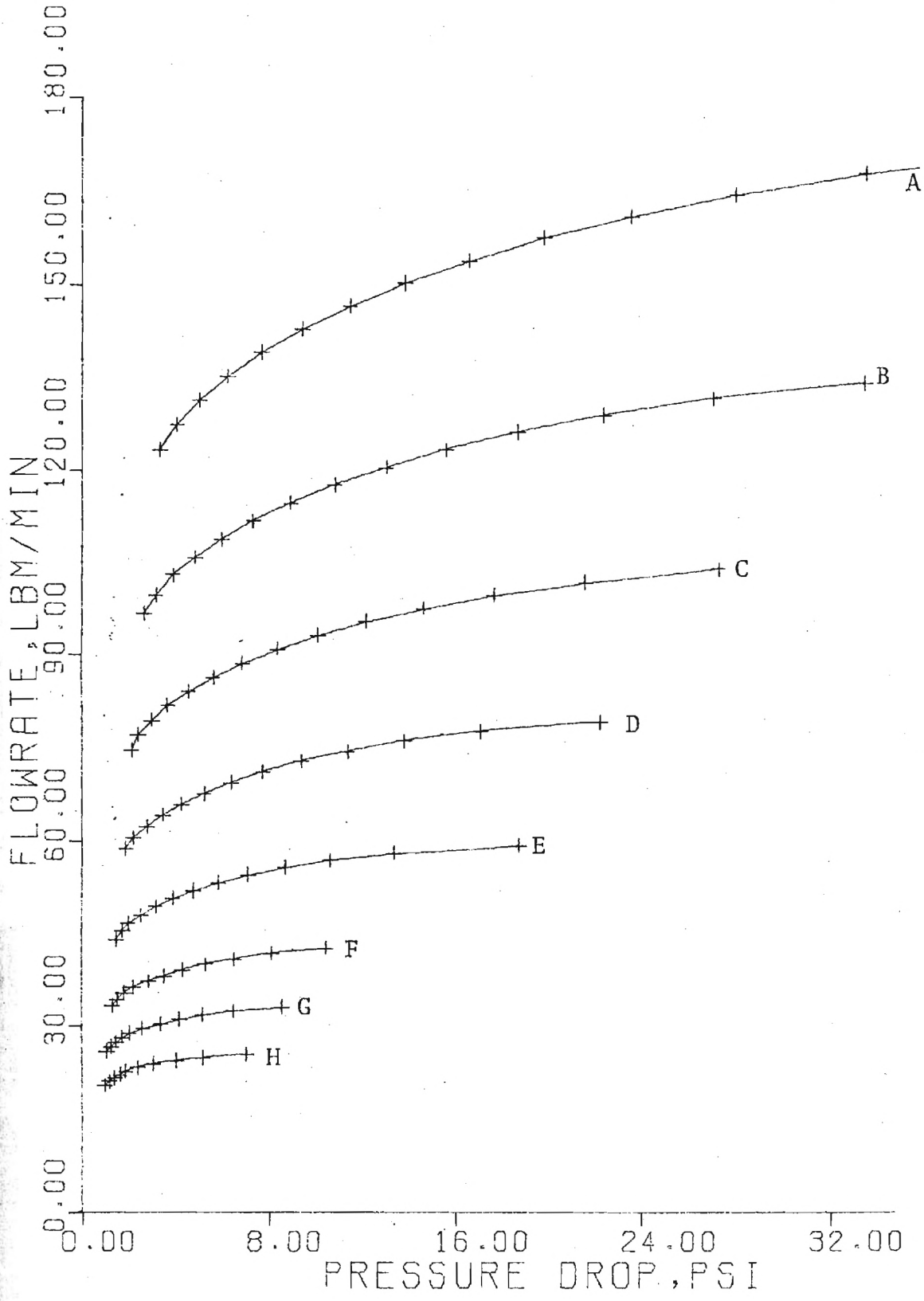

Figure 4-56. Case 2 Turbine Performance

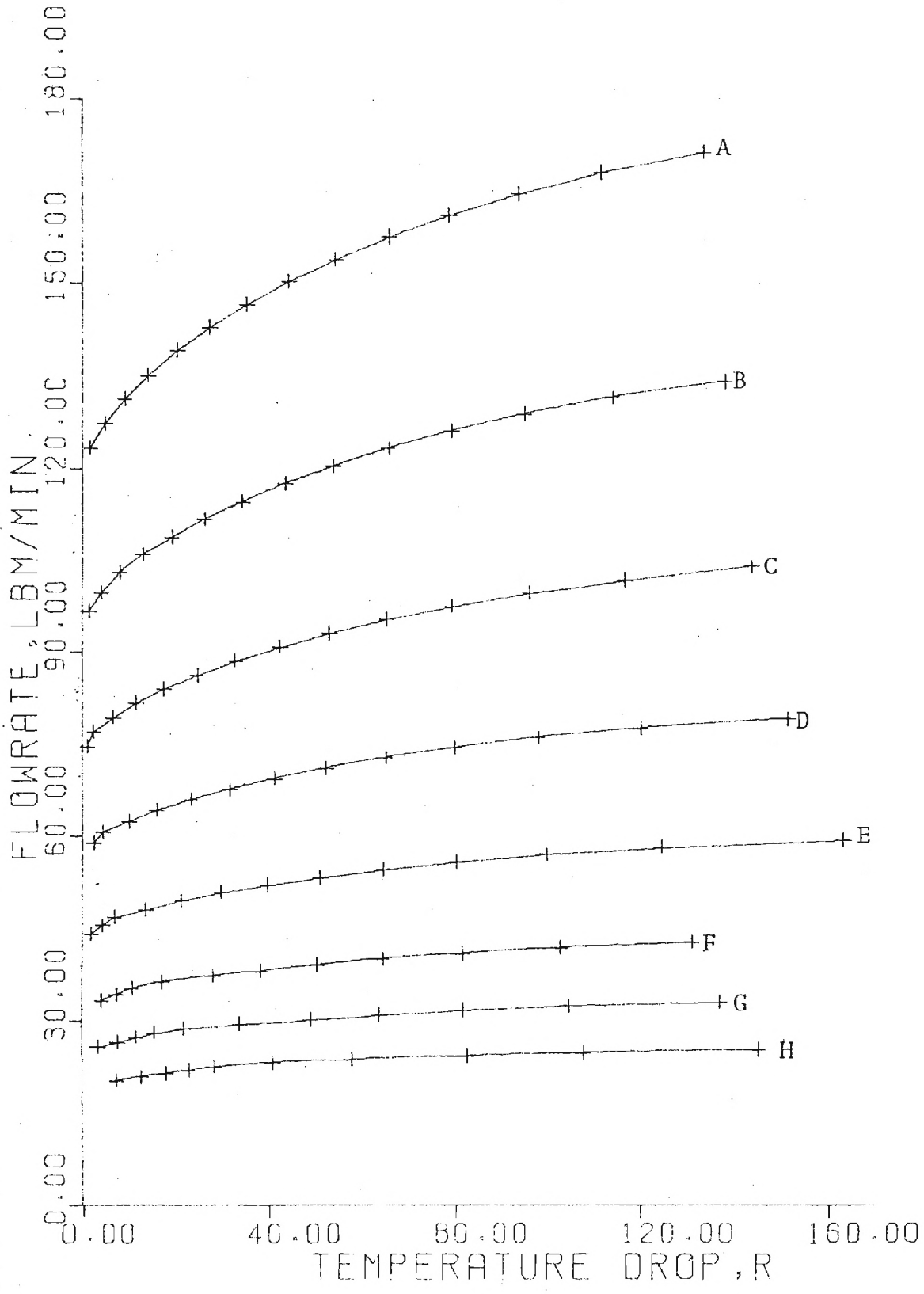

Figure 4-57. Case 2 Turbine Performance

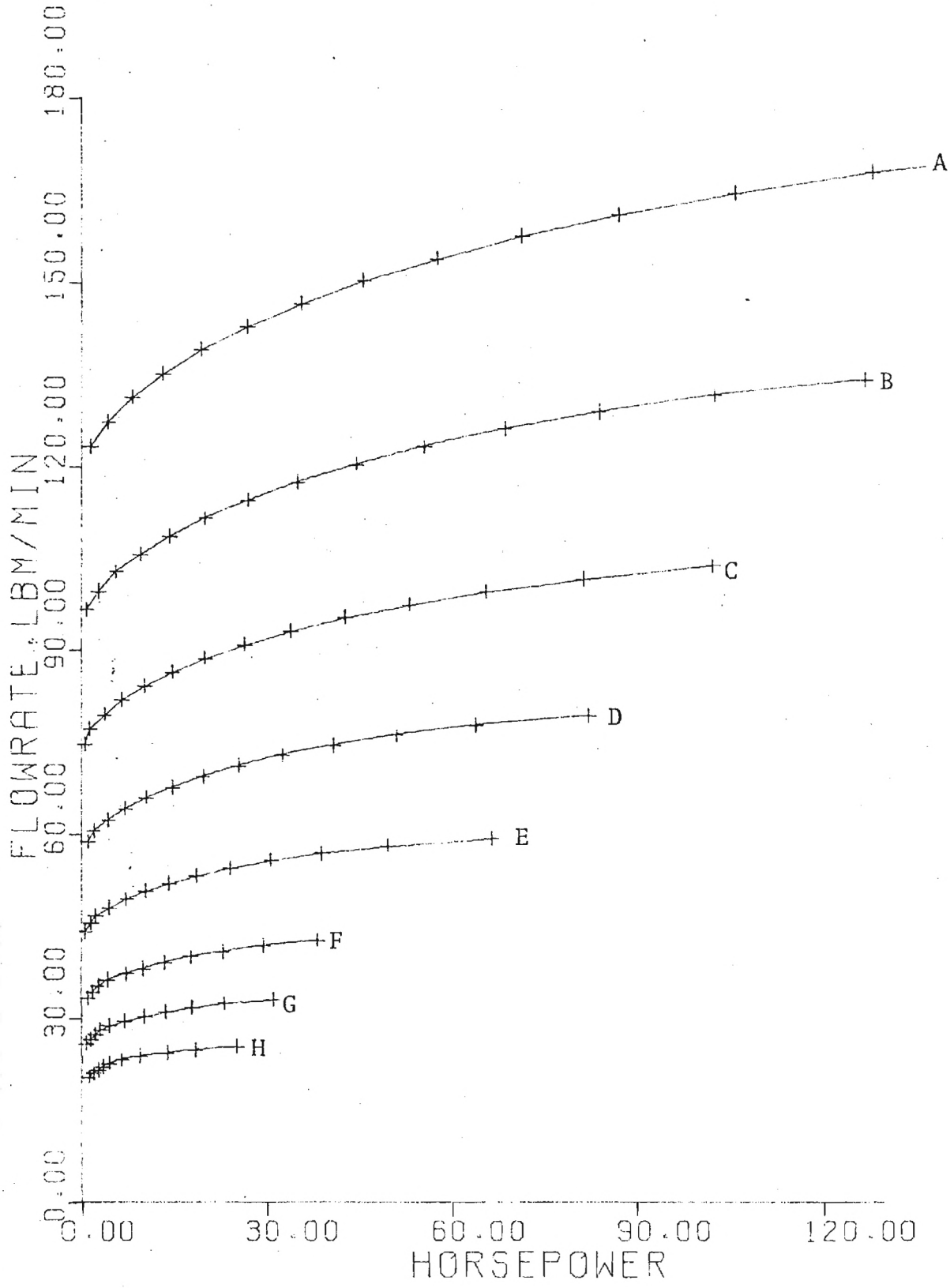

Figure 4-58. Case 2 Turbine Performance

Table 2. Turbine Entrance Conditions

	Case 1	Case 2
A	147 psia, 4000°R	147 psia, 4000°R
B	113.4 psia, 3889°R	113.4 psia, 4000°R
C	86.4 psia, 3775°R	84.4 psia, 4000°R
D	64.9 psia, 3658°R	64.2 psia, 4000°R
E	47.9 psia, 3538°R	46.6 psia, 4000°R
F	34.5 psia, 3413°R	34.5 psia, 4000°R
G	26.4 psia, 3310°R	26.2 psia, 4000°R
H	19.9 psia, 3205°R	18.8 psia, 4000°R

CHAPTER V

CONCLUSIONS AND RECOMMENDATIONS

This study has evaluated and optimized turbine performance on a theoretical basis. The results were shown to be valid by comparison with empirical data and limiting cases. Using the turbine performance characteristics, application as a topping turbine to a coal burning power plant was investigated.

Results indicate that single disk units such as shown in Figure 4-30 have low thermal efficiency and very low output. These are not considered practical for further study. However, using an axial compressor and a series of viscous turbines (Figure 4-38) very attractive efficiency and significant output was attained. Though the size of these units could be prohibitive, variable area geometry and supersonic turbines may offer alternatives to reduce equipment requirements at equivalent outputs.

In this manner, the viscous turbine may present a viable prospect to augment electrical power generation. Further study is recommended in the following areas:

1. Application to existing plants. A survey should be made of operating powerplants to determine the extent of applicability of a viscous topping turbine system. Effect

of the turbine on the steam cycle should also be evaluated. For example, will the boiler effectiveness be reduced when combustion occurs externally? What will refitting the existing plants to accommodate the turbine entail? Persons working in the power industry should be consulted in this portion of the study for suggestions and evaluation.

2. Heat transfer analysis. As discussed in Section 4-7 the heat transfer evaluations in this thesis represent two extremes: zero heat transfer or infinite resistance in the disk, and constant surface temperature or zero heat resistance in the disk. The difference was significant in regard to unit performance. Transient heat conduction analysis into the fins in conjunction with turbine operation needs to be performed in order to correctly ascertain the unit's potential. Possible surface coating of the disk with a high temperature insulative material may also be investigated.

3. Unit optimization. Analysis has indicated that unit efficiency, horsepower, and physical size are mutual tradeoffs. No attempt has been made to optimize the operation with regard to these quantities, because no valid basis for comparison was available. For example, which is the most practical, a 14 percent efficient 500 hp unit or a 9 percent efficient 1000 hp unit? Which is more practical, eight straight area series turbines at 14 percent or four variable area series turbines at 10 percent thermal efficiency.

Thorough optimization will be possible when these criteria are defined.

These recommendations are given in order of importance. Should the results of each study be found favorable, the next phase would be to build a prototype and test operational modes.

APPENDICES

APPENDIX A

VISCOUS TURBINE COMPUTER MODEL

```
      PROGRAM TURBINE(INPUT,OUTPUT,TAPE5=INPUT,TAPE6=OUTPUT)
      DIMENSION  VC(11),PC(11),TC(11),RHOC(11),FC(10),DDC(10)
      DIMENSION TO(99,10),C(99)
      DIMENSION HH(99,10),G(99)
      DIMENSION XX(99,10),YY(99,10),KA(10),KB(10),KD(10)
      DIMENSION X(99),Y(99),IBUF(512)
      DIMENSION PP(99,10),Z(99),BS(99,10),R(99)
      DIMENSION UE(99,10),U(99),HP(99,10),D(99)
      REAL N,MDOT,MA,MD,M,MM,MB
      CALL PLOTS(IBUF,512,9,00)
      CALL PLOT(2.0,1.5,-3)
      CALL FACTOR(1.2)
      PI=3.1416
    4 CONTINUE
C
C     KC AND KK ARE USED FOR PLOTTER INSTRUCTIONS
C     KC REPPESENTS THE NUMBER OF PLOTS,KK THE NUMBER OF CURVES
C
      KC=0
C
C     INPUT DATA
C
    1 READ(5,2) H,W,N,DIA,A3,S,T3,PRST
    2 FORMAT(8F10.0)
      IF(H.EQ.0.0) GO TO 99
      KC=KC+1
      H1=H
      RPM=S*60./PI/DIA
      WRITE(6,3)H,W,N,DIA,A3,S,T3,PRST
    3 FORMAT(8F15.7,/)
      DX=PI*DIA/180.
      KK=0
C
C     FLOWRATE IS CONTROLED BY MACH NUMBER
C
      DO 11 I=1,100,3
      D2=I
      MA=D2*.01
      C3=0.0
      DA=0.0
      H=H1
      QC=0.0
      AA=H1*W*N
C
C     ISENTROPIC ENTRANCE SECTION
C
      T=T3/(1.0+.2*(MA**2.0))
      P=PRST*((T/T3)**3.5)
      MDOT=P*AA*MA*.92/(T**.5)
      RHO=P/(T*639.6)
      V=MDOT/(RHO*AA)
      IF(S.GT.V) GO TO 11
      QC=0.0
```

```
      DRAG=0.0
      VC(1)=V
      PC(1)=P
      TC(1)=T
      RHOC(1)=RHO
C
C     MO IS FLOW THROUGH EACH SLOT
C
      MO=MDOT/N
      TW=2500.
      WRITE(6,44)V,RHO,P,T,MA,TW,MDOT
   44 FORMAT(7F15.5,/)
C
C     BEGIN ITERATION OF CONTROL VOLUMN ANALYSIS
C
      DO 21 J=1,10
      DA=J
      DO 19 IJ=1,10
      H=H*(1.+DA)
      IF(H/W.GT.10.0) GO TO 12
      AA=H*W*N
      D=2.0*H*W/(H+W)
C
C     CALCULATION OF FLUID PROPERTIES
C
      VIS=1.285*((TC(J)/560.0)**1.35)*(1000./(TC(J)+440.))*1.E-5
      CP=(((TC(J)/1000.)-1.0)*.02)+.2486
C
C     CALCULATION OF STRESSES AND CONVECTION FACTOR
C
      REW=(ABS(VC(J)-S))*D*RHOC(J)*12.0/VIS
      CALL FF (REW,FW)
      HW=RHOC(J)*CP*FW*(ABS(S-VC(J)))/8.0
      TAUW=FW*RHOC(J)*(ABS(S-VC(J)))*(S-VC(J))/3091.2
      REC=VC(J)*D*RHOC(J)*12.0/VIS
      CALL FF (REC,FX)
      TAUC=FX*RHOC(J)*(VC(J)**2.0)/3091.2
C
C     CALCULATION OF WORK,FORCE,AND HEAT TRANSFER
C
      DQC(J)=(TW-TC(J))*HW*((2.0*H)+W)*DX/MO
      FC(J)=TAUW*((2.0*H)+W)*DX
      DW=FC(J)*S/(MO*9336.0)
      C1=FC(J)/(H*W)-TAUC*DX/H
      C2=(DQC(J)+DW)/CP
      C6=MO/(H*W*TC(J)*53.3*32.2*144.0)
      C7=MO/(H*W*TC(J)*CP*32.2*778.*144.)
      BB=C3
      C3=C6-C7-(RHOC(J)/VC(J))
      IF(BB/C3.LT.0.0) GO TO 12
      C4=((C1/(53.3*TC(J)*12.0))-(C2*RHOC(J)/TC(J)))
C
C     COMBINATION OF FUNDAMENTAL EQUATIONS
```

```
C
      DV=C4/C3
C
C     CONTINUITY EQUATION
C
      DRHO=-RHOC(J)*DV/VC(J)
C
C     MOMENTUM EQUATION
C
      DP=-(MD*DV/(H*W*32.2*12.0))+C1
C
C     ENERGY EQUATION
C
      DT=C2-(VC(J)*DV/(CP*32.2*144.0*778.))
C
      IF(IJ.NE.1) GO TO 18
      WRITE(6,45)VC(J),TC(J),PC(J),DRAG,DT,C2,DV,DW,DQC(J),D8
      WRITE(6,46)DV,C1,C2,C6,C7,C3,C4,TAUW,TAUC,FW,H
   18 CONTINUE
      QC=QC+DQC(J)
      DRAG=DRAG+FC(J)*N
      VC(J)=VC(J)+DV
      M=VC(J)/12./(SQRT(2402.8*TC(J)))
      IF(M.GT.1.0) GO TO 12
      PC(J)=PC(J)+DP
      TC(J)=TC(J)+DT
      RHOC(J)=MDOT/(VC(J)*AA)
   19 CONTINUE
      VC(J+1)=VC(J)
      PC(J+1)=PC(J)
      TC(J+1)=TC(J)
      RHOC(J+1)=RHOC(J)
   21 CONTINUE
C
C     FINISH CONTROL VOLUMN ITERATION
C
      D8=11.0
      J=11
      WRITE(6,45)VC(J),TC(J),PC(J),DRAG,DT,C2,DV,DW,DQC(J),D8
      WRITE(6,46)DV,C1,C2,C6,C7,C3,HK,TAUW,TAUC,TC(J),M
   45 FORMAT(10F13.3)
   46 FORMAT(11E12.5,/)
      V=VC(11)
      T=TC(11)
      RHO=RHOC(11)
      P=PC(11)
      IF(P.LT.0.0) GO TO 12
C
C     ISENTROPIC EXIT SECTION
C
      MB=(V/12.0)/(SQRT(2402.8*T))
      PT=P*((1.0+.2*(MB**2.0))**3.5)
      DELP=PT-PRST
```

```
C
C     CALCULATION OF TURBINE EFFICIENCY,HORSEPOWER,AND SINGLE STAGE
C     UNIT EFFICIENCY
C
      WT=MDOT*CP*T3*(((PT/PRST)**.286)-1.)
      WA=DRAG*S/(778.*12.)
      EFF=WA/WT
      T2=530.*(((PRST/PT)**.286))
      WC=MDOT*.243*(T2-530.)/.8
      TA=(T2+T3)/2.
      CP=(((TA/1000.)-1.)*.02)+.2486
      QIN=MDOT*CP*(T2-T3)
      TEFF=(WA+WC)/QIN
      WRITE(6,47)DELP,MDOT,EFF,WA,TEFF
   47 FORMAT(8F15.4,/,/,/)
C
C     DATA PREPARED FOR PLOTTER
C
      KK=KK+1
      HP(KK,KC)=(WA+WC)/(-.707)
      PP(KK,KC)=DELP*(-1.)
      TO(KK,KC)=(WA*(-1.0))/(.29*MDOT)+(QC*(-1.0))/.29
      BS(KK,KC)=WA*(-1.0)
      XX(KK,KC)=MDOT*60.
      YY(KK,KC)=EFF*100.
      UE(KK,KC)=TEFF*100.
      HH(KK,KC)=H/H1
      KA(KC)=KK+1
      KB(KC)=KK+2
      KD(KC)=KK
   11 CONTINUE
   12 CONTINUE
      GO TO 1
   99 CONTINUE
C
C     PLOTTER INSTRUCTIONS
C
      CALL AXIS(0.0,0.0,"FLOWRATE,LBM/MIN",-16,5.0,0.0,0.0,10.)
      CALL AXIS(0.0,0.0,"PRESSURE DROP,PSI",17,6.0,90.0,0.0,5.0)
      KF=KC
      DO 97 KC=1,KF
      KE=KA(KC)
      O(KE)=-5.0
      C(KE)=0.0
      U(KE)=-1.0
      Y(KE)=0.0
      Z(KE)=0.00
      X(KE)=0.0
      KE=KB(KC)
      O(KE)=5.0
      C(KE)=40.0
      X(KE)=10.
      Z(KE)=5.0
```

```
      U(KE)=1.0
      Y(KE)=7.0
      KE=KC(KC)
      DO 96 L=1,KE
      U(L)=UE(L,KC)
      Z(L)=PP(L,KC)
      X(L)=XX(L,KC)
      Y(L)=YY(L,KC)
      C(L)=TC(L,KC)
      O(L)=HP(L,KC)
      G(L)=HH(L,KC)
      B(L)=BS(L,KC)
C
C     PRINT OUT PLOT DATA
C
      WRITE(6,47) X(L),Y(L),Z(L),U(L),O(L),B(L),C(L),G(L)
   96 CONTINUE
      CALL LINE(X(1),Z(1),KE,1,1,3)
   97 CONTINUE
      CALL PLOT(9.0,0.0,-3)
C
C     RETURN TO READ ADDITIONAL SETS OF DATA
C
      IF(A3.EQ.0.0) GO TO 4
      CALL PLOT(0.0,0.0,999)
      STOP
      END
```

APPENDIX B

SUBROUTINES

```
C      FRICTION FACTOR SUBROUTINE
C
       SUBROUTINE FF (RE,F)
       IF(RE.GT.2000.) GO TO 23
C
C      LAMINAR
C
       F=71.0/RE
       GO TO 26
C
C      TURBULENT
C
   23  F=.05
       D1=-.05
       DO 25 JJ=1,10
       D2=JJ
       F=F+D1*(2.0**(-D2))
       D3=1.0/(SQRT(F))
       D4=2.0*(ALOG10(RE*(SQRT(F))))-.8
       IF(D3.GT.D4) GO TO 24
       D1=-.05
       GO TO 25
   24  D1=.05
   25  CONTINUE
   26  CONTINUE
       RETURN
       END
```

```
      SUBROUTINE ISO (A1,A2,V,RHO,P,T,MDOT,MB)
      REAL MDOT,MB
      A=A1
      MB=(V/12.0)/(SQRT(2402.8*T))
      PT=P*((1.0+.2*(MB**2.0))**3.5)
      WRITE(6,34)A,V,P,T
   34 FORMAT(4E15.4)
      DO 30 K=1,100
      DO 33 KM=1,100
      MB=(V/12.0)/(SQRT(2402.8*T))
      X=((A2/A1)**.001)
      DA=((A*X)-A)*(ABS(1.0-MB))
      C8=-MDOT/(A*P*32.2*12.0)
      CP=(((T/1000.)-1.0)*.02)+.2486
      C9=V/(CP*T*32.2*144.0*778.)
      C10=(1.0/V)+C8+C9
      DV=-DA/(A*C10)
      DP=-(MDOT*DV)/(A*32.2*12.0)
      DT=-(V*DV)/(CP*32.2*144.0*778.0)
      A=A+DA
      V=V+DV
      T=T+DT
      P=PT/((1.0+.2*(MB**2.0))**3.5)
      IF(DA.LT.0.0.AND.A.LT.A2)GO TO 32
      IF(DA.GT.0.0.AND.A.GT.A2)GO TO 32
   33 CONTINUE
      WRITE(6,31)A,V,P,T,C8,C9,C10,MB
   31 FORMAT(8E15.4)
   30 CONTINUE
   32 WRITE(6,31)A,V,P,T,C8,C9,C10,MB
      RETURN
      END
```

APPENDIX C

VISCOUS COMPRESSOR AND TURBINE UNIT COMPUTER PROGRAM

```
      PROGRAM ENGINE1(INPUT,OUTPUT,TAPE5=INPUT,TAPE6=OUTPUT)
      REAL N,MDOT,MA,MD,M,MM,MB
      DIMENSION  VC(11),PC(11),TC(11),RHOC(11),FC(10),DQC(10)
      DIMENSION  VT(11),PT(11),TT(11),RHOT(11),FT(10),DQT(10)
      PI=3.1416
    1 READ(5,2) H,W,N,DIA,A3,RPM,T3,A4
    2 FORMAT(8F10.0)
      IF(H.EQ.0.0) GO TO 99
      WRITE(6,3)H,W,N,DIA,A3,A4,RPM,T3
    3 FORMAT(8F15.7,/)
      S=RPM*PI*DIA/60.0
      AA=H*W*N
      D=2.0*H*W/(H+W)
      DX=(PI*DIA/3.0)/10.
      DX=DX/10.
      MA=.5
      TW=2000.0
      D1=0.0
      QC=0.0
      QT=0.0
      QT=0.0
C
C     CONVERGENCE OF MDOT,TW
C
      DO 11 I=1,10
      D2=I
      MA=MA+D1*(2.0**(-D2))
      MA=D2*.1
      IF(QT+QC)15,16,17
   15 TW=TW+100.0
      GO TO 16
   17 TW=TW-100.0
   16 CONTINUE
C
C     ISENTROPIC 1 TO A
C
      T=530.0/(1.0+.2*(MA**2.0))
      P=14.7*((T/530.0)**3.5)
      MDOT=P*AA*MA*.92/(T**.5)
      RHO=P/(T*639.6)
      V=MDOT/(RHO*AA)
C
C     FLOW THROUGH COMPRESSOR
C
      QC=0.0
      DRAG=0.0
      MD=MDOT/N
      VC(1)=V
      PC(1)=P
      TC(1)=T
      RHOC(1)=RHO
      WRITE(6,44)V,RHO,P,T,MA,TW,MDOT
   44 FORMAT(7F15.5,/)
      DO 20 J=1,10
      D8=J
C
C     IF MACH RELATIVE TO WHEEL EXCEEDS ONE REDUCE RELATIVE VELOCITY
```

```
C
      M=(ABS(VC(J)-S))/12.0/(SQRT(2402.8*TC(J)))
      IF(M-1.0)21,21,22
   22 CONTINUE
      IF(S.GT.VC(J))D1=1.0
      IF(S.LT.VC(J))D1=-1.0
      GO TO 18
   21 CONTINUE
      DO 19 IJ=1,10
      VIS=1.485*((TC(J)/560.0)**1.35)*(1000./(TC(J)+440.))*1.E-5
      CP=(((TC(J)/1000.)-1.0)*.02)+.2486
      REW=(ABS(VC(J)-S))*D*RHOC(J)*12.0/VIS
C
C     CALCULATE FW,FC,TAU,HW   COMPRESSOR
C
      CALL FF (REW,FW)
      HW=RHOC(J)*CP*FW*(ABS(S-VC(J)))/8.0
      TAUW=FW*RHOC(J)*(ABS(S-VC(J)))*(S-VC(J))/3091.2
      REC=VC(J)*D*RHOC(J)*12.0/VIS
      CALL FF (REC,FX)
      TAUC=FX*RHOC(J)*(VC(J)**2.0)/3091.2
      DQC(J)=(TW-TC(J))*HW*((2.0*H)+W)*DX/MD
      DQC(J)=0.0
      FC(J)=TAUW*((2.0*H)+W)*DX
C
C     CALCULATE VELOCITY INCREMENT   COMPRESSOR
C
      DW=FC(J)*S/(MD*9336.0)
      C1=FC(J)/(H*W)-TAUC*DX/H
      C2=(DQC(J)+DW)/CP
      C6=MJ/(H*W*TC(J)*53.3*32.2*144.0)
      C7=RHOC(J)*VC(J)/(TC(J)*CP*32.2*778.*144.)
      C3=C6-C7-(RHOC(J)/VC(J))
      C4=((C1/(53.3*TC(J)*12.0))-(C2*RHOC(J)/TC(J)))
      DV=C4/C3
C
C     CONTINUITY EQUATION
C
      DRHO=-RHOC(J)*DV/VC(J)
C
C     MOMENTUM EQUATION
C
      DP=-(MD*DV/(H*W*32.2*12.0))+C1
C
C     ENERGY EQUATION
C
      DT=C2-(VC(J)*DV/(CP*32.2*144.0*778.))
C
      IF(IJ.NE.1) GO TO 18
      WRITE(6,45)VC(J),TC(J),PC(J),DRAG,DT,C2,DV,DW,DQC(J),D8
      WRITE(6,46)DV,C1,C2,C6,C7,C3,HW,TAUW,TAUC,C4,RHOC(J)
   46 FORMAT(11E12.5,/)
   45 FORMAT(10F13.3)
   18 CONTINUE
      QC=QC+DQC(J)*N
      DRAG=DRAG+FC(J)*N
      VC(J)=VC(J)+DV
```

```
      PC(J)=PC(J)+DP
      TC(J)=TC(J)+DT
      RHOC(J)=MDOT/(VC(J)*AA)
   19 CONTINUE
      VC(J+1)=VC(J)
      PC(J+1)=PC(J)
      TC(J+1)=TC(J)
      RHOC(J+1)=MDOT/(VC(J+1)*AA)
   20 CONTINUE
      D8=11.0
      J=11
      WRITE(6,45)VC(J),TC(J),PC(J),DRAG,DT,C2,DV,DW,DQC(J),D8
      WRITE(6,46)DV,C1,C2,C6,C7,C3,HW,TAUW,TAUC,TC(J),VC(J)
      V=VC(11)
      RHO=RHOC(11)
      P=PC(11)
      T=TC(11)
C
C     ISENTROPIC 8 TO 2
C
      CALL ISO (AA,A3,V,RHO,P,T,MDOT,M8)
      V2=V
      P2=P
      T2=T
      RHO2=RHO
C
C     COMBUSTION 2 TO 3
C
      CP=((((T3+T2)/2000.)-1.0)*.32)+.2466
      FUEL=MDOT*CP*(T3-T2)
      T=T3
      RHO=P/(53.3*T*12.0)
      RHO3=RHO
      V=MDOT/(RHO*A3)
      V3=V
C
C     ISENTROPIC 3 TO C
C
      CALL ISO (A3,AA,V,RHO,P,T,MDOT,MB)
      IF(T.LT.0.0) GO TO 10
      IF(MB.LT.1.0) GO TO 6
      D1=-1.0
      GO TO 10
    6 CONTINUE
C
C     FLOW THROUGH TURBINE
C
      QT=0.0
      PUSH=0.0
      VT(1)=V
      PT(1)=P
      TT(1)=T
      RHOT(1)=RHO
      DO 50 L=1,10
      D8=L
C
C     IF MACH RELATIVE TO WHEEL EXCEEDS ONE REDUCE RELATIVE VELOCITY
```

```
C
      M=(ABS(VT(L)-S))/12.0/(SQRT(2402.8*TT(L)))
      IF(M-1.0)51,51,52
   52 CONTINUE
      IF(S.GT.VT(L))D1=1.0
      IF(S.LT.VT(L))D1=-1.0
      GO TO 10
   51 CONTINUE
      DO 57 LI=1,10
      VIS=1.235*((TT(L)/560.0)**1.35)*(1000./(TT(L)+440.))*1.E-5
      CP=(((TT(L)/1000.)-1.0)*.02)+.2486
      REW=(ABS(VT(L)-S))*D*RHOT(L)*12.0/VIS
C
C     CALCULATE FW,FC,TAU,HW   TURBINE
C
      CALL FF (REW,FW)
      HW=RHOT(L)*CP*FW*(ABS(S-VT(L)))/8.0
      TAUW=FW*RHOT(L)*(ABS(VT(L)-S))*(VT(L)-S)/3091.2
      REC=VT(L)*D*RHOT(L)*12.0/VIS
      CALL FF (REC,FX)
      TAUC=FX*RHOT(L)*(VT(L)**2.0)/3091.2
      DQT(L)=(TW-TT(L))*HW*((2.0*H)+W)*DX/MD
      DQT(L)=0.0
      FT(L)=TAUW*((2.0*H)+W)*DX
C
C     CALCULATE VELOCITY INCREMENT   TURBINE
C
      DW=FT(L)*(-1.0*S)/(MD*9336.0)
      C1=-FT(L)/(H*W)-TAUC*DX/H
      C2=(DQT(L)+DW)/CP
      C6=MD/(H*W*TT(L)*53.3*32.2*144.0)
      C7=RHOT(L)*VT(L)/(TT(L)*CP*32.2*778.*144.)
      C3=C6-C7-(RHOT(L)/VT(L))
      C4=((C1/(53.3*TT(L)*12.0))-(C2*RHOT(L)/TT(L)))
      DV=C4/C3
C
C     CONTINUITY EQUATION
C
      DRHO=-RHOT(L)*DV/VT(L)
C
C     MOMENTUM EQUATION
C
      DP=-(MD*DV/(H*W*32.2*12.0))+C1
C
C     ENERGY EQUATION
C
      DT=C2-(VT(L)*DV/(CP*32.2*144.0*778.))
C
      IF(LI.NE.1) GO TO 58
      WRITE(6,45)VT(L),TT(L),PT(L),PUSH,DT,C2,DV,DW,DQT(L),D8
      WRITE(6,46)DV,C1,C2,C6,C7,C3,HW,TAUW,TAUC,C4,RHOT(L)
   58 CONTINUE
      QT=QT+DQT(L)*N
      PUSH=PUSH+FT(L)*N
      VT(L)=VT(L)+DV
      PT(L)=PT(L)+DP
      TT(L)=TT(L)+DT
```

```
      RHOT(L)=MDOT/(VT(L)*AA)
   57 CONTINUE
      VT(L+1)=VT(L)
      PT(L+1)=PT(L)
      TT(L+1)=TT(L)
      RHOT(L+1)=MDOT/(VT(L+1)*AA)
   59 CONTINUE
      D8=11.0
      L=11
      WRITE(6,45)VT(L),TT(L),PT(L),PUSH,DT,C2,DV,DW,DQT(L),D8
      WRITE(6,46)DV,C1,C2,C6,C7,C3,HW,TAUW,TAUC,TT(L),VT(L)
      V=VT(11)
      RHO=RHOT(11)
      P=PT(11)
      T=TT(11)
C
C     CHECK MACH LEAVING TURBINE
C
      M=(V/12.0)/(SQRT(2402.8*T))
      IF(M-1.0)95,95,96
   96 CONTINUE
C
C     SHOCK AT EXIT NEGLECTING DIFFUSER
C
      D5=(M**2.)*(1.+.2*(M**2.))/((1.+(1.4*(M**2.)))**2.)
      MM=1.0
      D1=-1.0
      DO 70 II=1,10
      D2=II
      MM=M1+D1*(2.0**(-D2))
      D6=(MM**2.)*(1.+.2*(MM*2.))/((1.+(1.4*(MM**2.)))**2.)
      IF(D5.GT.D6) GO TO 71
      D1=-1.0
      GO TO 70
   71 D1=1.0
   70 CONTINUE
      P=P*(1.0+(1.4*(M**2.)))/(1.0+(1.4*(MM**2.)))
      GO TO 97
C
C     ISENTROPIC EXPANSION THROUGH DIFFUSER
C
   95 CALL ISO (AA,A4,V,RHO,P,T,MDOT,M8)
C
C     IF P IS LESS THAN ATMOSPHERIC  REDUCE FLOWRATE
C
   97 IF(I.LT.10) GO TO 98
      WRITE(6,94) P
   94 FORMAT(F10.5)
   98 IF(P-14.7)75,12,76
   75 D1=-1.0
      WRITE(6,49) P,T,V,I
   49 FORMAT(4F15.5/,/,/)
      GO TO 10
C
C     IF P IS GREATER THAN ATMOSPHERIC  INCREASE FLOWRATE
C
   76 D1=1.0
```

```
      WRITE(6,49) P,T,V,M
      GO TO 10
   10 CONTINUE
C
C     CALCULATE OVERALL OUTPUT
C
   12 TORQUE=(PUSH-DRAG)*DIA/24.0
      POWER=TORQUE*6.2832*RPM/(778.*60.)
      EFF=POWER/FUEL
      WRITE(6,4)TORQUE,POWER,EFF,VC(1),MDOT,P2,T2,VT(11),M,V,P,T,TW
    4 FORMAT(7F15.7,/,6F15.7,/,/)
   11 CONTINUE
      GO TO 1
   99 STOP
      END
```

REFERENCES

1. Dusadeenoad, S., "Characteristics of a Viscous Flow Compressor," M.S. Thesis, Georgia Institute of Technology, September, 1970.

2. Caldwell, J. S., "Efficiency of a Viscous Flow Compressor," M.S. Thesis, Georgia Institute of Technology, June, 1973.

3. Colwell, G. T. and Jackson, T. W., Turbine-Compressor, United States Patent No. 3,751,908, August 14, 1973.

4. Yalcin. A. I., "Theoretical Study of a Viscous Turbine," M.S. Thesis, Georgia Institute of Technology, March, 1975.

5. Tesla, Nikola, Turbine, Official Gazette U. S. Patents No. 1061206 5/1913.

6. John, E. A., Gas Dynamics, First Edition, Allyn and Bacon Company, 1974.

7. Schlichting, H., Boundary-Layer Theory, Sixth Edition, McGraw-Hill Company, 1968.

8. White, F. M., Viscous Fluid Flow, First Edition, McGraw-Hill Company, 1974.

9. Reynolds, W. C., Thermodynamics, Second Edition, McGraw-Hill Company, 1968.

10. Kreith, F., Principles of Heat Transfer, Second Edition, McGraw-Hill Company, 1965.

11. Keenan and Kaye, Gas Tables, First Edition, Wiley Incorporated, 1966.

12. Cooper and Smith, Standard Fortran, First Edition, Houghton Mifflin, 1973.

E-25-658

1 cy

GEORGIA INSTITUTE OF TECHNOLOGY
ATLANTA, GEORGIA 30332

OFFICE OF
THE DIRECTOR OF
FINANCIAL AFFAIRS

March 1, 1977

United States Energy Research and
Development Administration
Oak Ridge Operations
Contract Division
P. O. Box E
Oak Ridge, Tennessee 37830

Attention: Mr. A. H. Frost, Jr.

Reference: Contract Number E-(40-1)-4959

Gentlemen:

Enclosed in triplicate is the Statement of Costs for Contract Number E-(40-1)4959 covering the period July 1, 1975 through June 30, 1976.

If you have any questions or desire additional information, please let us know.

Sincerely yours,

C. Evan Crosby

C. Evan Crosby
Associate Director of
Financial Affairs

CEC/bs
enclosure:
cc: Dr. S. P. Kezios
Dean J. R. Williams
Mr. E. E. Renfro
Mr. A. H. Becker
File E-25-658

GEORGIA INSTITUTE OF TECHNOLOGY, ATLANTA, GEORGIA
U. S. ENERGY RESEARCH AND DEVELOPMENT ADMINISTRATION
STATEMENT OF COSTS

1. Name and address of Contractor: Georgia Institute of Technology
Atlanta, Georgia 30332

2. Contract Number: E-(40-1)-4959

3. Beginning and ending date of pertinent contract period: July 1, 1975 thru June 30, 1976

4. Costs incurred during the pertinent contract period:

a.	Salaries and wages	$ 13,308.98
b.	Travel (all domestic)	481.47
c.	Other direct costs	2,255.66
d.	Total direct expenditures	$ 16,046.11
e.	Indirect costs - 65% of Salaries & Wages	8,650.84

5. Total costs for items under A-II (a) for the pertinent contract period. $ 24,696.95

6. Support Cost for the pertinent contract period. Using the percentage of 95% as set forth in Appendix "A" the amount chargeable to ERDA is $23,462.10. $ 23,462.10

7. Support Ceiling 25,000.00

8. Unexpended ERDA funds $ 1,537.90

I hereby certify that this report is true and correct to the best of my knowledge and belief and that the costs listed herein were incurred in connection with the performance of the research provided for under this contract and in accordance with the terms and conditions set forth therein.

Stothe P. Kezios, Director School of Mechanical Engineering
Name and Title of Principal Investigator

Stothe P Kezios
Signature

2-25-77
Date

C. Evan Crosby, Associate Director of Financial Affairs
Name and Title of Business Officer

C. Evan Crosby
Signature

3/1/77
Date